Detection of Cracks in a Cantilever Metal Plate Using Vibrational Techniques

By

Sharif Rezwan Shuvo

Student Number – 171011005

Supervised By

Dr. Md. Zahid Hossain

A thesis submitted to the Department of Mechanical and Production Engineering (MPE) in partial fulfillment of the requirement for the degree of Master of Science in Mechanical Engineering

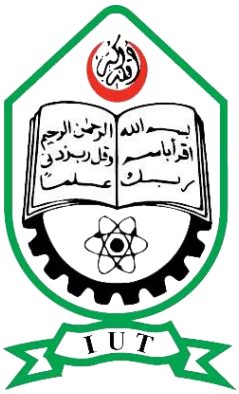

Department of Mechanical and Production Engineering (MPE)

Islamic University of Technology (IUT)

September 2020

Certificate of Approval

The thesis titled "Detection of Cracks in a Cantilever Plate Using Vibrational Techniques" submitted by Sharif Rezwan Shuvo bearing student number 171011005 of Academic Year 2019-2020 has been found as satisfactory and accepted as partial fulfillment of the requirement for the degree of Master of Science in Mechanical Engineering on 25 September, 2020.

Board of Examiners

…….	
Dr. Md. Zahid Hossain Head, Professor, Department of Mechanical and Production Engineering (MPE) Islamic University of Technology (IUT) Board Bazar, Gazipur, Bangladesh	Chairman (Supervisor) and Member (Ex-officio)
…….	
Dr. Md. Nurul Absar Chowdhury Professor, Department of Mechanical and Production Engineering (MPE) Islamic University of Technology (IUT) Board Bazar, Gazipur, Bangladesh	Member
…….	
Dr. Anayet Ullah Patwari Professor, Department of Mechanical and Production Engineering (MPE) Islamic University of Technology (IUT) Board Bazar, Gazipur, Bangladesh	Member
…….	
Dr. Md. Abdus Salam Akanda Professor, Department of Mechanical Engineering (ME), Bangladesh University of Engineering and Technology (BUET) Dhaka, Bangladesh	Member (External)

Candidate's Declaration

It is hereby declared that this thesis or any part of it has not been submitted elsewhere for the award of any degree or diploma.

Signature of the Candidate

…….

Sharif Rezwan Shuvo

Department of Mechanical and Production Engineering (MPE)

Islamic University of Technology (IUT)

Board Bazar, Gazipur,

Bangladesh.

Signature of the Supervisor

…….

Dr. Md. Zahid Hossain

Head, Professor,

Department of Mechanical and Production Engineering (MPE)

Islamic University of Technology (IUT)

Board Bazar, Gazipur,

Bangladesh.

Dedication

This thesis is dedicated to my parents and family.

Acknowledgement

The author is highly grateful to Almighty Allah for successful completion of the postgraduate thesis. The journey was not an easy one, rather it contained with lots of hard working, stressful office hours, many sleepless night and dedication, love and care of the family and the professors.

The author puts deepest gratitude to his supervisor, Dr. Zahid Hossain, Head, Professor of Mechanical and Production Engineering (MPE), Islamic University of Technology (IUT) for his constant guidance, recommendation and inspiration. The author will also not forget the tremendous effort of Mr. Nagib Mehfuz, Lecturer of Department of Mechanical and Production Engineering (MPE), Islamic University of Technology (IUT), for every stages of this thesis work.

Finally, the author is thankful to his beloved mother and family for providing financial and mental support and encouragement.

Despite of the careful and precise work, author ask forgiveness to readers for any mistakes, whatsoever, found in his report beforehand.

Abstract

The main objective of this research is to detect crack at different positions of the thin metal cantilever plate based on the natural frequency. Most of the researchers have investigated on beam. Few researchers have investigated on thin plate. The crack depth and crack thickness in standard convention of beam are considered as crack length and depth of crack respectively in this research for the thin metal plate. Some theoretical approach considering bilinear stiffness have been found in some literatures. Numerical and experimental analysis due to crack in cantilever beam or plate have been investigated by different researchers.

In this research work, a thin plate is considered made of aluminum alloy and structure steel. A slit crack is considered for different cases of investigations. The crack length, width, depth, location, etc. are taken as parameters. These are investigated on the change of natural frequencies through modal analysis due to the mentioned parameters change.

The study confirms that when the crack length affects the most in frequency drop than that of crack width and crack depth. The drop of frequency is massive when the crack length increases. However, when the crack width increases the drop of frequency remains constant. Moreover, thorough crack on a plate shows more drop of frequency than that of a plate with crack, which is not thorough. Therefore, thorough cracks on plates are more detectable

Along the longitudinal direction (Z-axis), the effect of transverse edge crack is more significant and visible (with large frequency drop) than that of longitudinal crack (surface defect). The maximum drop in frequency in both the bending and torsional modes is shifted to free end along the relative distance on the plate. While along transverse direction (X-axis) of free end of the thin plate, the effect of longitudinal edge cracks are visible in torsional modes with massive frequency drop. In this case, the frequency of transverse cracks (surface defects) found in bending modes is greater than healthy plate and longitudinal curve. Surface defects, i.e., the

longitudinal crack along the longitudinal direction and the transverse crack along the transverse direction, along the edge of the plate remain undetectable. Although, the longitudinal embedded crack remain undetectable, the transverse embedded crack is traceable by the aid of bending modes only. Angle between 75^{o} to 105^{o} of the inclined cracks are more prone to detection. The effect of stiffness on the crack position on the plate near a bend or a twist (found in mode shape) is greater than any other region. Crack located in this region is more likely to be detected.

In static structural analysis along the longitudinal direction, stress concentration and total deformation is maximum while the first natural frequency is the minimum at fixed end. While at free end stress and deformation becomes minimum but first natural frequency becomes maximum. It is also found that, for healthy plate and plate with crack near free ends (with relative distance > 70%), the maximum von-Mises stress is located near fixed region of the plate. While for crack positions near fixed end and at mid-region (0% ≤ relative distance ≤ 70%), the maximum von-Mises stress is located at the tip of the crack. It is also observed that the pattern of normalized frequency curve in metal (structural steel) and metal alloy (aluminum alloy) are same. An analytical FEM approach has been performed for without crack condition and numerical validation with published paper has been done and found in good agreement.

Table of Contents

List of Tables

List of Figures

Nomenclature and Terminology

Particulars	Nomenclature
Length of the Plate	L or l
Width of the Plate	B
Thickness of the Plate	H
Length of the Crack	a
Width of the Crack	b
Depth of the Crack	c
Location of Crack along Z-axis	x
Location of Crack along X-axis	y
Natural Frequency	f or ω
Natural Frequency of healthy plate	f_o
Normalized Frequency	f/f_o or p
Relative Distance along Z-axis	x/L or n
Relative Distance along X-axis	y/B
Crack Length to Plate Length Ratio	a/L
Crack Width to Plate Length Ratio	b/L
Crack Depth to Plate Thickness Ratio	c/H
Mass of the beam	m
Density of the material	ρ
Cross section Area	A
Young's Modulus	E
Aluminum Alloy	AA
Structural Steel	SS

Chapter 1

Introduction

1.1 Definition of Crack and Breathing Crack

A crack is a discontinuity of stress concentration in a solid body creating some separation extent (crack length and depth) leading to metal failure (crack propagation) due to material separation by opening or sliding effects. For a beam to fail, cracks can occur due to increased shear stress or bending stress, compression failure (mechanical or thermal fatigue) and corrosion (corrosion fatigue). The number, position (embedded or edged), size (crack depth and length) and mode (opening, in-plane shear and out-of-plane shear) of the crack plays important role in detection of the crack. In mechanical vibration, considering only linear behavior of a crack might bring unrealistic result because it becomes insufficient to describe behavior of the crack. In our research we will consider, “Breathing Phenomena” in a crack. This progression is non-linear in nature consisting of alternating opening and closing of crack depending on the damping characteristic of the experimental material.

1.2 Why Crack Detection is Important?

Crack detection is one of the important aspect of structural safety. It is also essential in designing stage to know the behavior of the material based on natural frequency for with and without crack condition. Early detection of crack in an object could avoid severe accidents from occurring hence save a lot of currency. There are two ways to detect cracks, first the destructive testing and the second is the non-destructive testing. Destructive testing is carried out until the objects fails to find out the behavior of the material. While non-destructive testing undergoes investigation without any physical damage of the object. This analysis based on natural frequency could be a useful tool in reducing failure rate, accidents and costs.

1.3 Research Objectives

In this research, vibration methods are used to study different types of cracks, positon of cracks and identification of their status are verified. The linear characteristics are only considered to identify the crack initiation and progression. Moreover, the frequency drop and gain at different

beam locations are also considered to identify the most significant position and orientation of the crack along the plate. In short, our research will focus on:

a. To study intensively on different types of cracks at various locations on the plate using vibration analysis

b. To verify simulation results with theoretical and experimental results.

c. Intensive study to crack identification due to parametric changes.

The benefits of our research will add advantage to improve the technique currently used and to make certain applications like cantilever constructions, buildings, bridges etc. safer and more durable.

1.4 Possible Outcomes

From our research, we are looking forward to following outcomes:

a. From different types of cracks and their parametric change, crack identification will be possible.

b. Experimental results will establish the simulation result.

c. This work will have a good contribution in identifying cracks intensively.

1.5 Outline of Methodology

We have outlined our research into three phase:

1.5.1 Step 1

SolidWorks will be used to design a thin rectangular metal plate. For the crack design, initially a small through rectangular slit is considered. ANSYS Workbench will be used to simulate the design imported from SolidWorks through finite element modelling (FEM). Different boundary condition of the plate will be applied. The position of the slit will be located at the fixed end of the plate for primary validation purpose. For modal analysis, the natural frequency of the healthy rectangular plate without crack will be simulated and natural frequencies of first twenty modes will be recorded. Similarly, the natural frequencies of the rectangular plate with

crack will be noted to compare the variation. Once validation is completed, the slit position will be changed, depending on the type of operations and simulation conditions and first six modes of natural frequencies will be recorded.

1.5.2 Step 2

ANSYS 16.0 workbench will be used to perform static structural analysis. For different cases, maximum von-Mises stress and total deformation will be recoded. The findings will be compared with the modal frequency curves to establish any relationships for changing crack positions along beam, crack orientations or crack sizes.

Harmonic analysis will also be performed through simulation. The results will be found in bode plot. To check for the non-linearity of the design, the range of frequency of first three natural frequencies are considered and increase the solution interval. If any abrupt amplitude change is not observed then system is linear, in that case increasing the width of the crack to achieve non-linearity. Secondary peak for non-linear response located at the corresponding natural frequency multiplied by the factor 3, 5 and 7 times or 1/3, 1/5 and 1/7 times, known as the sub and super-harmonic response respectively.

1.5.3 Step 3

The experimental setup will be prepared using aluminum alloy as the material with the exact dimension is used for simulation. The experimental equipment and apparatus are used for the experiment will be: Clamping Device (Vice), ECL 202e Driver (Sensor Controller), U12 Non-Ferrous (Sensor), PCB 2007 mini-shaker (Shaker), Oscilloscope and a Power Supply. The results obtained from modal and harmonic analysis will be compared with the simulation results.

Chapter 2

Literature Review

Before 1970s, most of the vibrational techniques researchers used were associated with boundary conditions and derivation of single edge fatigue crack ignoring the opening and closing phenomena of the crack. Afterwards, researcher put emphasis on this issue to make it more realistic. Shen and Chu [1] had introduced a fatigue crack in a uniform beam in the form of breathing crack, which open when the normal strain at the crack tip is positive and vice versa. The objective was to investigate the contact effect of the crack on the structural dynamic behavior and its changes with time. A governing equation was derived for the beam by applying Galerkin procedure to formulate a bilinear stiffness equation of motion for each vibration mode for a simply supported beam. The result deduced that the changes in dynamic behavior is non-linear and can be used to identify the crack size and crack location. Chondros et al. [2] used different boundary conditions on a simply supported beam with a breathing crack. The bilinear characteristics of the stiffness system were solved separately over their respective domain. Open cracks shows larger natural frequency than fatigue breathing crack. The experimentation results with aluminum beam matches with the analytical finding. Tao et al. [3] investigated a thin cantilever rectangular plate with thorough crack on the fixed end edge to measure the change of natural frequencies and mode shapes. The plate was made of aluminum. First, the time-average electronic speckle pattern interferometry (ESPI) was used as experimental techniques. PZT actuator was fixed with the face surface to measure the natural frequency. This experiment determined non-linear vibration response of cracked plate. The technique provides whole field and real time measurement for vibration analysis. Later, the experimental data with validated with the finite element modeling (FEM) calculation using ANSYS. The study also showed the principal mode shape of super-harmonic vibration but failed to describe the detection of crack in the structure. This scientific paper is used for validation purpose.

Orhan [4] showed single and two V-shaped edge cracks were assessed on top and bottom surface of the cantilever beam. Natural frequencies were calculated using free vibration

numerically. The sinusoidal forced vibration was applied on free end to measure the harmonic response of the beam. The numerical analysis was done with ANSYS for healthy and cracked beam. It was found that as the crack depth increased natural frequency decreased. Natural frequency of top crack was more than bottom crack. Moreover, for constant crack depth, as crack location increased natural frequency increased. Natural frequency of bottom crack was more than top crack. Modal analysis was found more effective in identifying two cracks, while harmonic analysis showed better approach in single crack detection. Tufisi et al. [5] conducted numerical analysis to achieve on six natural frequencies and stress distribution for various crack positions along the 2% range of the fixed cantilever beam made of structural steel. It was observed that the stress concentration was disturbed by introduction of crack and its movement along the positions on the beam. Two linear regression curves were plotted to show first natural frequency and deflection. These curves had a good match against fixed end crack positions found from numerical analysis. It was shown that the highest frequency drop for a crack is located at the fixed end but result obtained could be misleading for detecting crack unless regression curve is plotted to clarify both deflection and natural frequency. Shinde and Katerkar [6] investigated on a single transverse crack for various crack depths and crack locations experimentally on a cantilever beam with mild steel beam. The experiment was performed by dropping a spherical object 400mm above at 50mm of free end and first three natural frequency were observed. From graphical representations of crack depth against natural frequency and crack length against natural frequency were plotted. It was conclude the natural frequencies decreases with increase in crack depth and the first natural frequency increases as the crack position moves away from fixed end and vice versa.

Praisach et al. [7] had developed analytical calculus valid for calculating natural frequency of a damaged cantilever beam (effective for all Euler-Bernoulli Type damaged beam). They considered crack on the damaged beam as open on the entire width of the beam. Later the crack

was placed at different locations of the beam and simulations were conducted. The researchers concluded the derived analytical calculus matches the FEM modal analysis. The study could give a clear understanding on material behavior based on static and dynamic response. Another important finding was that due to change of crack position, there were considerable amount of relative shift in natural frequency. The thoroughly investigations have not been found properly.

Gillich et al. [8] investigated the effect of natural frequencies due to the change of location and dimension of the cracks for a cantilever beam. For this purpose, the influence of mass loss and stiffness change were considered due to presence of transverse crack in a cantilever beam. The study also concentrates these influences on breathing cracks in open and closing stages along the cracked beam (i.e. geometrical discontinuity) both analytically and with numerical analysis. An equation was derived to calculate the frequency of the beam, which showed loss of mass analytically. This equation was found in terms of mass of the beam and squared of mode shape of curvature. The length of the crack is same of the width of the beam in this investigation. This investigation mainly focused on the change of natural frequencies due to the location of the crack for the beam. Mode shapes changes are not investigated thoroughly due to the change of crack.

There was only 0.2% variation when the numerical simulation found from ANSYS was compared with the derived equation. Another set of equations were generated in terms of mass of the beam and squared of mode shape of curvature. These were used to analytically calculate the natural frequency of damaged beam with decrease in stiffness (with and without loss of mass). In numerical simulation, a relation between frequency and damaged width were shown. A linear and asymptotic relationship were found for larger and smaller frequencies respectively. Another finding was found in relation with frequency and relative beam length (x/L). Breathing crack frequency (analytical) is more than frequency of open crack (FEA). The

mathematical equations proposed were used to estimate the frequency shifts due to structural changes in beam, when the crack was open or with breathing crack or crack with mass loss.

Andreaus and Baragatti [11] worked on breathing crack and its detection using aluminum alloy and steel beam. Instead of beam, this research deals with thin plate of the same materials. Charalambides and Fang [13] worked with a cantilever beam with horizontal embedded cracks subjected to transverse force. Lie et al. [14] investigated on a cantilever beam with closed embedded horizontal crack. In this research, both transverse embedded crack and longitudinal embedded crack are used along the mid axis of the Z-axis. Soliman [15] worked on impact of crack inclination angle on a cracked beam. While Jena and Parhi [16] made parametric study on response analysis of different structures of cracks – one of which is inclined type in their study. This research includes inclined cracks to analyze the behavior of crack at different positions. Gillich et al. [17] developed an improved frequency evaluation algorithm based on damaged location indicator and damage signature for early detection of damage in beam-like structures. Barad et. al. [18] showed that in crack detection the effect of crack location and crack depth are vital because they significantly affect the natural frequency. In this research, the crack length represents as the crack depth by the researcher. Elshamy et al. [19] obtain similar results. They not only performed it using finite element analysis but also experimentally validate it. They determined the transverse breathing crack would introduce flexibility in cantilever beam where the system stiffness and natural frequency would reduce. Gillich et al. [20] processed mathematical association among deflection, stored energy and natural frequencies for detection of cracks. It was found that, when the crack is located where the bending moments are not maximum, the effect on the natural frequency is not weakened once it is compared with the healthy beam with the normalized square of the mode shape of curvature of the crack.

In this research work, detection of crack in a thin rectangular plate is investigated. The type of crack analyzed here is thorough on the edge of the plate. The thorough parametric investigation has been done in this research work to understand the change of natural frequencies due to the slit crack. Mode shapes have been also investigated to explain the phenomenon properly. Modal analysis has been done through ANSYS to determine the natural frequencies and mode shapes. The mode shapes and normalized frequency response curves are considered in determining the presence of the crack. Two types of modes, namely bending modes and torsional modes, have been observed. Validation of published paper has been made and a theoretical investigation is done for the healthy (without crack) plate. The results have been found in a very good agreement.

Chapter 3

Modeling, Numerical Analysis and Problem Specification

3.1 Modeling of Cantilever Plate

In this research, SOLIDWORKS Premium 2019 is used to model of the thin metal plate. The dimension of the plate is 165mm x 80mm x 1.43mm. This remains fixed throughout the research. The plate drawn on SOLIDWORKS is shown in Figure 3.1.

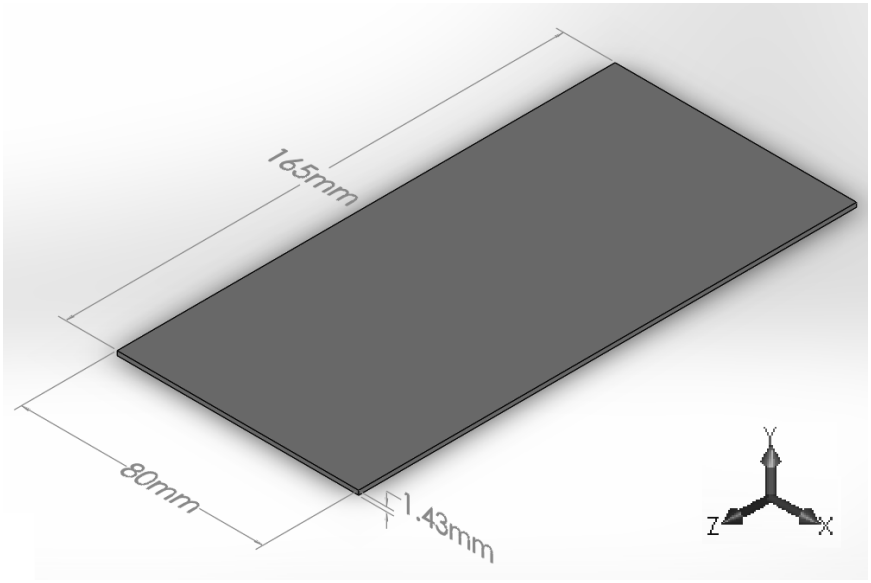

(a) Healthy Metal Plate

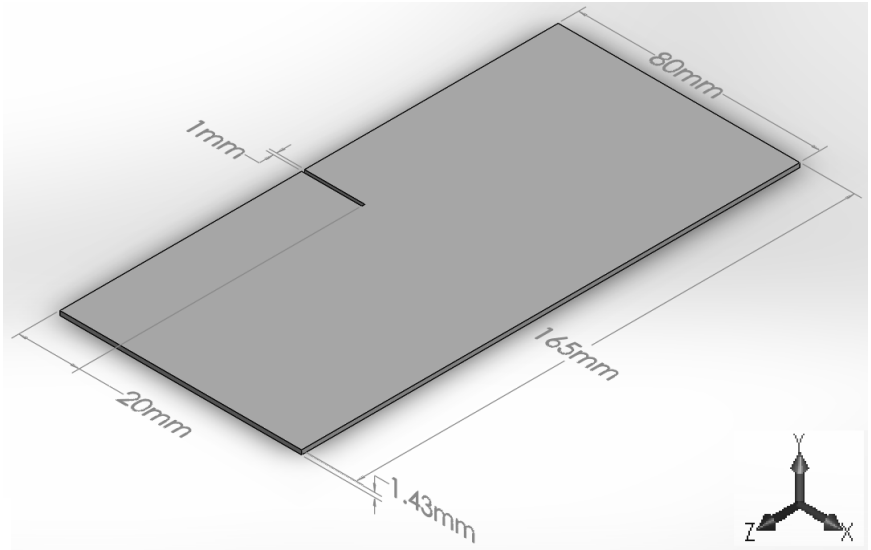

(b) Cracked Metal Plate

Figure 3.1: SOLIDWORKS Design of Thin Metal Plate

On the cantilever thin plate, a thorough crack of different dimensions and orientation is taken to meet certain research scenario. The crack positions are also changed along Z-axis (longitudinal direction) and X-axis (transverse direction). Different cases are considered for investigation shown in the next chapter. Some of the important parameters of the plate and the crack are shown in the table 3.1 along with nomenclature and values. The basic dimension of crack is 20mm x 1mmx 1.43mm.

Table 3.1: Dimension and Material Properties of the Plate and the Crack

Particulars	Value/mm	
	Standard	**Range**
Plate Properties		
Length of the Plate	165	165
Width of the Plate	80	80
Thickness of the Plate	1.43	1.43
Crack Properties		
Length of the Crack	20	10-70
Width of the Crack	1	0.5-20
Depth of the Crack	1.43	0.143-1.43

Material Properties	**Value**
Aluminum Alloy	
Density	2700 kg/m^3
Young's Modulus	70 GPa
Poisson's Ratio	0.33
Structural Steel	
Density	7850 kg/m^3
Young's Modulus	200 GPa
Poisson's Ratio	0.3

Change of Crack Location Along Axis	
Location of Crack along Z-axis	x
Location of Crack along X-axis	y
Crack Orientation	
Transverse Crack	Crack vertical to Z-axis
Longitudinal Crack	Crack vertical to X-axis
Inclined Crack	Crack at various angles 0^o to 180^o
Crack Movement Axis	
Longitudinal Direction	Z-Axis
Transverse Direction	X-Axis
Depth Direction	Y-Axis

3.2 Numerical Analysis

In this research, ANSYS 16.0 Workbench is used for conducting modal analysis and static structural analysis. Some important steps are taken into account are shown below.

Table 3.2: Important Steps of Numerical Analysis Procedures

STEP 1	:	Create New Project at ANSYS Workbench
STEP 2	:	Open: (a) Modal (b) Static Structural
STEP 3	:	Edit Engineering Data to add Material Properties & Type
STEP 4	:	Import Geometry from SOLIDWORKS
STEP 5	:	Open Model of Each Analysis
STEP 6	:	Add Mesh & Generate
STEP 7	:	Add analysis specification at Analysis Settings
STEP 8	:	Define Boundary Conditions
STEP 9	:	Add Input Load or Force
STEP 10	:	Define Solution Information
STEP 11	:	Solve
STEP 12	:	Collect Data as per recommendation

Aluminum alloy is used for validation. Later both structural steel and aluminum alloy are used for particular cases for the numerical analysis.

3.2.1 Modal Analysis

Initially, SolidWorks is used to design a thin rectangular metal plate. For the crack design, specification mentioned on the previous chapter is used. The design is imported from SolidWorks to ANSYS 16.0 workbench to simulate through finite element modelling (FEM). Table 3.2 shows the flow of the processes. Boundary conditions and mesh size are added on simulation settings. For validation, the position of the crack is located at the fixed end of the plate. The natural frequency of the healthy rectangular plate is recorded because this is utilized for comparing the natural frequency of cracked plate. Once validation is complete, the crack

positions are changed, depending on the operations and simulation conditions. In modal analysis, first six natural frequencies are extracted.

3.2.2 Static Structural Analysis

Static structural analysis is conducted using ANSYS 16.0 workbench to illustrate the stress concentration throughout the thin metal plate. In this case, a fixed end is defined and a small load of 1N on negative Y-axis applied at the free end. This are shown in the Figure 3.2. The Maximum von-Mises stress and total deformation are recorded when the position of the crack along the plate is changed. These findings are compared with the result of modal analysis to establish any relationships.

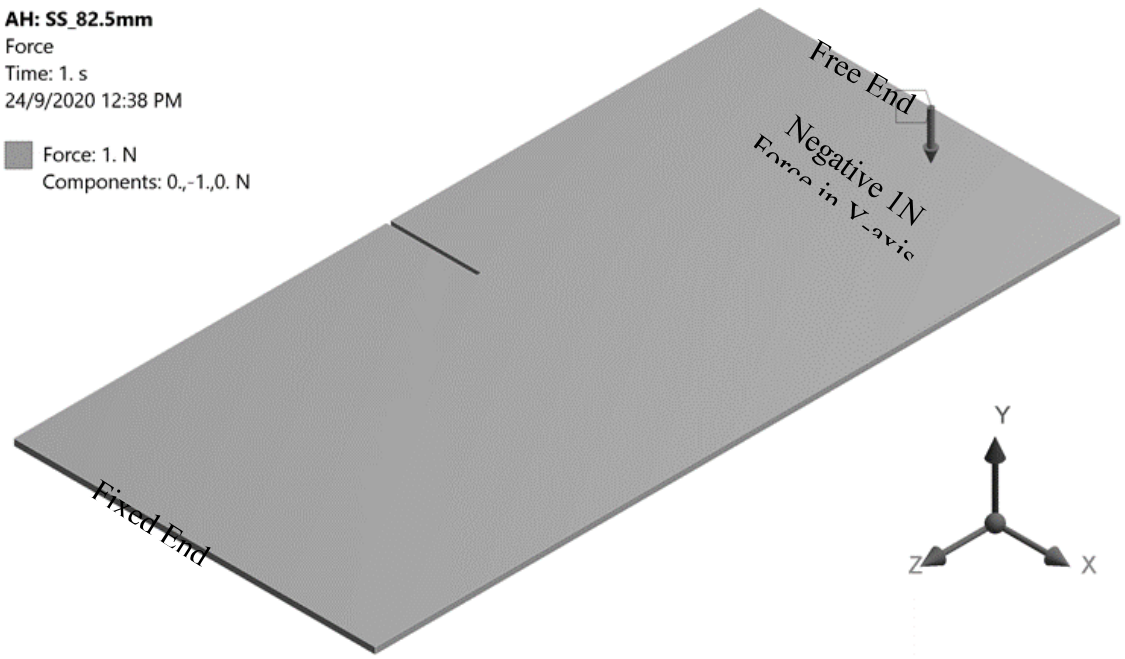

Figure 3.2: Schematic Diagram for Indicating Fixed End and Application of Load on Metal Plate

3.2.3 Boundary Condition and Meshing

For setting up a cantilever plate, we defined a fixed end. This is shown in the Figure 3.2. In a thin healthy metal plate, there are 13483 nodes and 1860 elements. For a cracked plate with crack length 20mm, number of nodes are from 13666 to 14527 and the number of elements are from 1874 to 2007. Solid186 element type is used. The advantage of this element type is that it is functional for three-dimensional nodes for higher order. It displays quadratic displacement nature for 20 nodes having three degree of freedom per node, i.e., translation in nodal x, y and z directions. The element is valid for plasticity, hyper-elasticity, creep, stress stiffening, large deflection, and large strain capabilities. It also has mixed formulation capability for simulating deformations of nearly incompressible elastoplastic materials, and fully incompressible hyper-elastic materials.

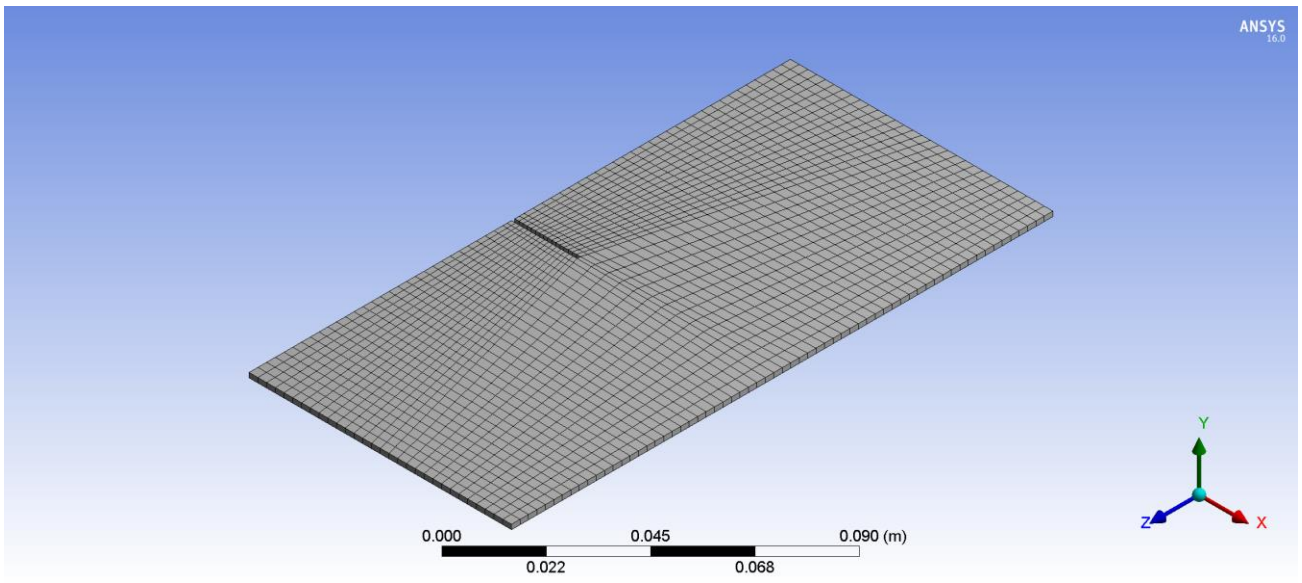

Figure 3.3: Meshing on Metal Plate

In ANSYS, the relevance center of the meshing i.e., mesh size, is set to fine mode during simulation in which the minimum edge length is 1mm. Though medium and coarse mesh size only deviate by about 1% in compared to fine mode, fine mesh size is used throughout the research for higher precision.

3.3 Convention for Measuring Plate and Beam Dimension

In most scientific papers, the dimensions of beam with crack are as shown in the Figure 3.4[12]. In this case, the nomenclature used are put in Table 3.3.

Table 3.3: Nomenclature for Beam and Crack According to Standard Convention

Nomenclature	Description
l	Length of the beam
w	Width of the beam; Thickness of the Crack
d	Depth of the beam
d_c	Depth of the crack
x_c	Location of the crack

The standard convention is to use full thickness of the crack along the width of the beam as shown in Figure 3.4 (b).

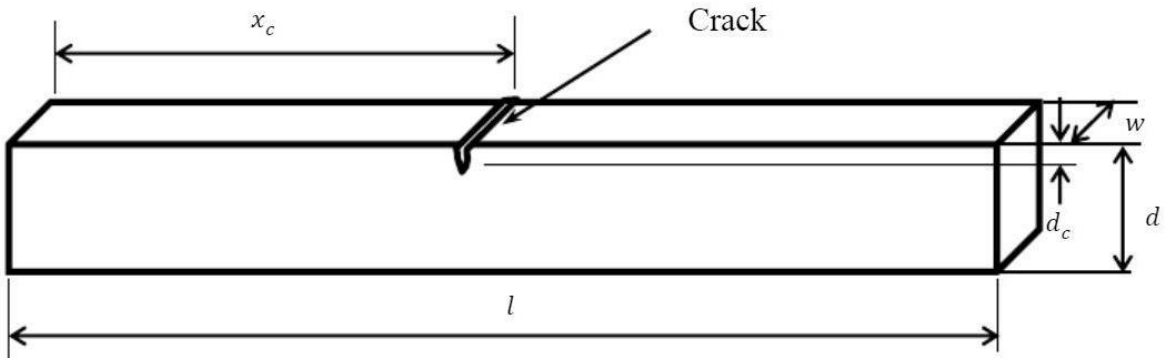

(a) ISO View

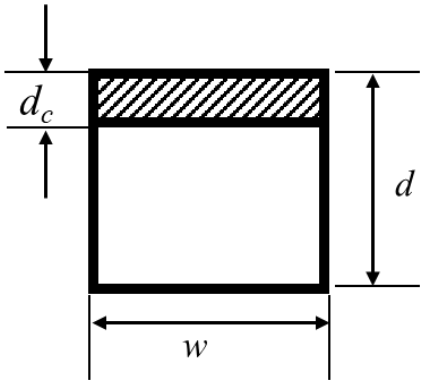

(b) RHS View

Figure 3.4: Convention for Measuring Beam and Crack Dimension

In Figure 3.5, dimensions used for this research are illustrated; where L, B and H – length, width and thickness of the plate respectively. While a, b and c are length, width and depth of crack respectively. All the nomenclatures are added in Nomenclature and Terminology section. The thickness of the beam and thickness of the crack are along the same direction as shown in 3.5 (a). Comparing both figures, it is noticed that the standard crack depth d_c (Figure 3.4) is in the direction of crack length a in this research (Figure 3.5). Furthermore, the standard crack thickness w (standard beam width) is in the direction of depth of crack c in this research.

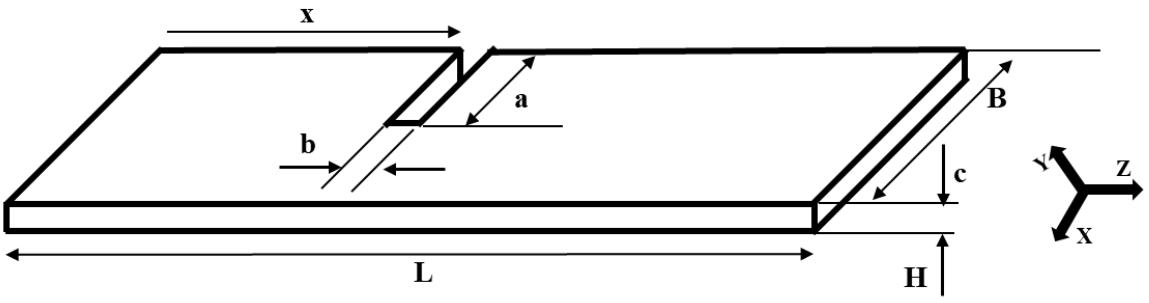

(a) ISO View

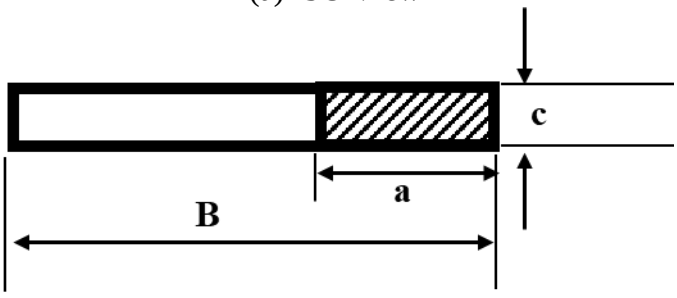

(b) RHS View

Figure 3.5: Standard Used in this Research for Thin Plate

3.4 Problem Specification

In this study, normalized frequency is used over relative distance of crack along longitudinal and transverse direction of the plate. A comparison is made keeping the natural frequency of the healthy plate as a base. Set of simulations are conducted with different crack length, crack width and crack depth along the edge of the plate. Moreover, the study also include similar study on metal and metal alloys to note any difference. The orientation of the crack is also changed from transverse to longitudinal along the edge and mid-axis.

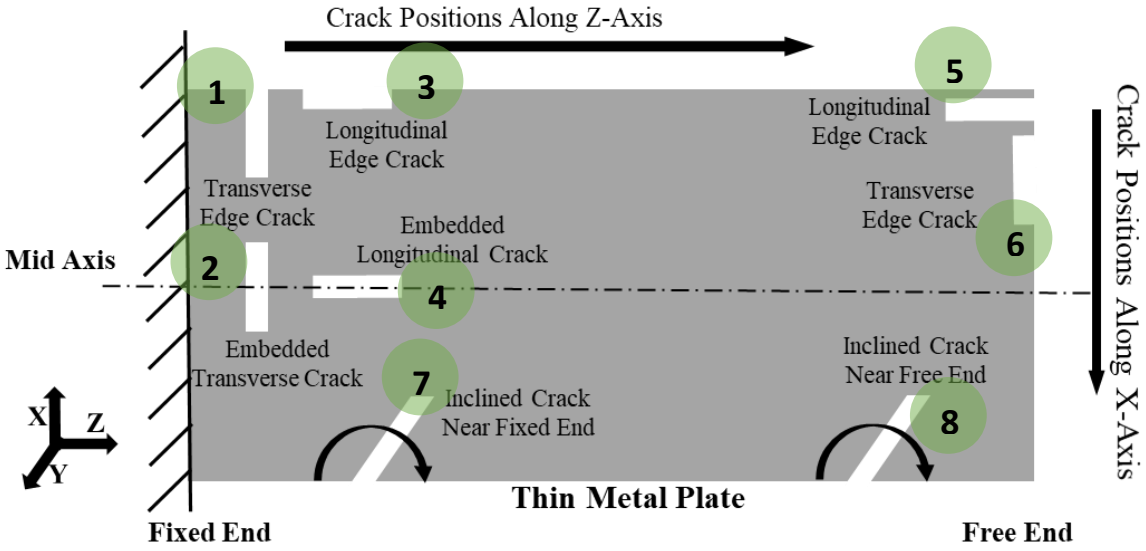

Figure 3.6: Illustration of All the Cases

Table 3.4: Brief Case Descriptions of all the Cases

Case Number	Case Description	Legends on Fig 3.6
Case-1	Change of Transverse Edge Crack Positions along Z-axis (Longitudinal Direction)	1
Case-2	Change of Transverse Crack Lengths on the Edge along Z-axis (Longitudinal Direction)	1
Case-3	Change of Transverse Crack Widths on the Edge along Z-axis (Longitudinal Direction)	1
Case-4	Study of Effect on Normalized Frequency due to Change of Crack Depths along Y-axis (along Depth Direction)	1

Case-5	Change of Transverse Edge Crack Positions along Z-axis (Longitudinal Direction) with Structural Steel	1
Case-6	Change of Embedded Transverse Crack Positions along Mid Z-axis	2
Case-7	Change of Longitudinal Edge Crack (Surface Defect) Positions along Z-axis (Longitudinal Direction)	3
Case-8	Change of Embedded Longitudinal Crack Positions along Mid Z-axis	4
Case-9	Change of Longitudinal Edge Crack Positions along X-axis (Transverse Direction)	5
Case-10	Change of Transverse Edge Crack (Surface Defect) Positions along X-axis (Transverse Direction)	6
Case-11	Inclined Crack Positions at Relative Distance of 21% on Z-axis	7
Case-12	Inclined Crack Positions at Relative Distance of 79% on Z-axis	8

The inclined cracks at different angles are placed at two distinct positions. The first scenario is for inclined cracks at the free end and the other one is at the fixed end, to check for any outcome. Finally, a static structure analysis is conducted to visualize the stress concentration and total deformation when a little load is applied at free end.

Chapter 4

Results of Numerical Simulation and Discussion

4.1 Validation of the Scientific Work

In this section, results of the validation with a scientific paper is overviewed. The title of the paper is “Investigation on Non-Linear Vibration Response of Thin Plates with Crack Using Electronic Speckle Pattern Interferometry” [3] published in the “The International Conference on Experimental Mechanics 2018 (ICEM18), Brussels, Belgium”. The author of the paper is Nan Tao, Yinhang Ma, Hanyang Jiang, Meiling Dai and Fujun Yang. The dimension of the plate is 165mm x 80mm x 1.43mm. Taking aluminum alloy as the material of the simulation, the properties of it depicted on Table 4.1. Specimen 1 is the healthy plate, while from specification 2 to specification 5; the crack length is 20mm, 40mm, 60mm and 70mm respectively. Figure 4.1 shows all the specimens mentioned below. In all the cases, the crack is placed at the fixed end of the cantilever plate.

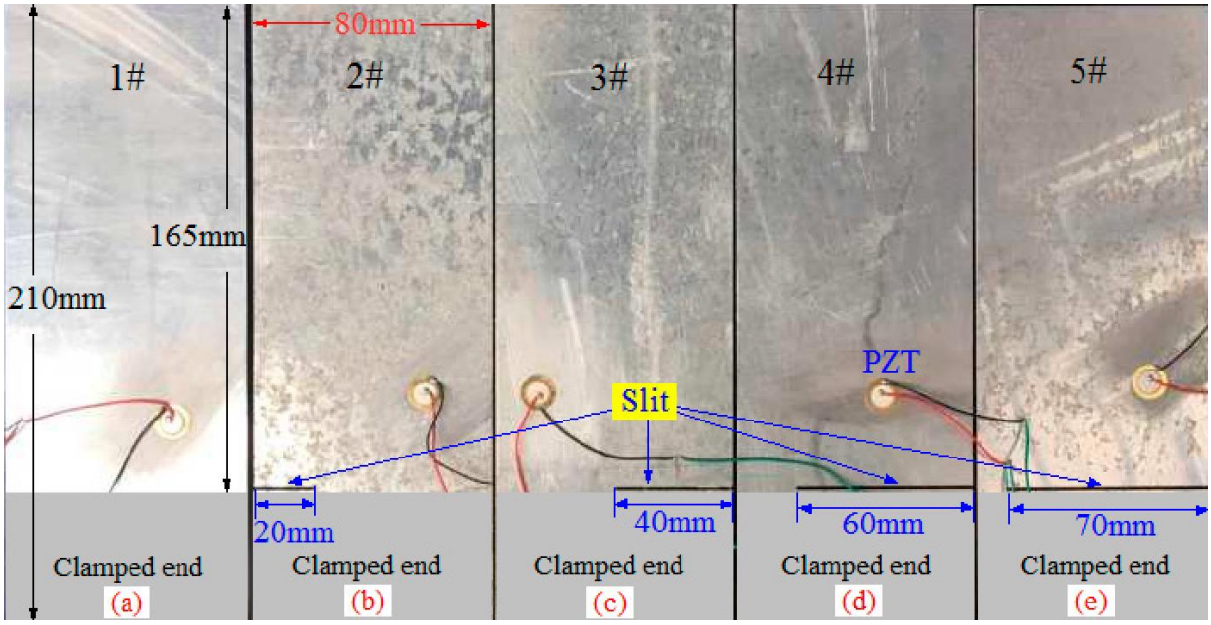

Figure 4.1: Illustration of Specimen from Scientific Paper [3]
(a) Specimen 1# Plate with No Crack (b) Specimen 2# Plate with Crack Size 20mm (c) Specimen 3# Plate with Crack Size 40mm (d) Specimen 4# Plate with Crack Size 60mm (e) Specimen 5# Plate with Crack Size 70mm

From Table 4.1 and Table 4.2, we can conclude that the natural frequency found in the scientific paper and the result obtained in our simulation is very close. The average percentage error is from 0.80 to 0.86, which is less than 1%. This means our simulation work validates with the scientific work in the paper. Moreover, the mode shapes of our results are similar with the paper shown in Figure 4.2 and Figure 4.3.

Table 4.1: Validation Result of Specimen-2 & Specimen-3

	Natural Frequency								
	Specimen-1 (No Crack)			**Specimen-2 (Crack Size 20mm)**			**Specimen-3 (Crack Size 40mm)**		
Mode	***Result from Paper[3]***	***Obtained from ANSYS***	***% Error***	***Result from Paper[3]***	***Obtained from ANSYS***	***% Error***	***Result from Paper[3]***	***Obtained from ANSYS***	***% Error***
1	44.176	44.596	0.95	42.698	43.084	0.90	38.359	38.722	0.95
2	191.79	193.36	0.82	182.52	184	0.81	159.33	160.74	0.88
3	274.96	277.56	0.95	266.34	268.7	0.89	249.52	251.73	0.89
4	623.69	628.87	0.83	589.87	594.74	0.83	489.99	494.3	0.88

5	771.77	778.97	0.93	748.34	754.91	0.88	703.39	709.34	0.85
6	1195	1205.2	0.85	1113.4	1122.8	0.84	898.68	905.84	0.80
7	1265.2	1274.3	0.72	1258.1	1267.3	0.73	1251	1260.4	0.75
8	1527	1541.5	0.95	1480.1	1492.7	0.85	1314.5	1324.3	0.75
9	1690.4	1703.3	0.76	1614.9	1627.5	0.78	1529.8	1541.6	0.77
10	1968.4	1985.5	0.87	1844.5	1859.9	0.83	1717.2	1730.2	0.76
11	2352	2370.6	0.79	2233.1	2251.2	0.81	2051.7	2067	0.75
12	2546.2	2569	0.90	2413.5	2432.8	0.80	2294.3	2312.1	0.78
% Error			**0.86**			**0.83**			**0.82**

Table 4.2: Validation Result of Specimen-4 & Specimen-5

	Natural Frequency					
	Specimen-4 (Crack Size 60mm)			**Specimen-5 (Crack Size 70mm)**		
Mode	***Result from Paper[3]***	***Obtained from ANSYS***	***% Error***	***Result from Paper[3]***	***Obtained from ANSYS***	***% Error***
1	31.802	31.397	1.27	25.662	25.95	1.12
2	122.07	123.26	0.97	98.036	99.082	1.07
3	229.2	231.2	0.87	216.11	218.01	0.88
4	385.16	388.28	0.81	350.88	353.62	0.78
5	659.81	665.18	0.81	632.32	637.55	0.83
6	815.589	821.62	0.74	797.7	803.53	0.73
7	1218.6	1228.2	0.79	1142.4	1151.7	0.81

8	1258.9	1268	0.72	1251.4	1260.6	0.74
9	1474	1485	0.75	1424.4	1434.7	0.72
10	1631.6	1644.1	0.77	1579.5	1591.3	0.75
11	1926.1	1940.9	0.77	1822.3	1835.9	0.75
12	2099.3	2114.8	0.74	2069.9	2084.8	0.72
13	2554.2	2573.4	0.75	2521.1	2540.2	0.76
14	2662.1	2680.8	0.70	2571.9	2589.3	0.68
15	3026.7	3049	0.74	3010.2	3032.2	0.73
Average % Error			**0.81**			**0.80**

Number of Modes

1 2 3 4 5 6 7 8 9 10 11 12

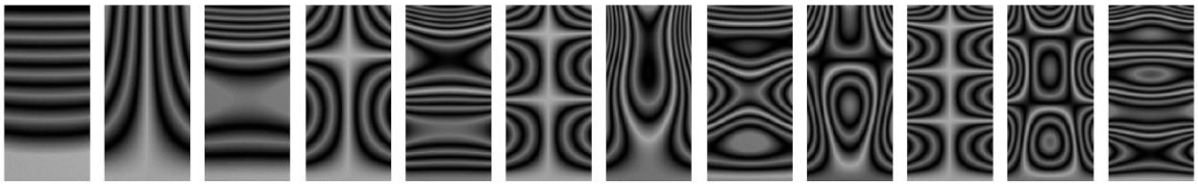

(a) FEM from Scientific Paper[3]

Number of Modes

1 2 3 4 5 6 7 8 9 10 11 12

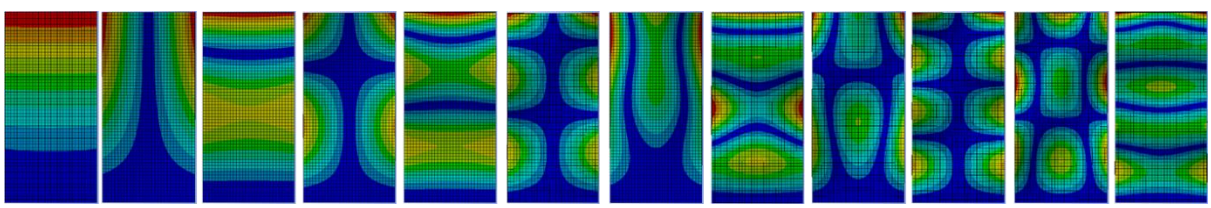

(b) Results obtained from ANSYS 16.0

Figure 4.2: Comparison of Mode Shape for Specimen-1

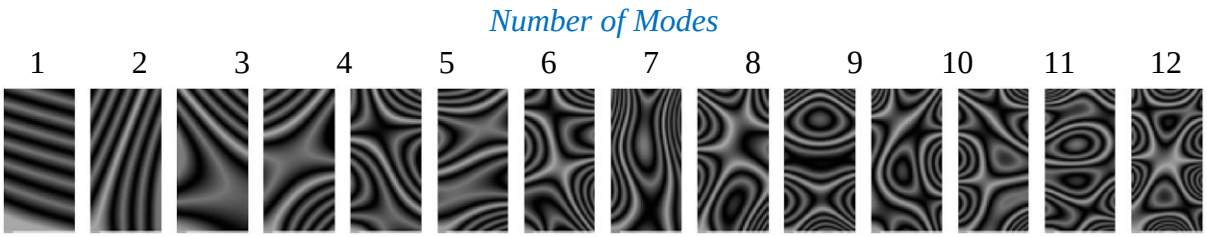

(a) FEM from Scientific Paper[3]

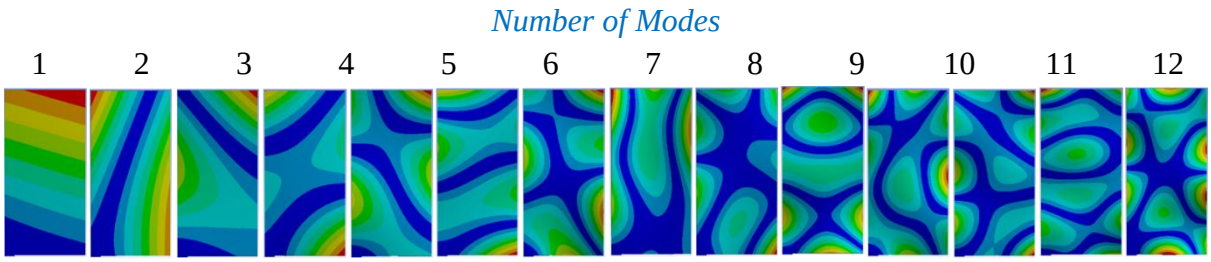

(b) Results obtained from ANSYS 16.0

Figure 4.3: Comparison of Mode Shape for Specimen-5

4.2 Theoretical Calculation for Bending Vibration Beam Element Theory

Three are two types of modes shapes, namely bending modes and torsional. In bending mode, the motion of the plate is observed in the linear direction along the axis of motion. In torsional vibration, motion of the plate is observed at angular motion along the axis of rotation. First, third and fifth mode shapes are the bending modes. While, second, fourth and sixth mode shapes are torsional modes.

In this section, the natural frequencies for this first three bending mode are calculated theoretically. Here, the Euler-Bernoulli beam model is used where the cross-section is perpendicular to the bending line. Shear deformation is not taken into consideration. The beam element has two nodal points and two degrees of freedom in each node: the translation and

rotation along the x-direction. There are four equations of motion. Therefore, the mass and stiffness matrix are 4x4 matrix which is given below.

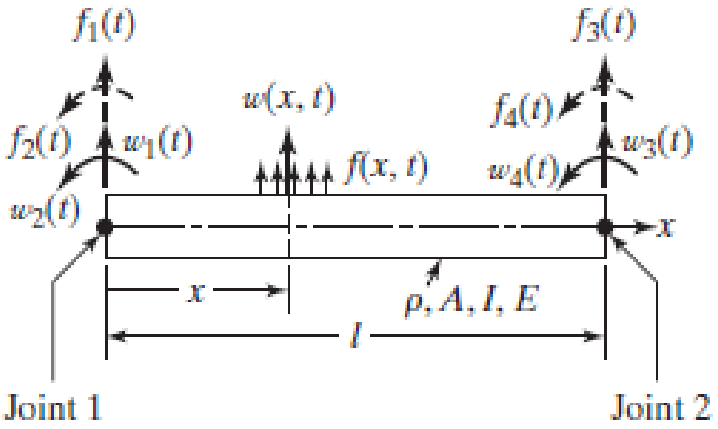

Figure 4.4: Uniform Beam Element [9]

The mass matrix is

$$[m] = \frac{\rho Al}{420}[156\ 22l\ 54\ -13l\ 22l\ 4l^2\ 13l\ 3l^2\ 54\ 13l\ 156\ -22l\ -13l\ -3l^2\ -22l\ 4l^2\ ]$$

The stiffness matrix is

$$[k] = \frac{EI}{l^3}[12\ 6l\ -12\ 6l\ 6l\ 4l^2\ -6l\ 2l^2\ -12\ 6l\ 12\ -6l\ 6l\ 2l^2\ -6l\ 4l^2\ ]$$

Then Finite element method was applied in this beam to get a more accurate result. So, the total beam is divided into 20 elements. Then common nodal points between two elements are taken as one nodal point. Finally, 42x42 mass and stiffness matrix is formed. For the boundary

condition of a cantilever beam, the deflection and slope are zero so the matrix reduced to 40x40 matrix. For free vibration the equation of motion is

$$\{[k] - \omega^2[m]\}x = 0$$

Where ω is the angular velocity and by divided it with 2π, the natural frequencies are found.

The first three bending frequencies are 42.24 Hz, 269.39 Hz and 759.75 Hz, which matched with the natural frequencies found from ANSYS simulation: 44.6 Hz, 277.56 Hz and 778.59 Hz in good agreement.

4.3 Case-1: Change of Transverse Edge Crack Positions along Z-axis

In this study, we use aluminum alloy as the material. Material properties like, density, Young's modulus, Poisson's ratio, along with plate and crack properties are mentioned in the Table 4.1. In this case, the transverse edge crack positions are moved from fixed to free end i.e. along Z-axis or in longitudinal direction. The crack positions are changed at 5mm intervals. The dimension of the crack is 20mm x 1mm x 1.43mm. Schematic diagram of the movement of crack is illustrated in Figure 4.5.

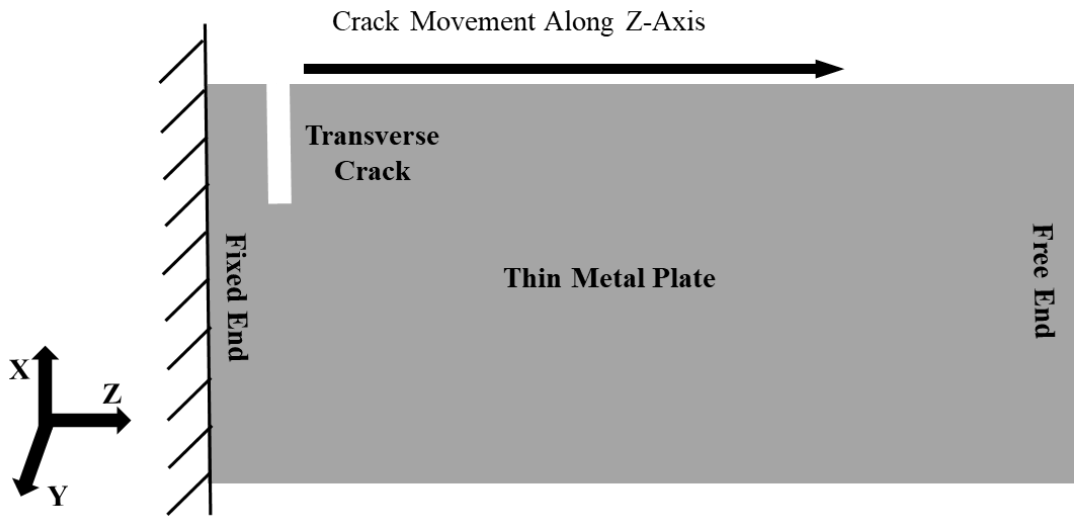

Figure 4.5: Schematic Diagram for the Change in Transverse Crack Positions along Z-axis

Two types of modes shapes found from ANSYS simulation, namely bending modes and torsional modes shown in Figure 4.6. In bending mode, the motion of the plate is observed in the linear direction along the axis of motion. In torsional vibration, motion of the plate is observed at angular motion along the axis of rotation. First, third and fifth mode shapes are the bending modes. While, second, fourth and sixth mode shapes are torsional modes. For first bending mode, there is one nodal point or (or bends). For second and third bending modes, two and three nodal points exist respectively. Similarly, for torsional modes there one, two and three nodal points (or twists) for first, second and third torsional modes respectively.

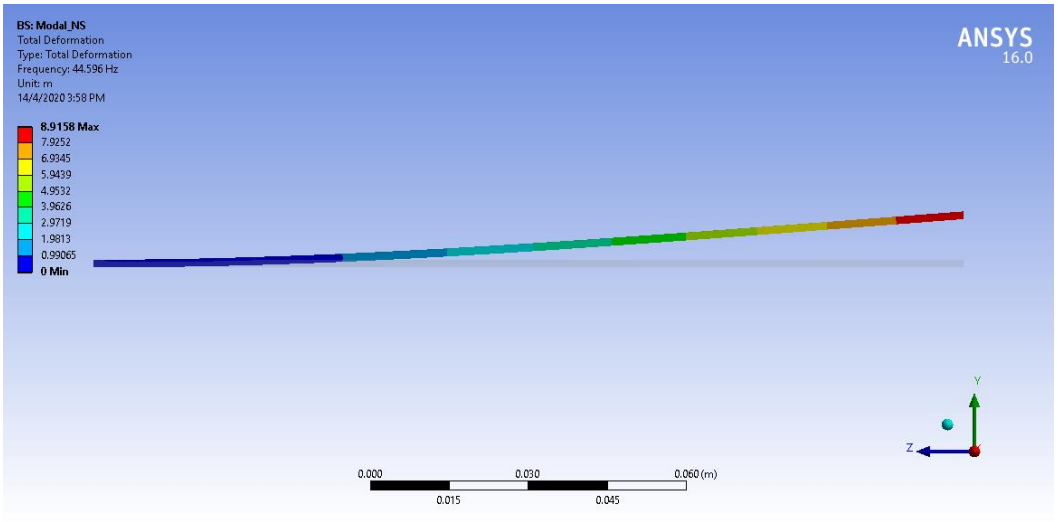

(a) First Mode (First Bending Mode)

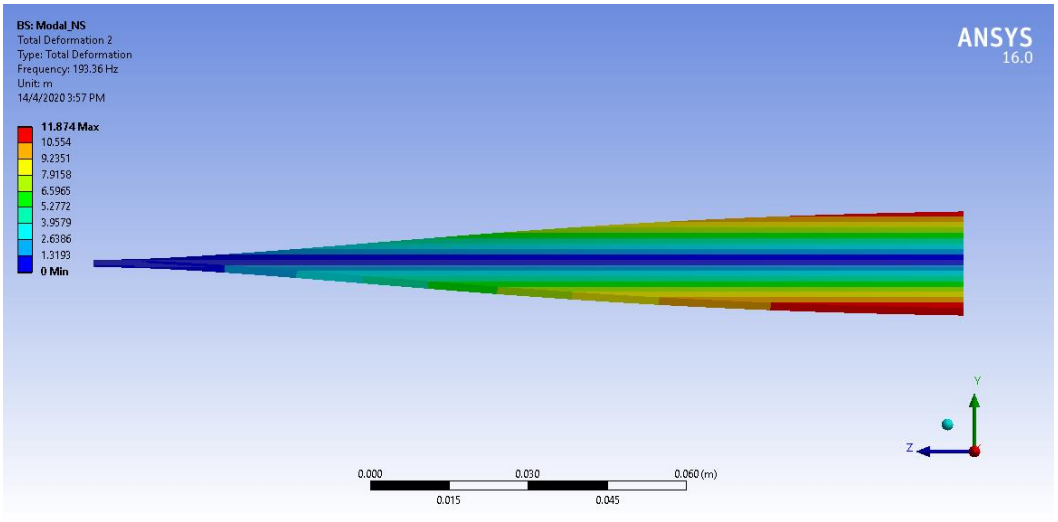

(b) Second Mode (First Torsional Mode)

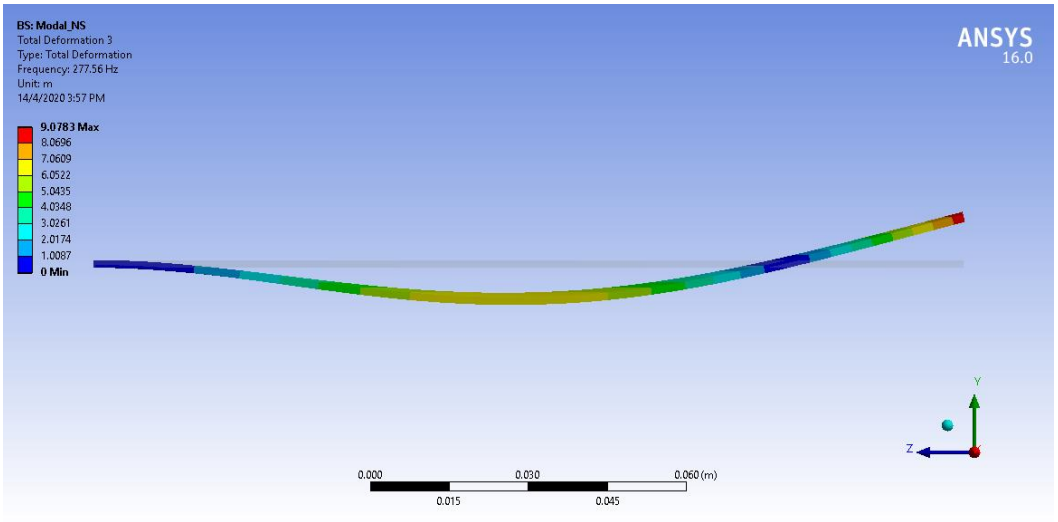

(c) Third Mode (Second Bending Mode)

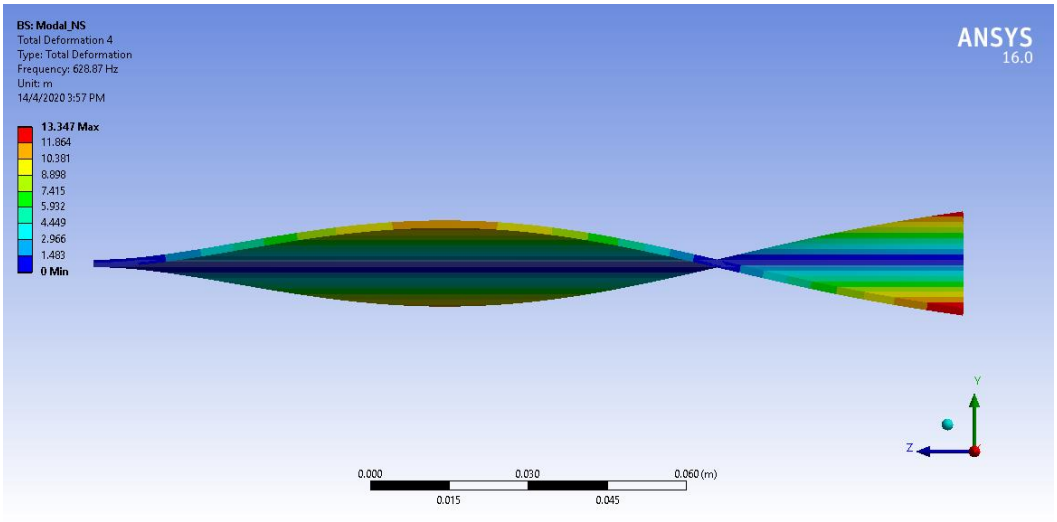

(d) Fourth Mode (Second Torsional Mode)

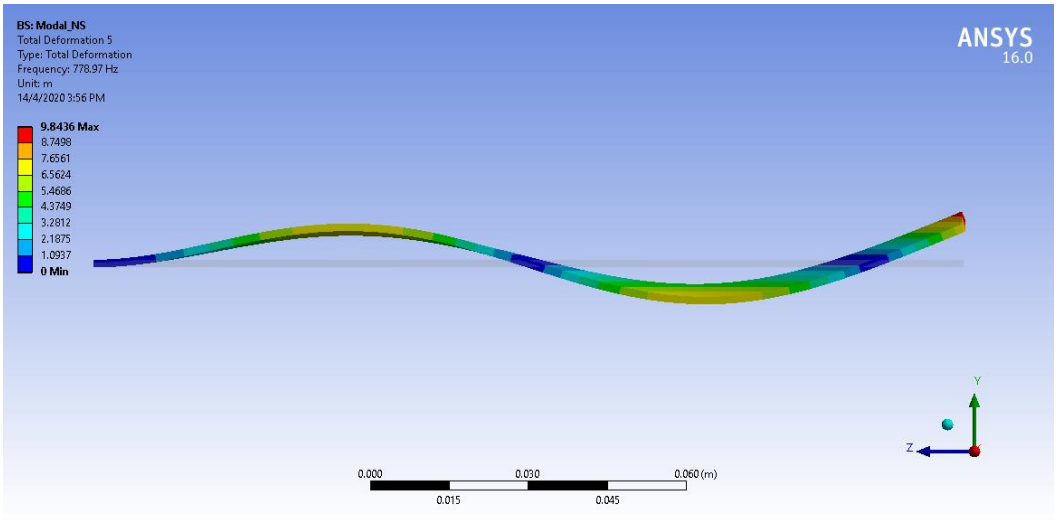

(e) Fifth Mode (Third Bending Mode)

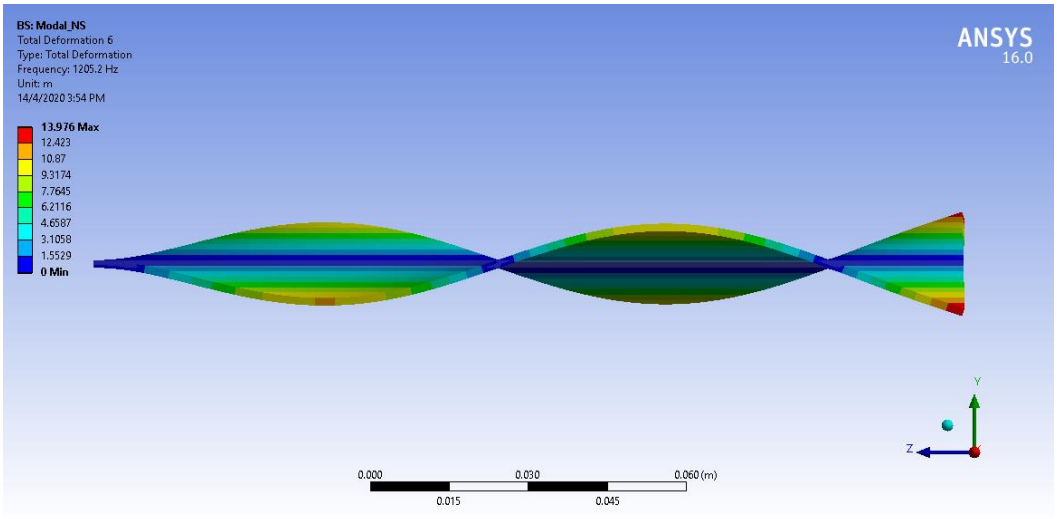

(f) Sixth Mode (Third Torsional Mode)

Figure 4.6: Mode Shape Deformation of a Healthy Metal Plate

The Figure 4.7 compares the first six natural frequencies of a healthy plate with plates having crack at various positions along the edge. It is found that for all the six modes there are significant frequency drop at relative distance from 0 to 12% (near fixed end) of the plate. For torsional mode, the most significant frequency drop is 7.4% at relative distance 84.8% on 6th mode. For bending modes, the most significant frequency drop is 5.88% at relative distance 9.1% on 1st mode. The study also shows that the torsional modes give significantly larger drop (overall 3.3 to 5%) in frequencies than bending modes (overall 2 to 2.9%).

For bending modes (first, third and fifth modes), it is observed that the maximum drop in frequency compared to the healthy plate shifted along the relative distance. For first bending mode, at 9.1% relative distance, the frequency drop is 5.9%. For second bending mode, 4.4% frequency drop is found at relative distance 54.5%. For third bending mode the frequency drop is 5.0% at relative distance 69.7%. Similar pattern is observed in torsional modes as well. For all the six modes at certain relative distance at the free end region, the natural frequency of the cracked plate demonstrates higher natural frequency than healthy plate. In this research, the relative distance of crack where these two curves crosses is called “Intersection Point”. For a 20mm crack, it occurs at relative distance of 78.8% in first mode, at 93.9% in second and third modes and at 99.4% for rest of the modes.

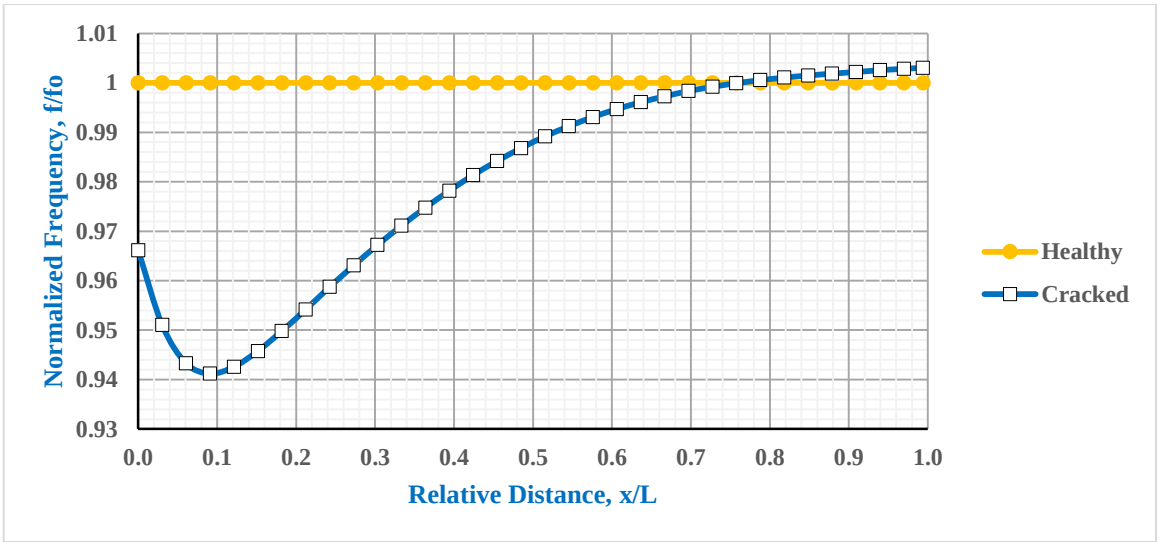

(a) First Mode

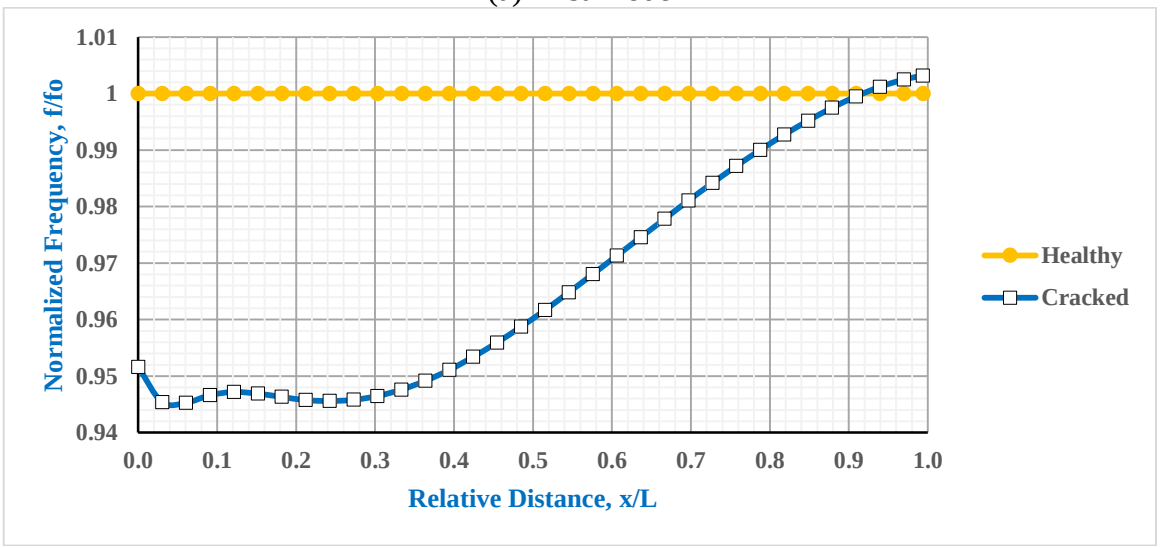

(b) Second Mode

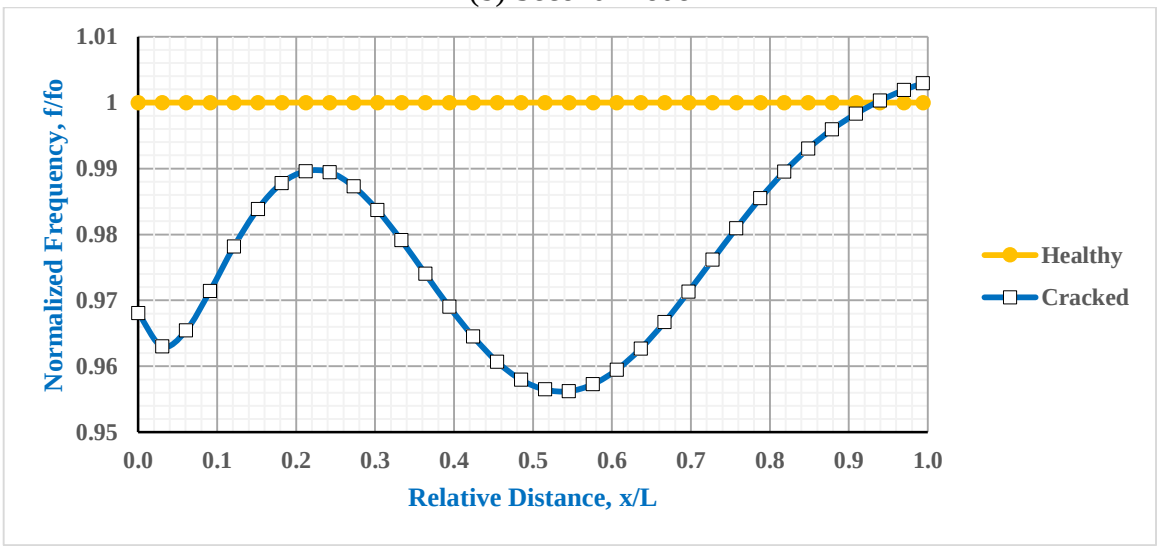

(c) Third Mode

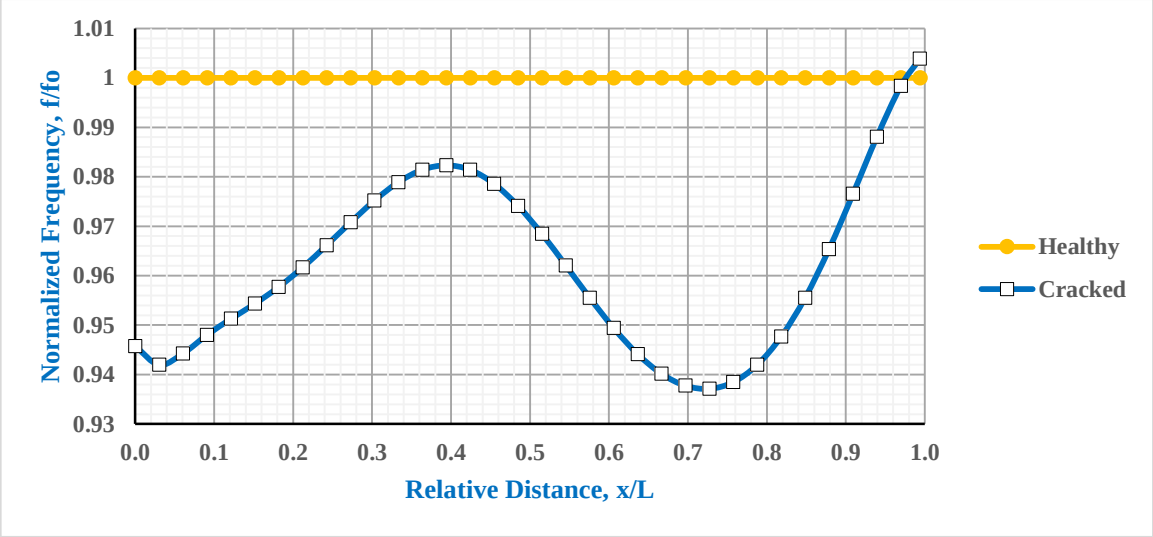

(d) Fourth Mode

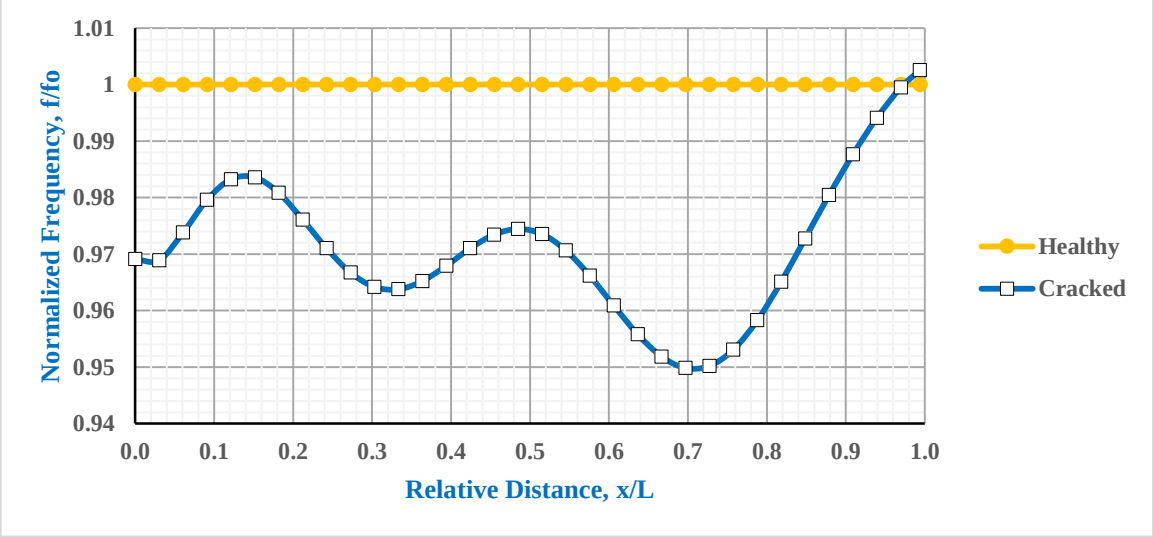

(e) Fifth Mode

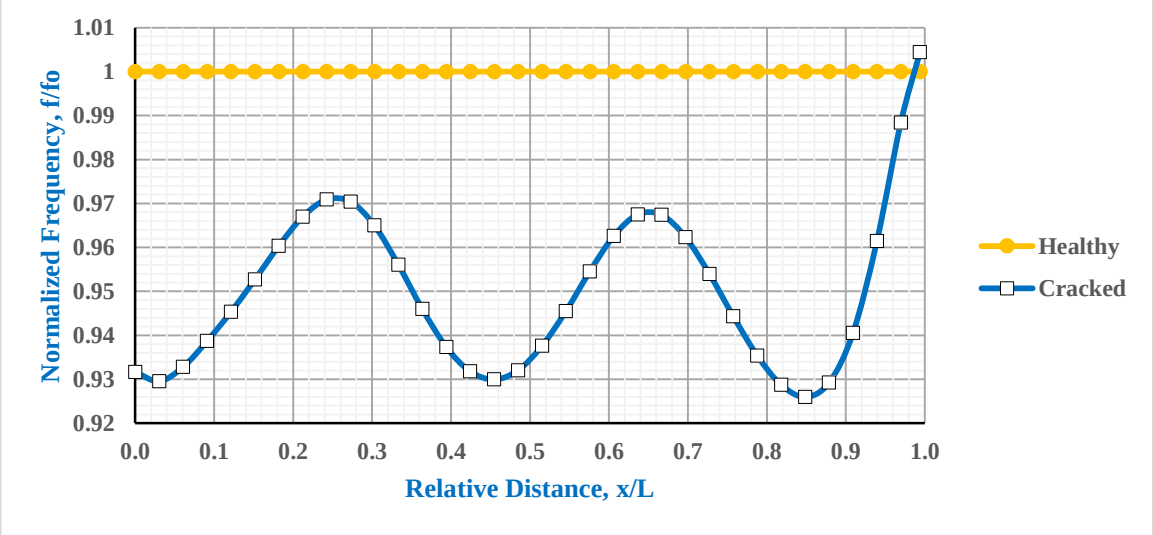

(f) Sixth Mode

Figure 4.7: Normalized Frequency over Relative Distance along Z-axis

4.4 Case-2: Change of Transverse Crack Lengths on the Edge along Z-axis

This is a similar study done in case-1 for three different transverse crack lengths of 10mm, 20mm (case-1) and 30mm with aluminum alloy. The other properties of the material and plate dimensions are same as depicted in Table 3.1. The movement of crack is at 5mm intervals along the edge of the Z-axis. Figure 4.8 illustrates the schematic diagram of the movement of crack of different lengths along longitudinal direction.

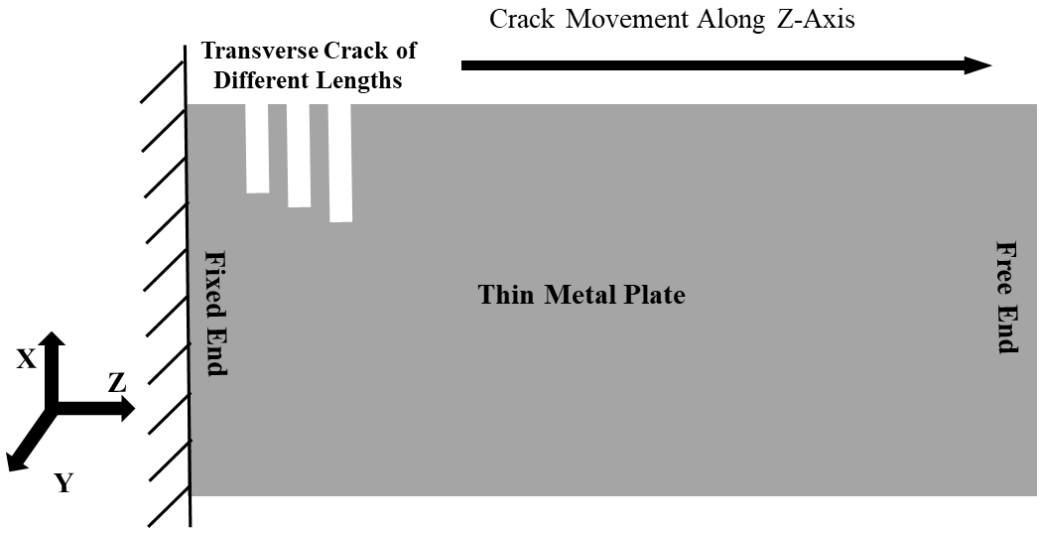

Figure 4.8: Schematic Diagram for the Change of Transverse Crack Length on the Edge along Z-axis

Figure 4.9 shows the results of this case scenario. Similar trend and pattern are observed in all the six normalized frequency curves with different variations of frequency drop. It is found that the larger the crack length the higher is the frequency drop. For bending modes, the maximum significant frequency for the crack length of 10mm, 20mm and 30mm are 1.8%, 5.9% and 11.4% respectively at relative distance 9.1% on the first mode. For torsional modes, the maximum significant frequency for the above mentioned crack lengths are 1.4%, 7.4% and 20% for relative distance of 81.8%, 84.8% and 90.9% respectively on the 6th mode. It is also observed that for small cracks ($a \leq 10$mm), fixed end region has more drop in frequencies than mid-region and free end regions.

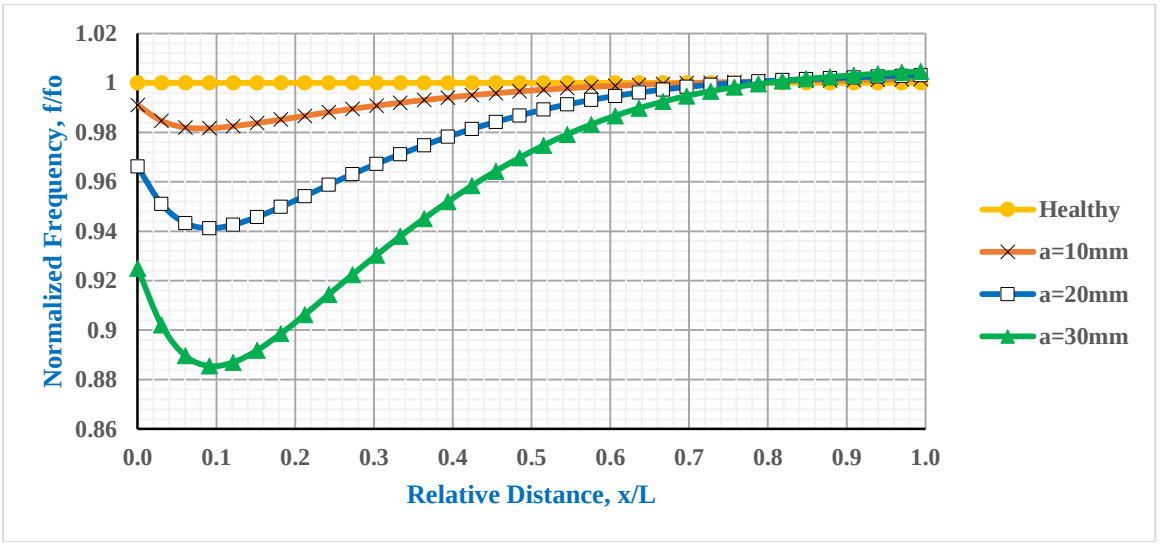

(a) First Mode

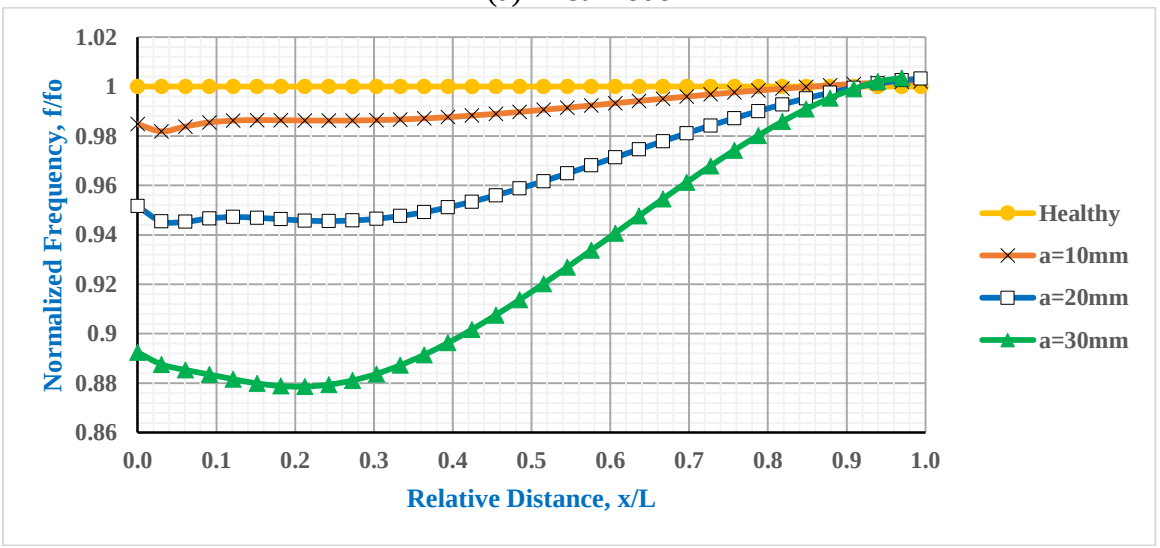

(b) Second Mode

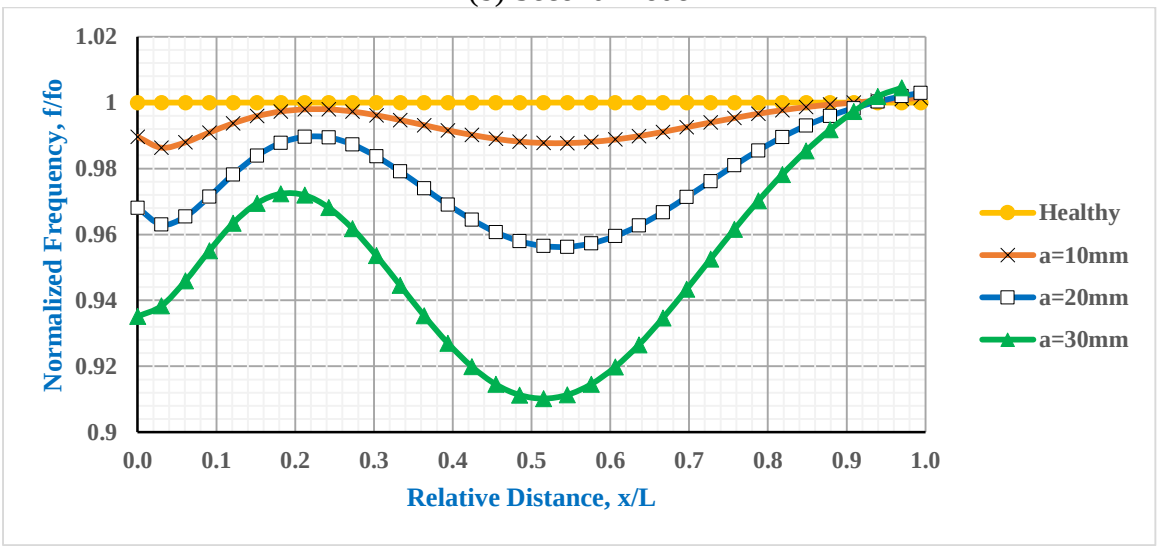

(c) Third Mode

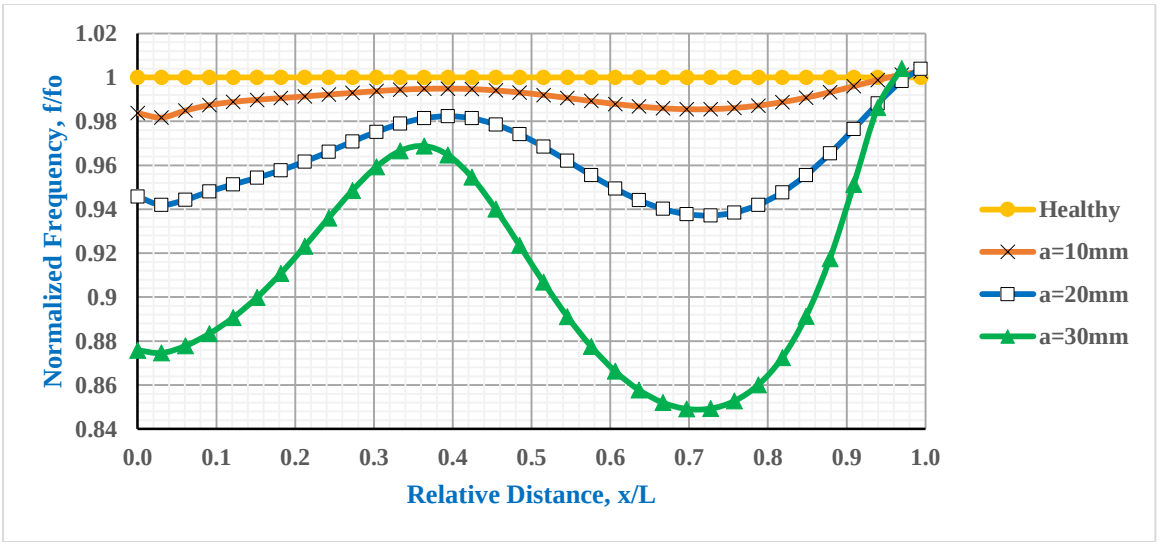

(d) Fourth Mode

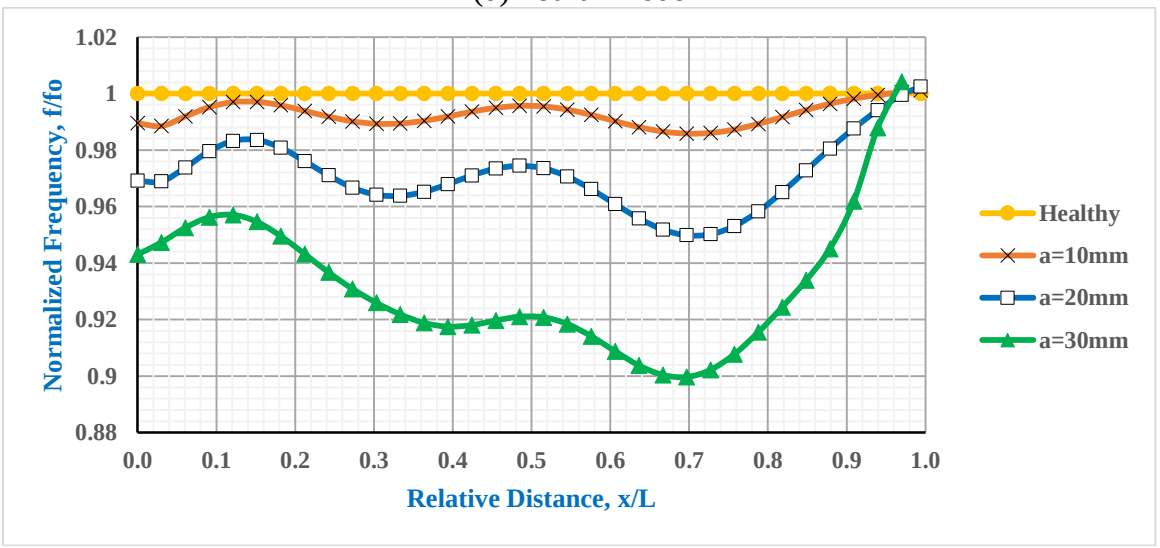

(e) Fifth Mode

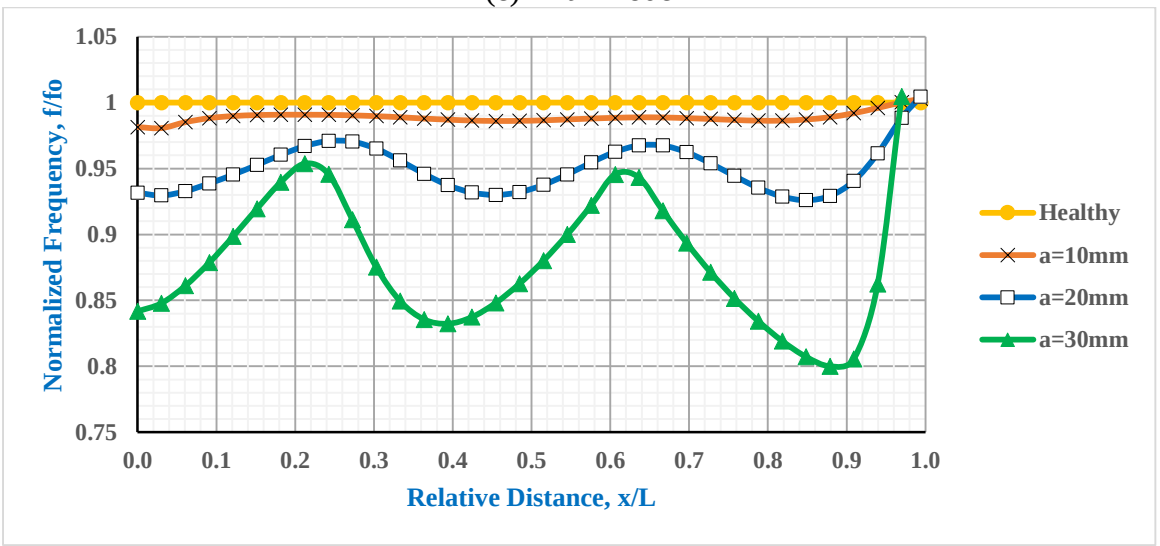

(f) Sixth Mode

Figure 4.9: Normalized Frequency over Relative Distance along Z-axis for Transverse Crack Length of 10mm, 20mm and 30mm

The Table 4.3 below shows the intersection point on the normalized frequency curve of the first mode. As the crack length increases, the intersection point moves towards the free end. To determine the exact relative distance of the intersection point we deduced regression equation of sixth polynomial for the curve of the first mode and found the solution as 70.07%, 74.6% and 77.40% for 10mm, 20mm and 30mm respectively. These points in this case also seems to move towards free end with increases crack length.

The regression equations for crack length 10mm, 20mm and 30mm are respectively:

For a=10mm: $p = 1.6849n^6 - 5.7195n^5 + 7.6358n^4 - 5.0438n^3 + 1.6602n^2 - 0.2057n + 0.9902$

For a=20mm: $p = 3.7773n^6 - 13.067n^5 + 17.926n^4 - 12.312n^3 + 4.2663n^2 - 0.5517n + 0.9649$

For a= 30mm: $p = 5.1548n^6 - 18.087n^5 + 25.393n^4 - 18.077n^3 + 6.5767n^2 - 0.8774n + 0.9238$

Here, $p = f/f_o$ (normalized frequency), and $n=x/L$ (relative distance)

Table 4.3: Key Findings of Case-2 for Different Crack Lengths

Region on Cantilever Plate	**% of Max Frequency Drop on Sixth Mode**		
	a=10mm	**a=20mm**	**a=30mm**
Fixed End (x/L: 0-15%)	1.8%	7.0%	16.1%
Mid-Region (x/L: 42-55%)	1.4%	7.0%	16.8%
Free End (x/L: 85-99%)	1.3%	7.4%	20%

Methods	**Relative Distance of Intersection Pint on First Mode**		
	a=10mm	**a=20mm**	**a=30mm**
Normalized Frequency Curve	72.7% (x=120mm)	78.8% (x=130mm)	81.8% (x=135mm)
Regression Equation	70.07% (x=115.61mm)	74.60% (x=123.09mm)	77.40% (x=127.71mm)

4.4.1 Further Study on Different Crack Lengths

The study is conducted to find the relationship between normalized frequencies over various crack length to plate length ratio (a/L). In this case, seven samples are taken, shown in Table 4.4, for three different crack locations: 15mm (near fixed end), 82.5mm (mid-region) and 140mm (near free end), keeping crack width and crack depth constant.

Table 4.4: Seven Samples of Crack Dimension with Various Crack Lengths

Sample	Crack Length a/mm	Crack Width b/mm	Crack Depth c/mm	a/L
1	70	1	1.43	0.4242
2	60	1	1.43	0.3636
3	40	1	1.43	0.2424
4	20	1	1.43	0.1212
5	15	1	1.43	0.0909
6	10	1	1.43	0.0606
7	5	1	1.43	0.0303

Figure 4.10 illustrates the frequency drop of six modes for changing crack length. It is found that for all six modes in three distinct regions (fixed end, mid-region and free end) there is increase in frequency drop with increase in crack length and all these modes are below the frequency line of the healthy plate. The first two modes show a good pattern where the fixed region have more drop in frequency than free end. The fifth and sixth mode have more drop at free end than fixed end. In third and fourth mode, the drop in these regions overlap with each other and cannot be predicted at mid-region.

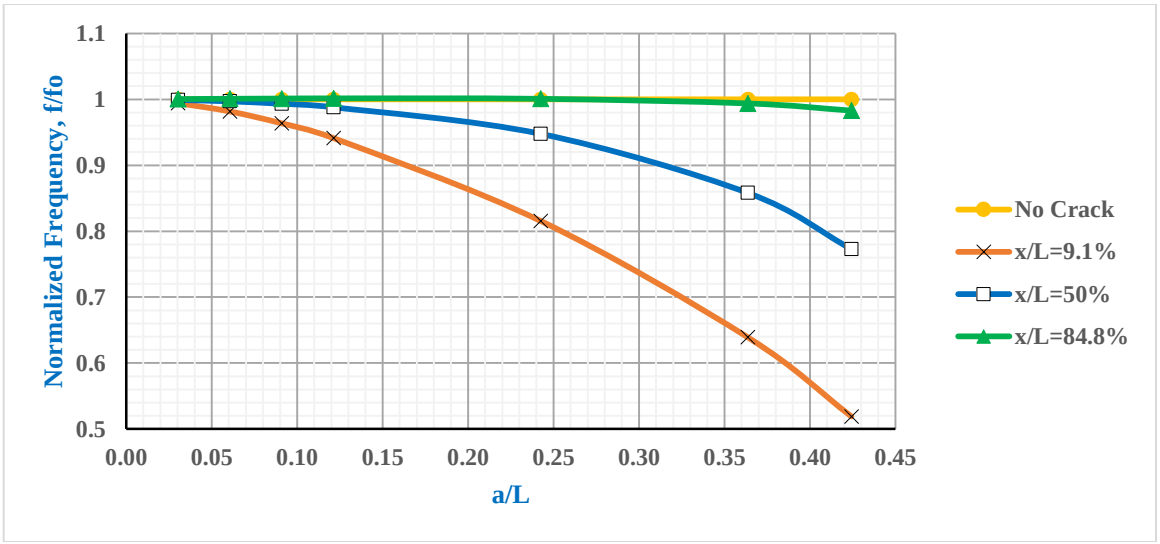

(a) First Mode

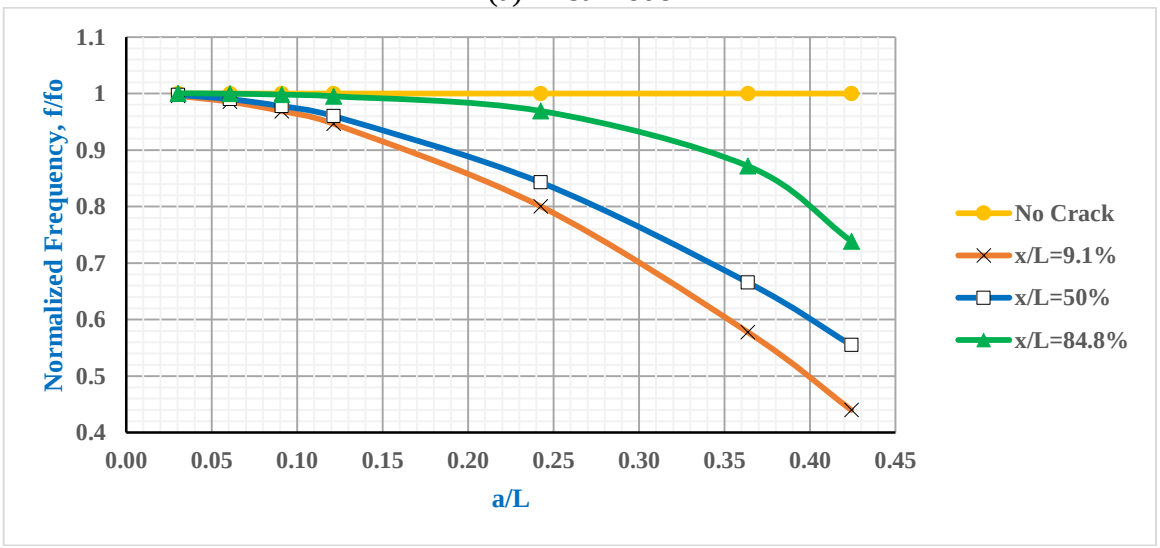

(b) Second Mode

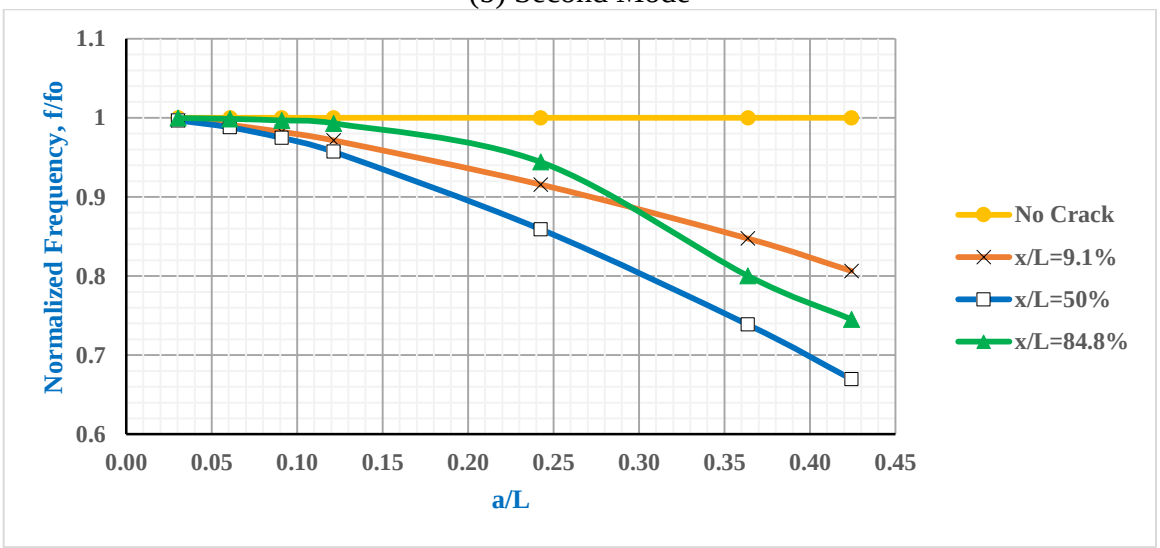

(c) Third Mode

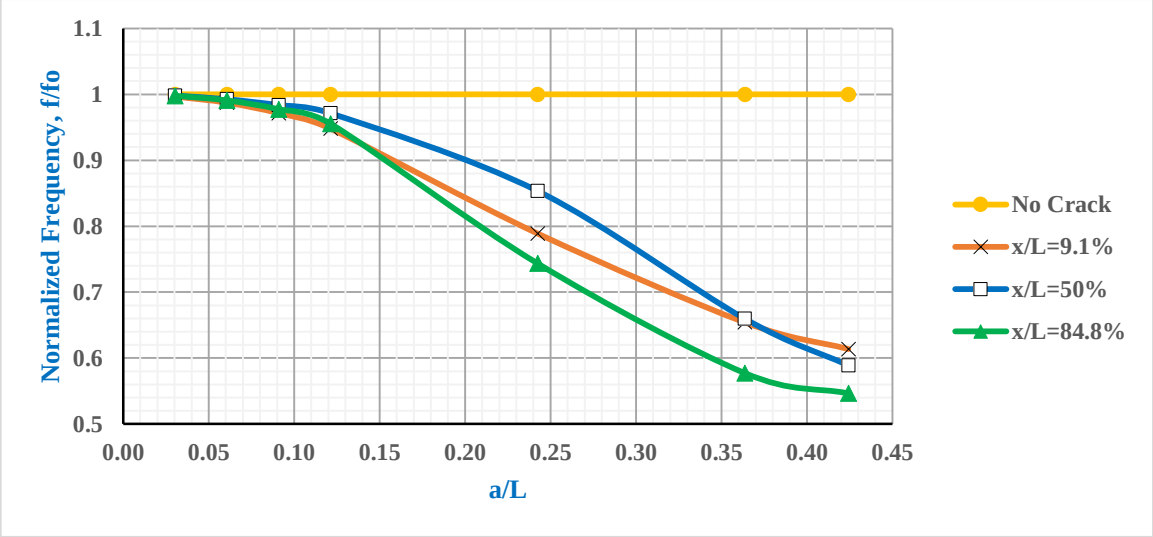

(d) Fourth Mode

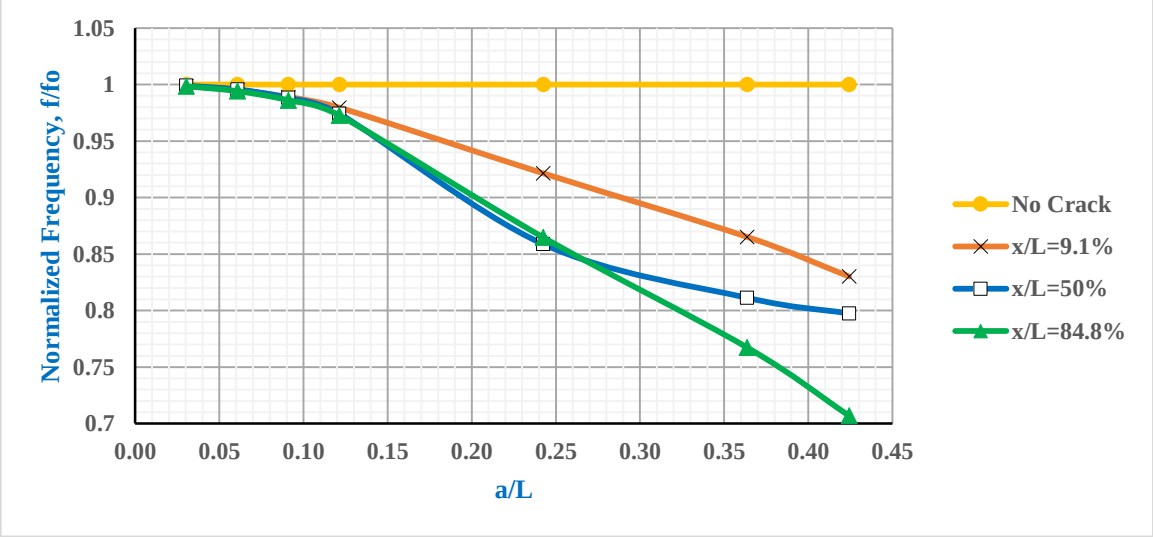

(e) Fifth Mode

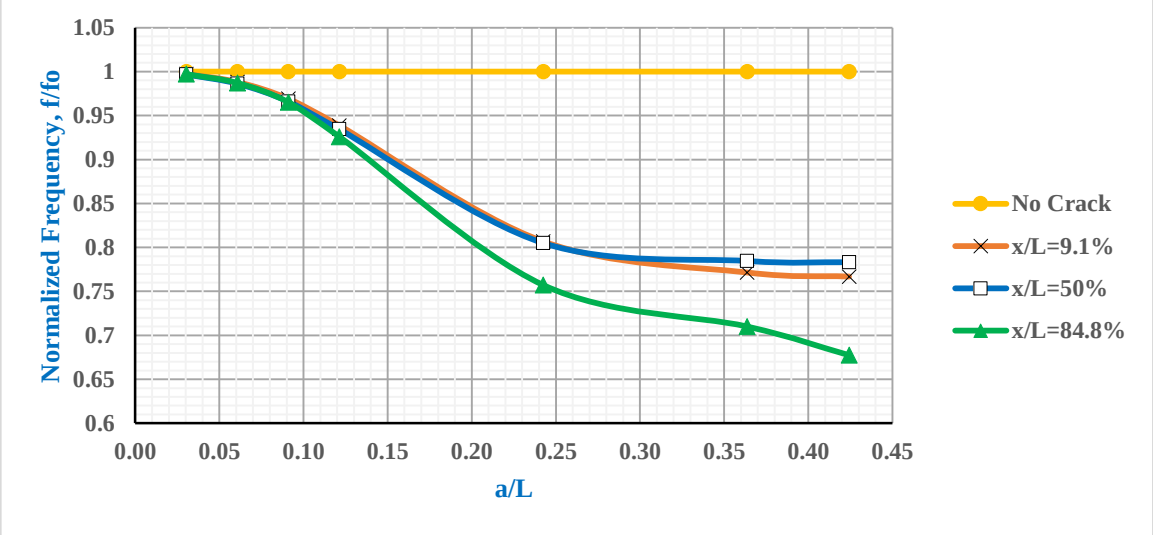

(f) Sixth Mode

Figure 4.10: Normalized Frequency Curve over Different Crack Length to Plate Length Ratio

Table 4.5 shows the maximum significant difference in frequency drop for cracks in three regions. Fixed end region have more frequency drop than free end for a particular crack dimension.

Table 4.5: Frequency Drop for Cracks at Three Distinct Regions for Different Crack Length

Region on Cantilever Plate	**Significant Difference in Frequency Drop (%) (In Sample 1)**			
	Mode 1	**Mode 2**	**Mode 5**	**Mode 6**
Fixed End (x/L=9.1%)	48.1%	56%	17%	23.3%
Mid-Region (x/L=50%)	22.7%	44.5%	20.3%	21.7%
Free End (x/L=84.8%)	1.7%	26.1%	29.3%	32.3%

4.5 Case-3: Change of Transverse Crack Widths on the Edge along Z-axis

This is a similar study done in case-1 for three different transverse crack widths of 0.5mm, 1mm (case-1) and 1.5mm with aluminum alloy. The other properties of the material and plate dimensions are same as depicted in Table 3.1. The movement of crack is at 5mm intervals along the edge of the Z-axis. Figure 4.11 illustrates the schematic diagram of the movement of crack of different width along longitudinal direction.

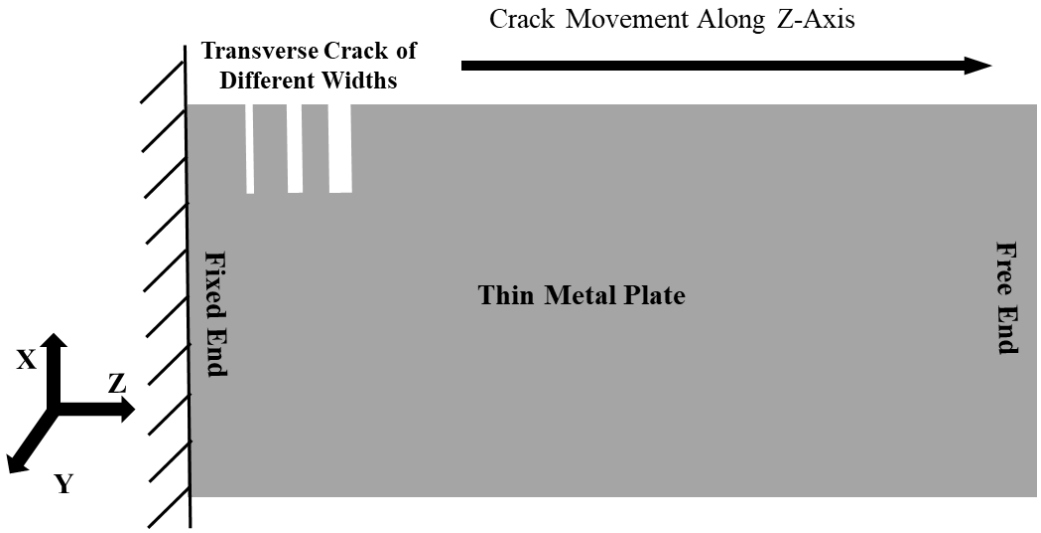

Figure 4.11: Schematic Diagram for the Change of Transverse Crack Width on the Edge along Z-axis

The results displayed in the Figure 4.12 shows that as the crack widths changes there is very little variations of frequency drop in all the six normalized frequency curves. These curves have similar pattern as in case-1. For bending modes, the maximum significant frequency for the crack width of 0.5mm, 1.0mm and 1.5mm are 5.7%, 5.9% and 6.0% respectively at relative distance 9.1% on the 1st mode. For torsional modes, the maximum significant frequency for the crack width of 0.5mm, 1.0mm and 1.5mm are 7.1%, 7.4% and 7.6% respectively at relative distance 84.8% on the 6th mode.

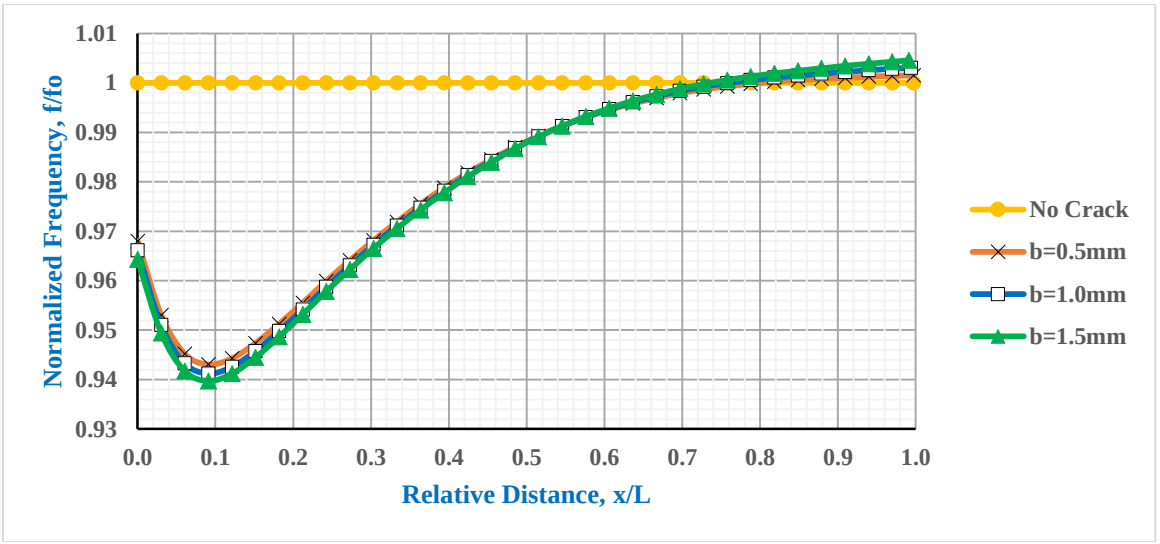

(a) First Mode

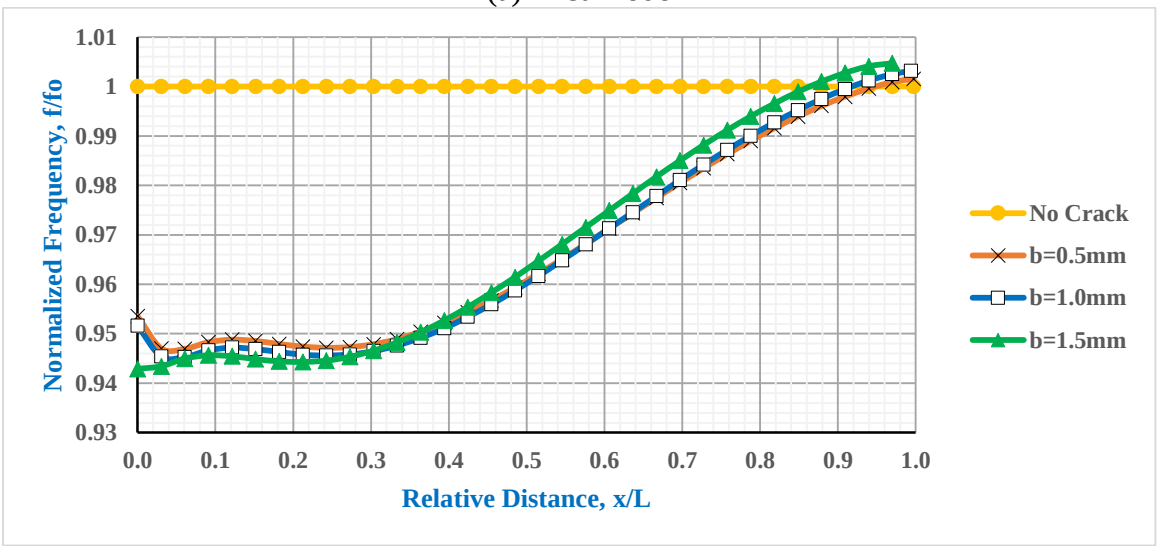

(b) Second Mode

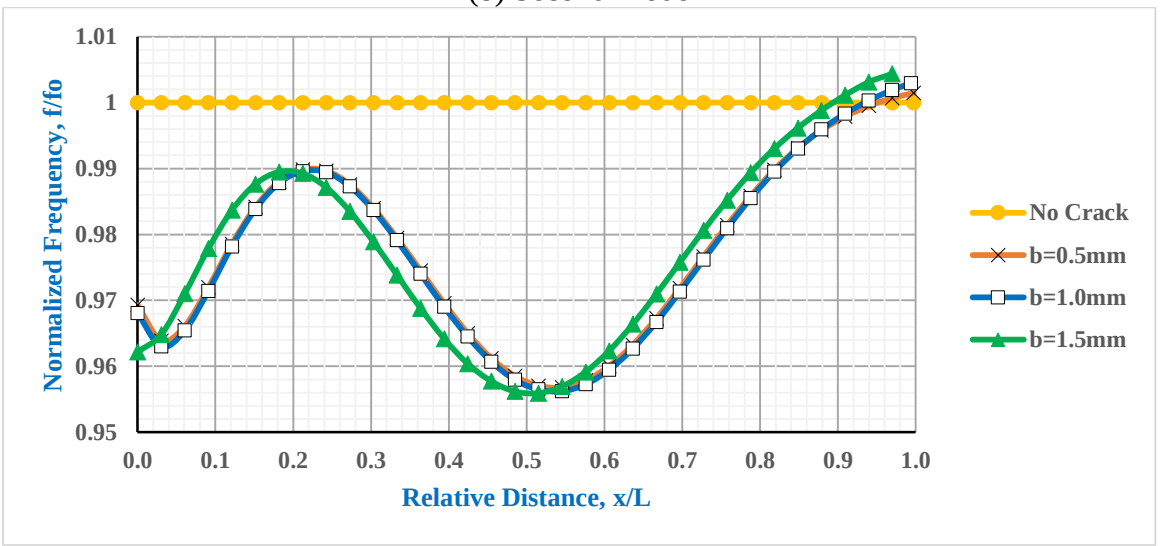

(c) Third Mode

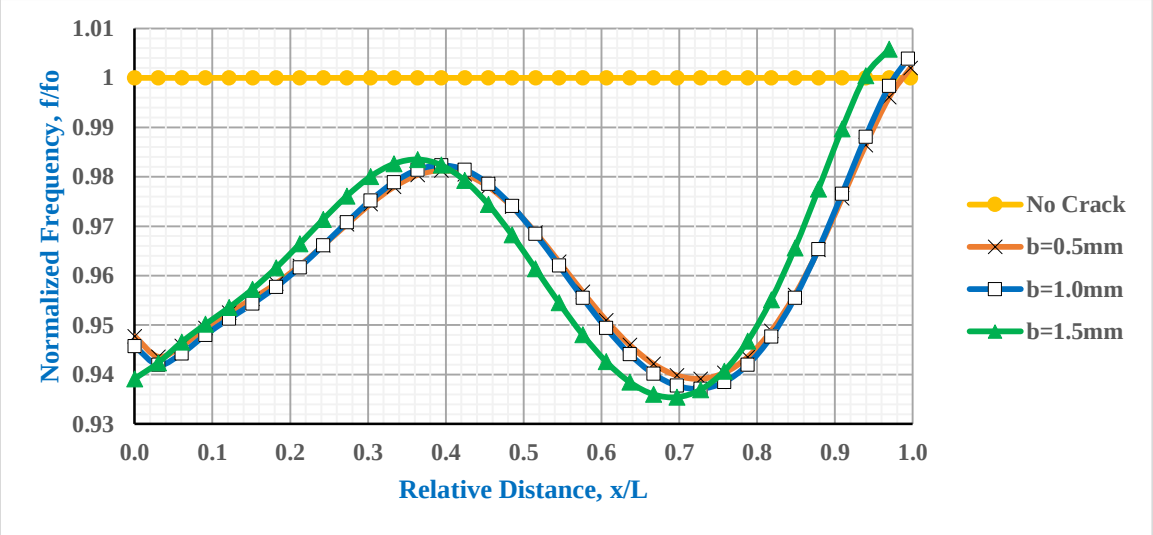

(d) Fourth Mode

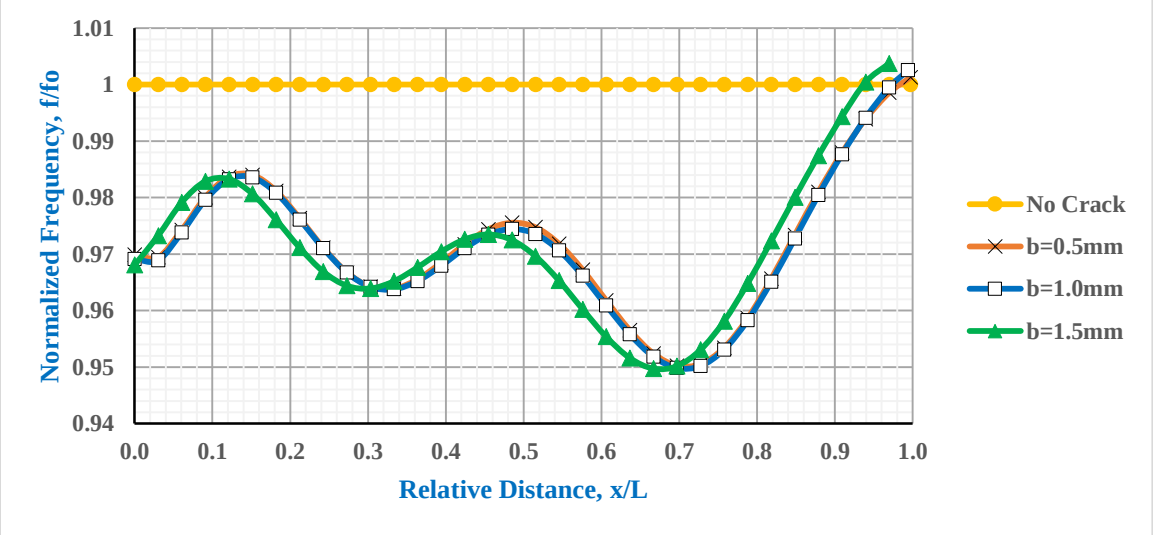

(e) Fifth Mode

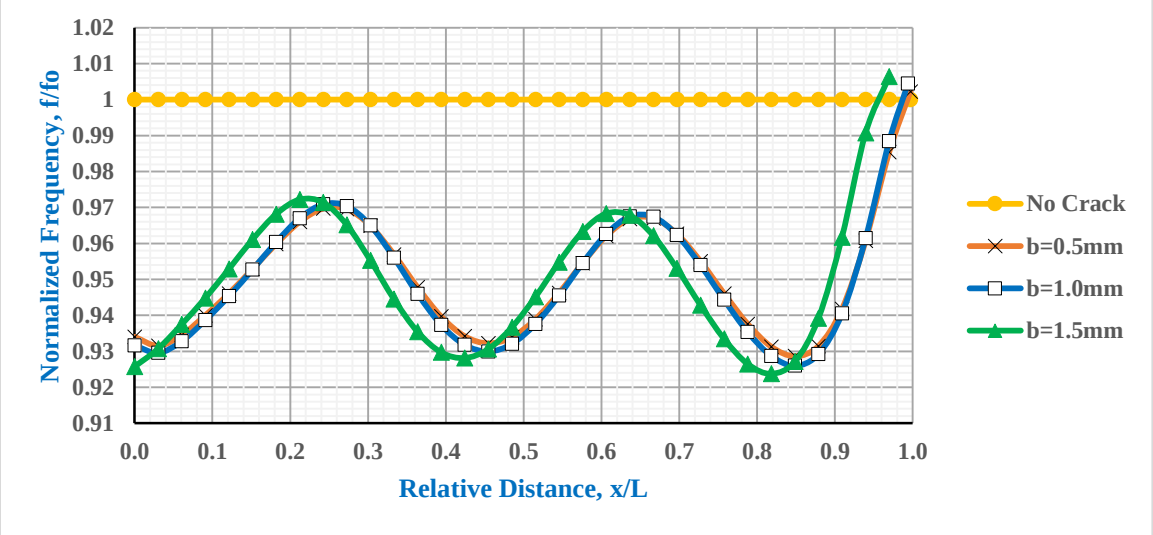

(f) Sixth Mode

Figure 4.12: Normalized Frequency over Relative Distance along Z-axis for Transverse Crack Width of 0.5mm, 1mm and 1.5mm

The frequency drop remains almost equal for varying the crack width over the Z-axis. It is observed that all the regions in the plate, free end, mid-region and fixed end, have almost similar frequency drop ranging from 6.8% to 7.6% given on Table 4.6. The maximum significance frequency drop compared to the frequency of healthy plate for 0.5mm, 1mm and 1.5mm are 7.1%, 7.4% and 7.6% at 6th mode at relative distance of 84.8% for all the cases.

Table 4.6: Key Findings of Case-3 for Different Crack Widths

Region on Cantilever Plate	**% of Max Frequency Drop on Sixth Mode**		
	b=0.5mm	**b=1mm**	**b=1.5mm**
Fixed End (x/L: 0-15%)	6.8%	7.0%	7.4%
Mid-Region (x/L: 42-55%)	6.8%	7.0%	7.2%
Free End (x/L: 85-99%)	7.1%	7.4%	7.6%

Methods	**Relative Distance of Intersection Point on First Mode**		
	b=0.5mm	**b=1mm**	**b=1.5mm**
Normalized Frequency Curve	81.8% (x=135mm)	78.8% (x=130mm)	75.8% (x=125mm)
Regression Equation	75.84% (x=125.14mm)	74.60% (x=123.09mm)	72.37% (x=119.40mm)

The regression equations for crack width 0.5mm, 1mm and 1.5mm are respectively:

For b=0.5mm: $p = 3.748n^6 - 12.968n^5 + 17.792n^4 - 12.22n^3 + 4.2354n^2 - 0.5512n + 0.9669$

For a=1mm: $p = 3.7773n^6 - 13.067n^5 + 17.926n^4 - 12.312n^3 + 4.2663n^2 - 0.5517n + 0.9649$

For a=1.5mm: $p = 3.7842n^6 - 13.099n^5 + 17.981n^4 - 12.353n^3 + 4.2788n^2 - 0.5494n + 0.9632$

Here, $p = f/f_o$ (normalized frequency), and $n=x/L$ (relative distance)

The Table 4.6 also shows the intersection point on the normalized frequency curve of the first mode. As the crack width increases, the intersection point moves towards the fixed end, unlike the case of increasing the crack length. To determine the exact relative distance of the

intersection point we deduced regression equation of sixth polynomial for the curves of the first mode and found the solution as 75.84%, 74.60% and 72.37% for 0.5mm, 1mm and 1.5mm respectively. These points in this case also seems to move towards fixed end with increases crack width.

4.5.1 Further Study on Different Crack Widths

The study is conducted to find the relationship between normalized frequencies over various crack width to plate length ratio (b/L). Table 4.7 shows five samples that are taken for three different crack locations: 15mm (near fixed end), 82.5mm (mid-region) and 140mm (near free end). In this case, crack length and crack depth are kept constant.

Table 4.7: Five Samples of Crack Dimension with Various Crack Widths

Sample	Crack Length a/mm	Crack Width b/mm	Crack Depth c/mm	b/L
1	20	1	1.43	0.0061
2	20	5	1.43	0.0303
3	20	10	1.43	0.0606
4	20	15	1.43	0.0909
5	20	20	1.43	0.1212

Figure 4.13 illustrates the frequency drop of six modes for changing crack width in three distinct regions of the cantilever plate. The frequency drop at mid-region, the normalized frequency curve of fifth mode and sixth mode cannot be explained for the random overlapping of the curves. In the first four mode, it is observed that as the crack width increases the frequency drop increases at fixed region. On the other hand, there is frequency gain at free end. All the six modes consistently drop below the frequency of the healthy plate over the subsequent increase in modes. The maximum significant difference in frequency drop is found at fixed region for mode 1 Sample 5 (b=20mm) with the value of 9.7%.

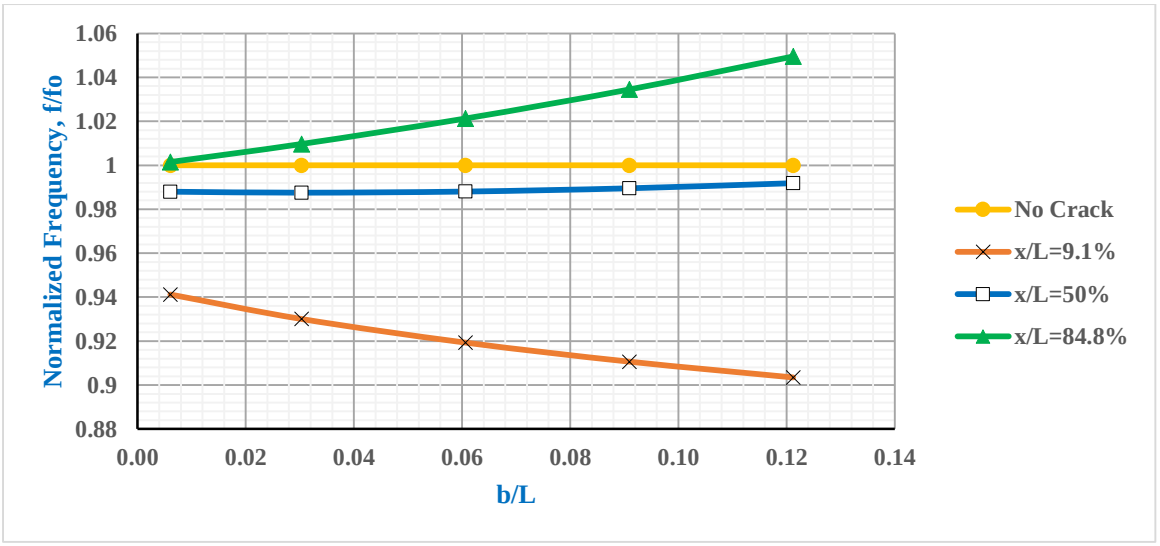

(a) First Mode

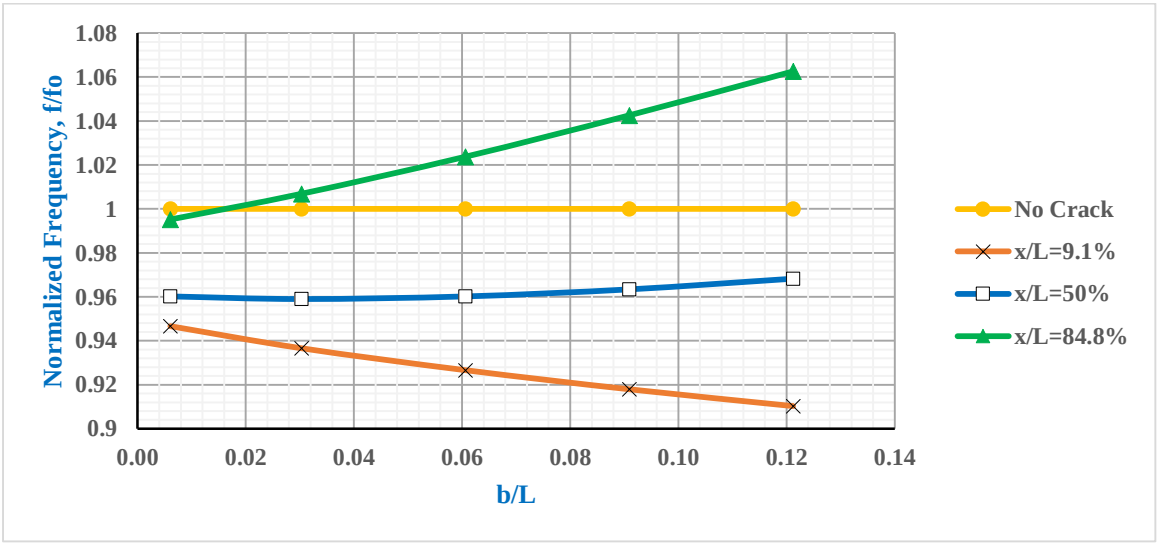

(b) Second Mode

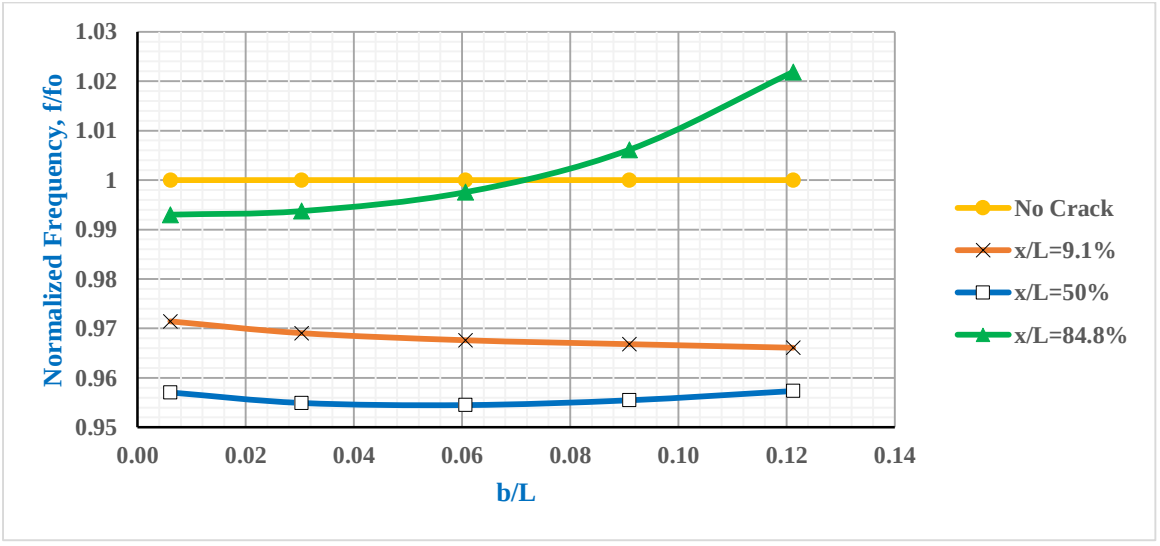

(c) Third Mode

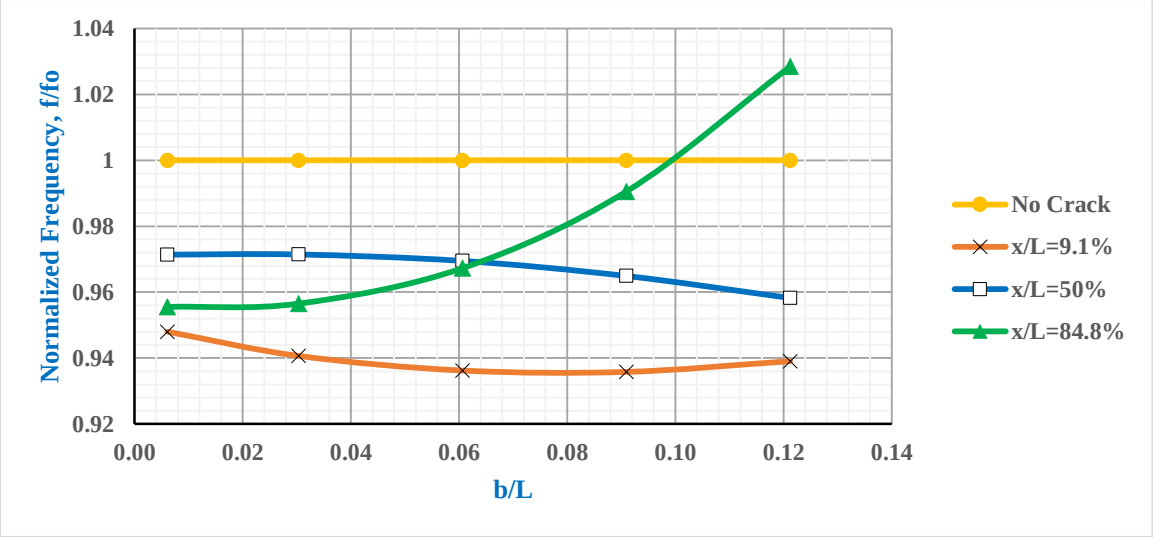

(d) Fourth Mode

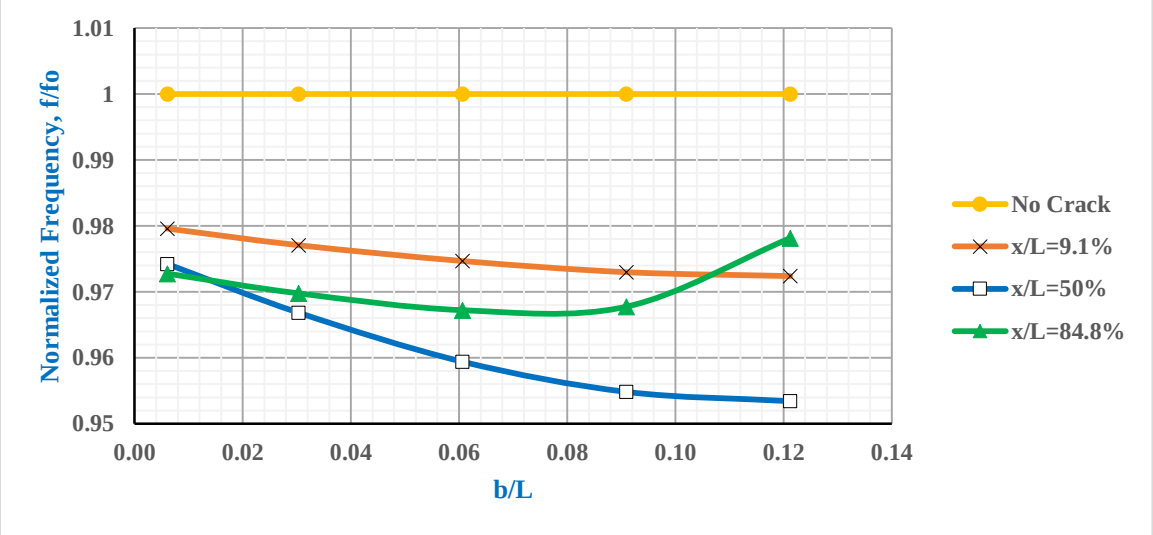

(e) Fifth Mode

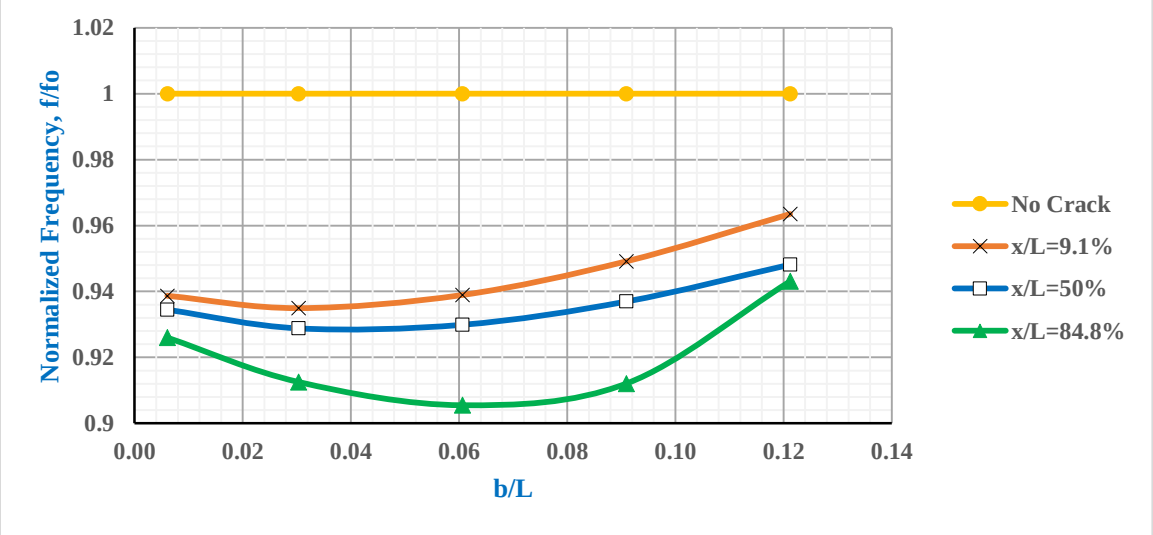

(f) Sixth Mode

Figure 4.13: Normalized Frequency Curve over Different Crack Width to Plate Length Ratio

4.6 Case-4: Study on Effect of Normalized Frequency due to Change of Crack Depths along Y-axis

The study is conducted, to find the relationship between normalized frequencies over various crack depths, to plate thickness (c/H) along Y-axis (depth direction). Table 4.8 shows five samples that are taken for three different crack locations: 15mm (near fixed end), 82.5mm (mid-region) and 140mm (near free end). In this case, crack length and crack width are kept constant.

Table 4.8: Five Samples of Crack Dimension with Various Crack Depths

Sample	Crack Length a/mm	Crack Width b/mm	Crack Depth c/mm	c/H
1	20	1	1.43	1.0000
2	20	1	1.0725	0.7500
3	20	1	0.715	0.5000
4	20	1	0.3575	0.2500
5	20	1	0.143	0.1000

Figure 4.14 illustrates the frequency drop of six modes for changing crack depth in three distinct regions of the cantilever plate. For all the six modes, there is no frequency drop until the crack depth is 75% of the plate thickness (i.e., c/H=75%). It is also found that curve generated up to this point is parallel to the line of the healthy plate. After this point there is a rapid frequency drop until the crack is thorough (i.e., c/H=100%).

For bending modes, the maximum frequency drop for thorough crack (sample 1) and non-thorough crack (sample 2) is 5.9% and 0.87% respectively near fixed end on the 1st mode. For torsional modes, the maximum frequency drop for thorough crack (sample 1) and non-thorough crack (sample 5) is 7.4% and 0.92% respectively near free end on the 6th mode.

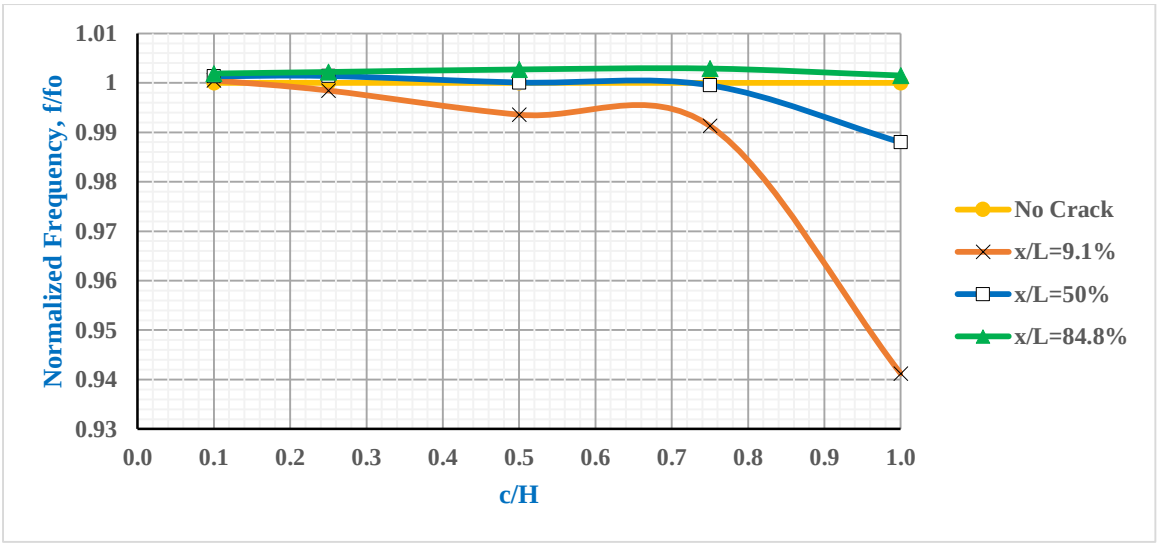

(a) First Mode

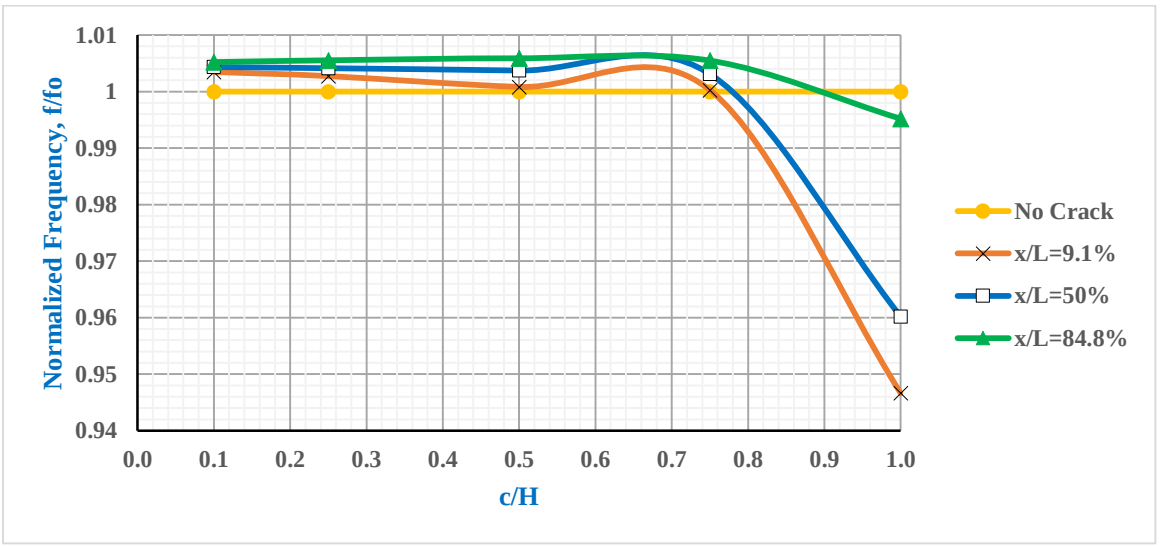

(b) Second Mode

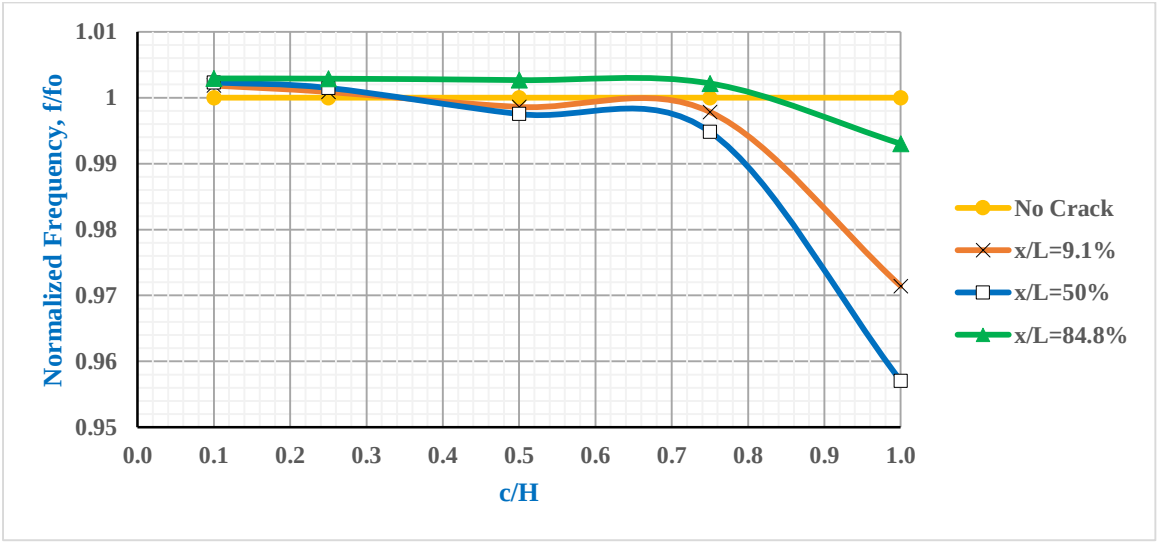

(c) Third Mode

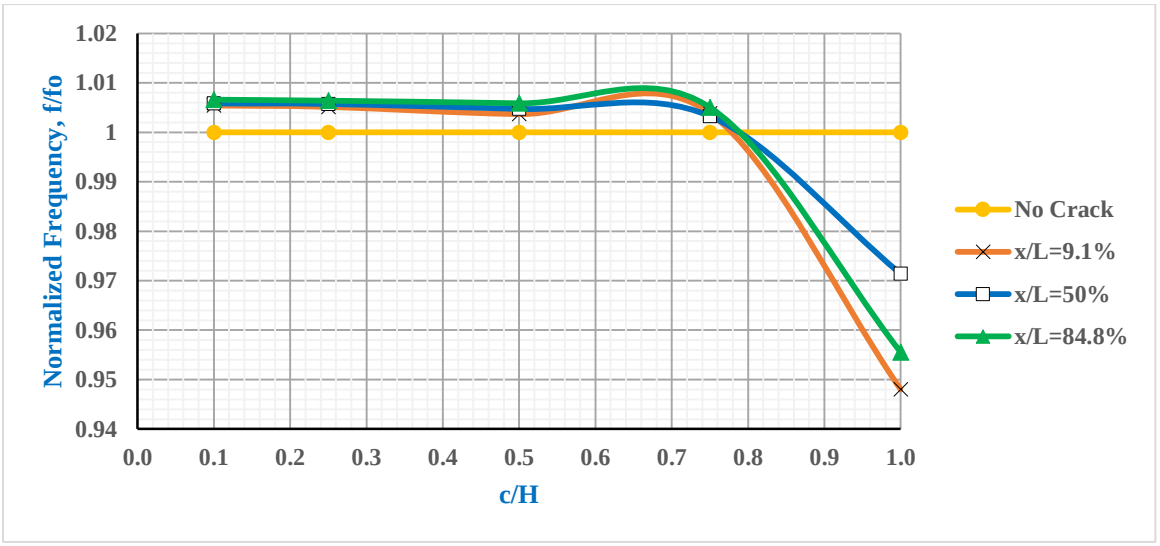

(d) Fourth Mode

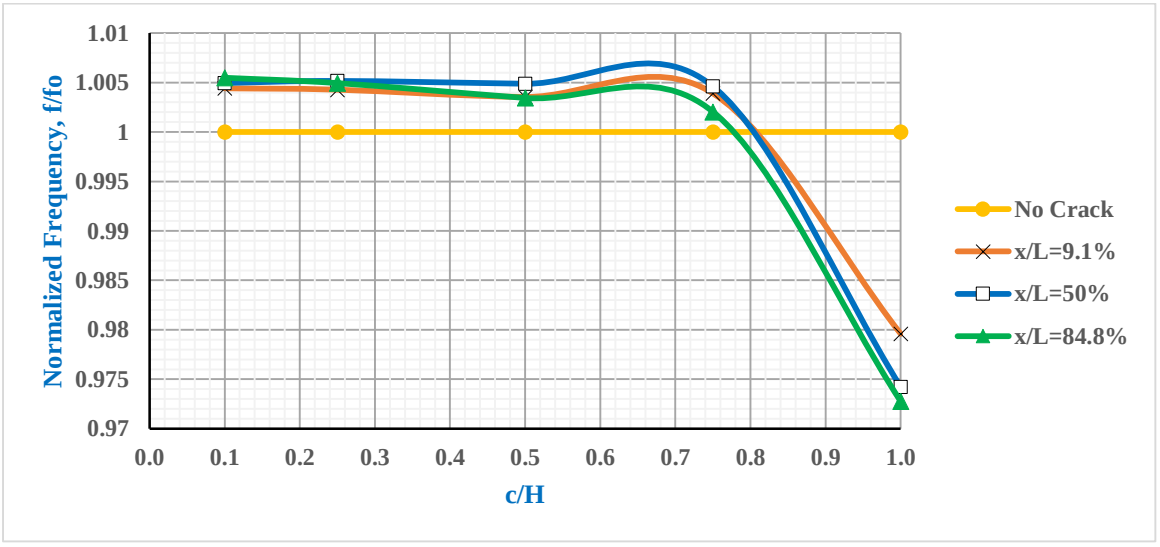

(e) Fifth Mode

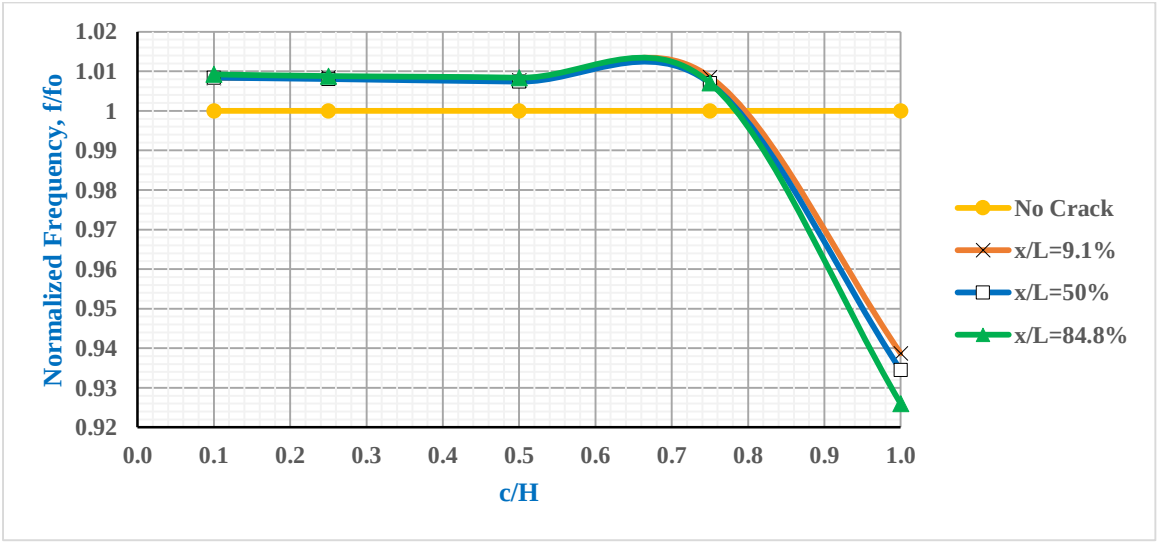

(f) Sixth Mode

Figure 4.14: Normalized Frequency Curve over Different Crack Depth to Plate Thickness along Y-axis

4.7 Case-5: Transverse Edge Crack Positions along Z-axis with Structural Steel

This is a similar study like case-1 where transverse edge cracks are changed along Z-axis. The only difference here is that the material is changed to structural steel. Table 3.1 shows the properties of the cantilever plate and the crack. The orientation of crack position is transverse in nature. Figure 4.15 shows the normalized frequency over the relative distance for six modes. The result found in case-1 with aluminum alloy is plotted in the same figure with case-5 with structural steel to compare any differences. Schematic diagram of the movement of crack is illustrated in Figure 4.5.

It is found that for all the six modes there are significant frequency drop at relative distance from 0 to 12% (near fixed end) of the plate. For torsional mode, the most significant frequency drop is 7.3% at relative distance 84.8% on 6th mode. For bending modes, the most significant frequency drop is 5.8% at relative distance 9.1% on 1st mode. For a 20mm crack, the intersection point occurs at relative distance of 78.8% in first mode, 93.9% in second and third modes and at 99.4% for rest of the modes.

All natural frequencies of aluminum alloy are found greater than that of structural steel along Z-axis showing that the former has a higher stiffness. Moreover, normalized frequency curves of both these cases (case-1 and case-5) follow the same pattern and trend as shown in the Figure 4.15. The normalized curves in torsional modes share the same line of progression with little difference. On the other hand, though the normalized curve of the bending modes have the same pattern, their progression takes place at certain gap. As both these materials share the common trends, structural steel is used in later cases in the research. AA stands for Aluminum Alloy and SS stand for Structural Steel in the figures and tables below.

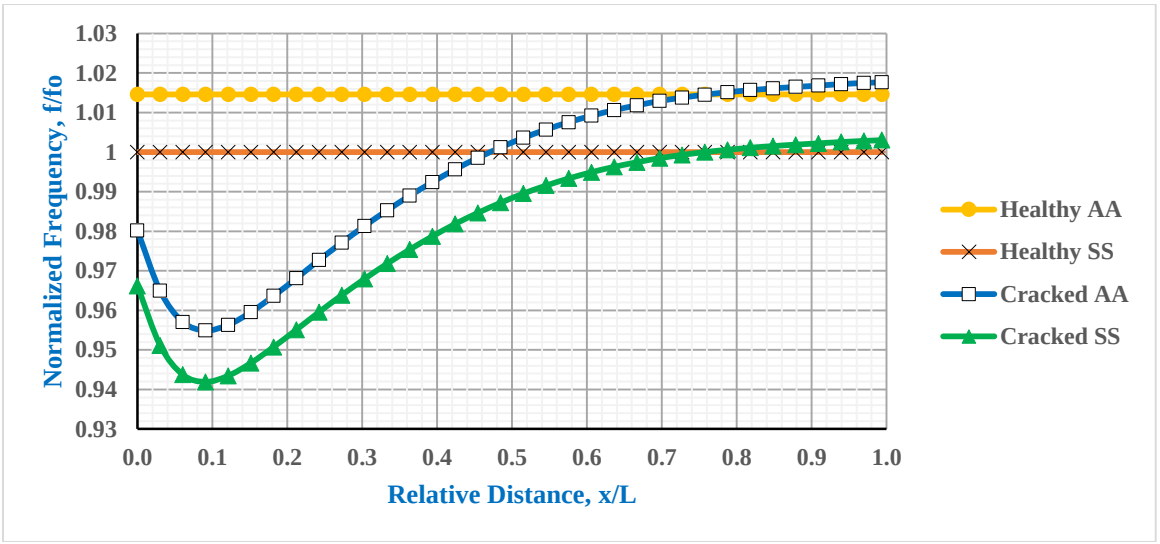

(a) First Mode

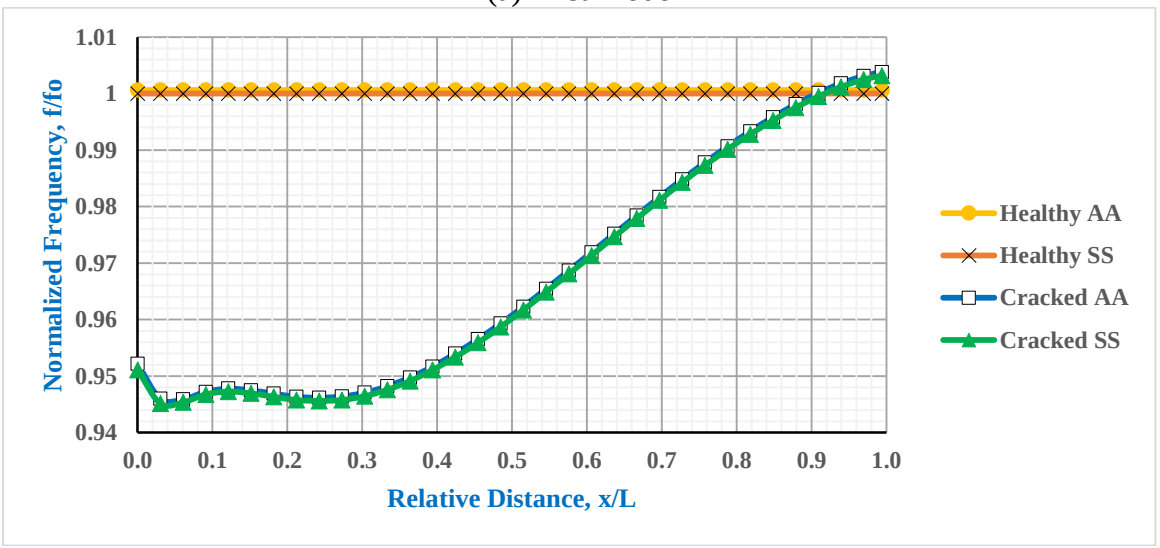

(b) Second Mode

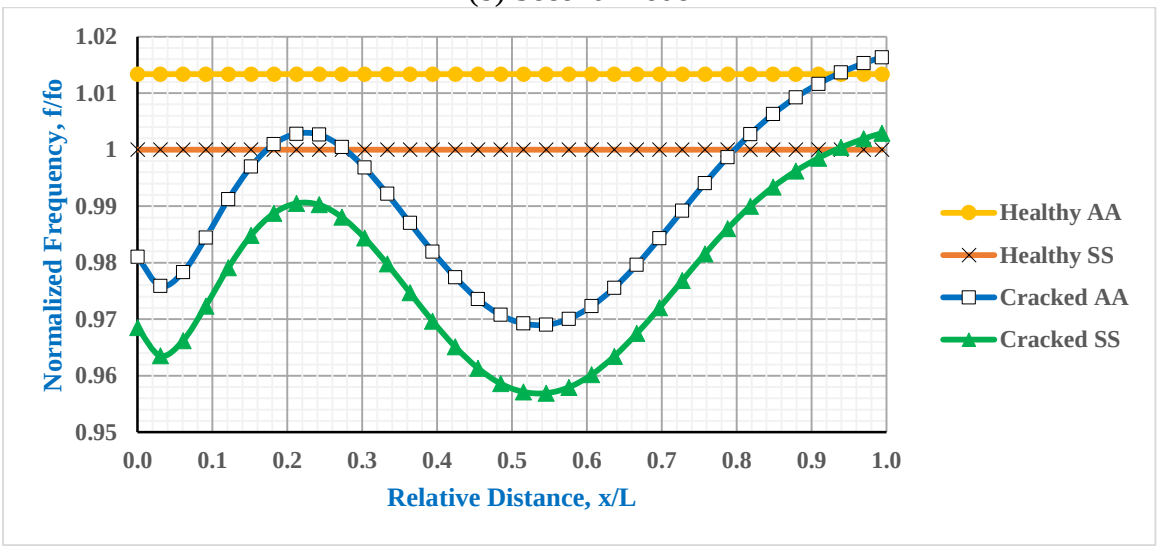

(c) Third Mode

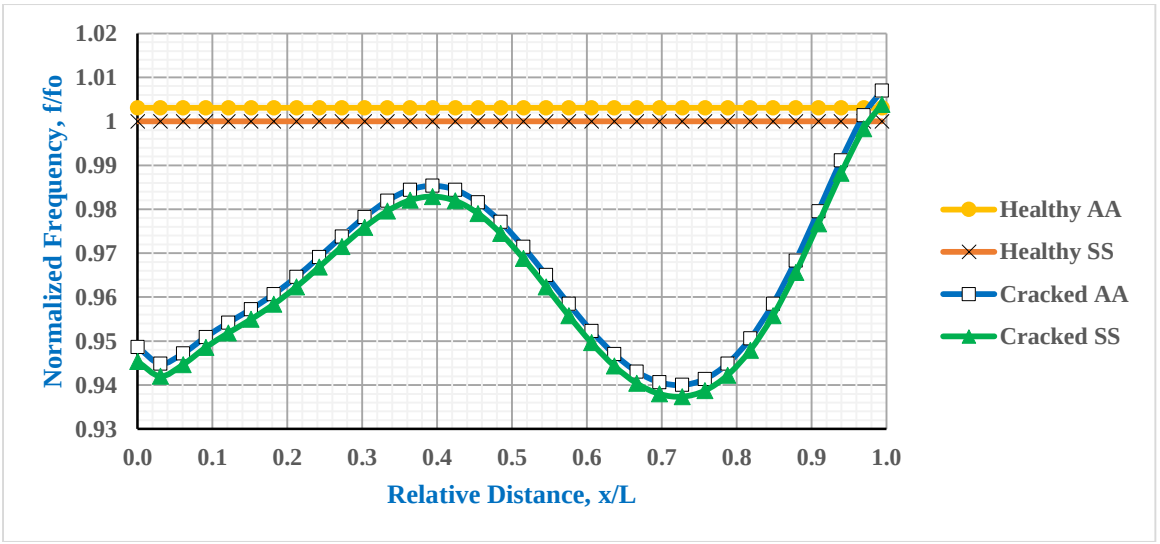

(d) Fourth Mode

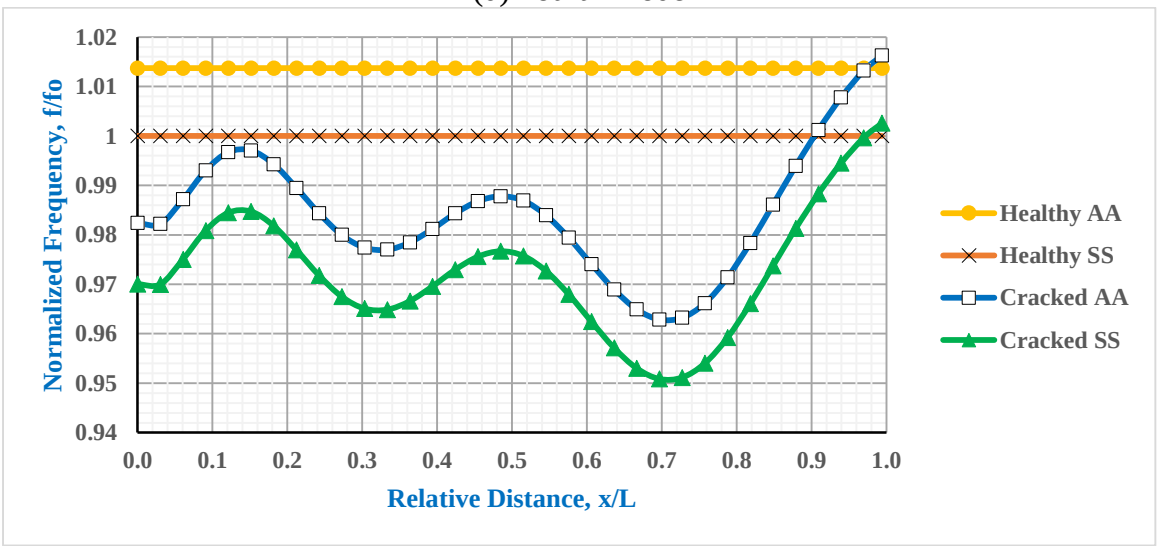

(e) Fifth Mode

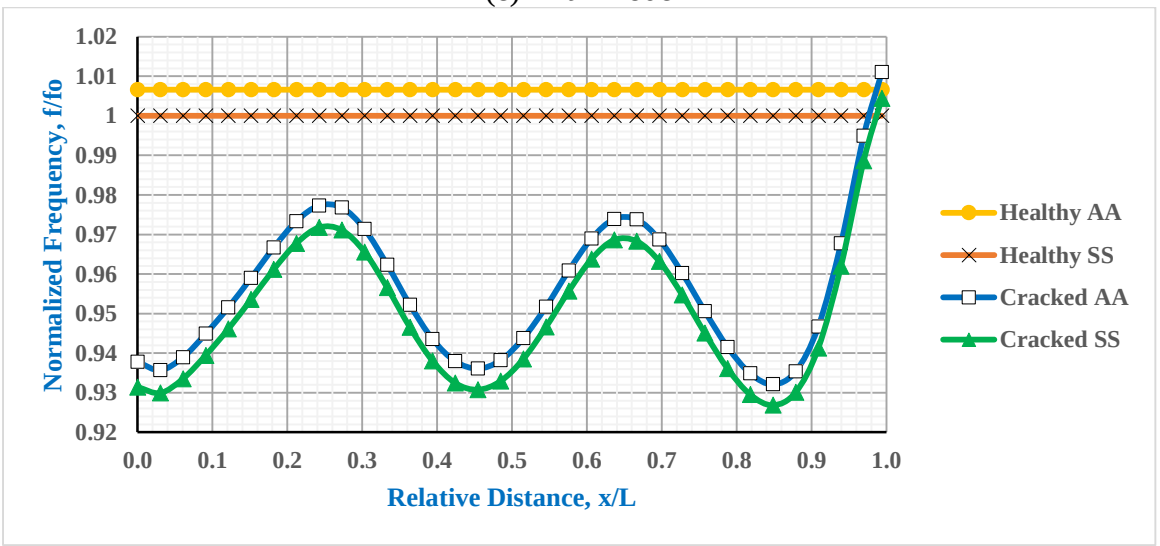

(f) Sixth Mode

Figure 4.15: Normalized Frequency Between Aluminum Alloy (Case-1) and Structural Steel (Case-5)

4.8 Case-6: Change of Embedded Transverse Crack Positions along Mid Z-axis

This is a similar study mentioned in case-5 where the transverse cracks are moved along the edge of the Z-axis using structural steel. In this case, material used is structural steel. However, the crack positions are changed along the mid-line of the Z-axis. This type of crack, which is not at the edge of the plate, are known as embedded crack. This is shown in the Figure 4.16. Table 3.1 shows the properties of the cantilever metal plate and the crack.

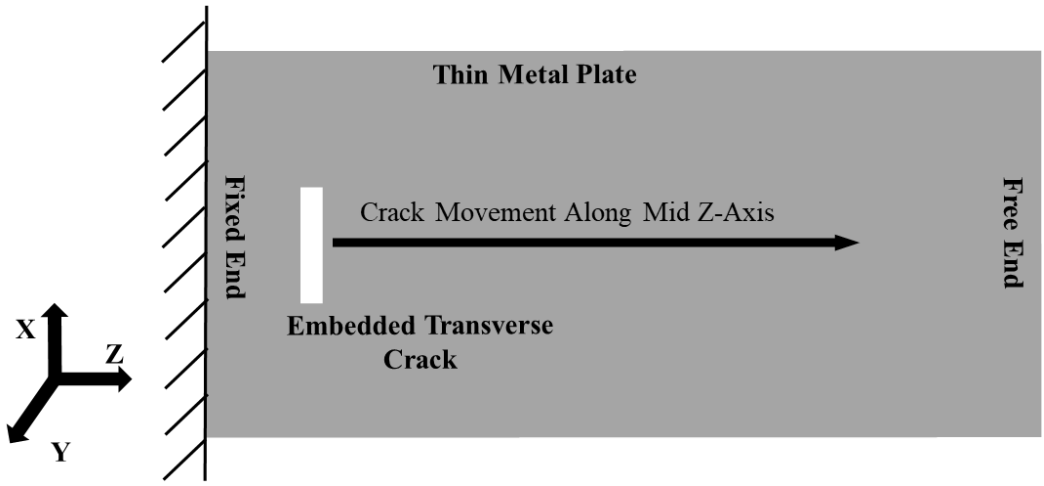

Figure 4.16: Schematic Diagram for the Change in Embedded Transverse Crack Positions along Mid Z-axis of the Plate

Figure 4.17 compares the first six normalized frequencies of a healthy plate with the plates having crack. In bending modes, the normalized frequency curves of embedded crack and edge crack follow the same pattern. However, the frequency drop of edge crack is massive than that of mid-crack. The bending modes in mid-cracks have frequency drop near the fixed end. With the subsequent increase in bending mode, the maximum frequency drop moves towards the free end. For bending modes, the maximum frequency drop is 4.2% at relative distance 6.1% on 1st mode. In torsional modes of embedded crack has no significant frequency drop. This is because the angle of twist in this axis is zero. The maximum frequency drop in torsional mode is 0.26% at relative distance 90.9% on 6th mode. This phenomenon could be used to predict the presence of embedded crack with transverse orientation. In Figure 4.17, the embedded crack is mentioned as “Mid Crack”.

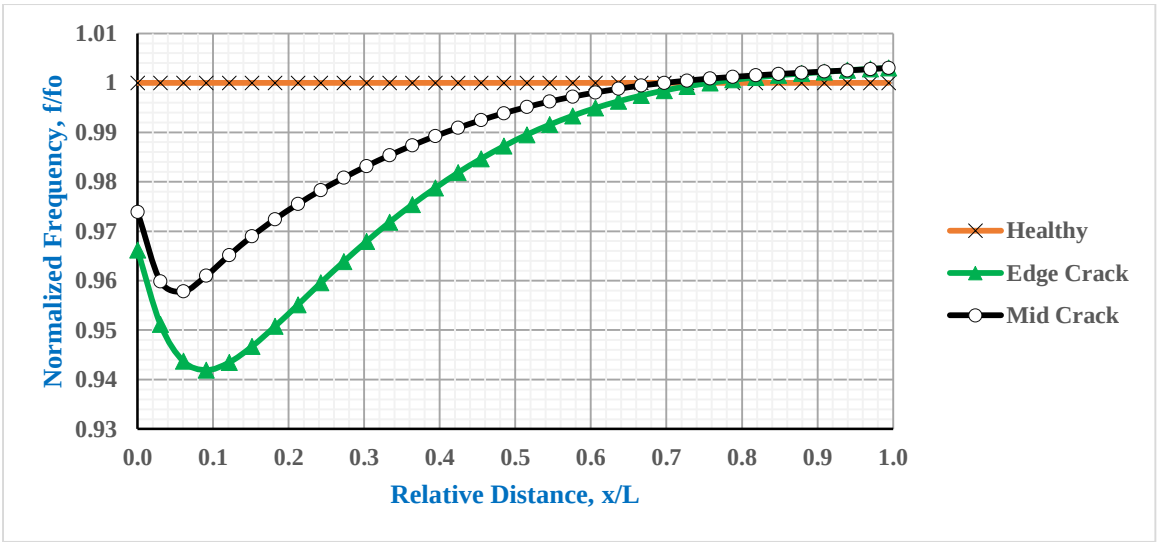

(a) First Mode

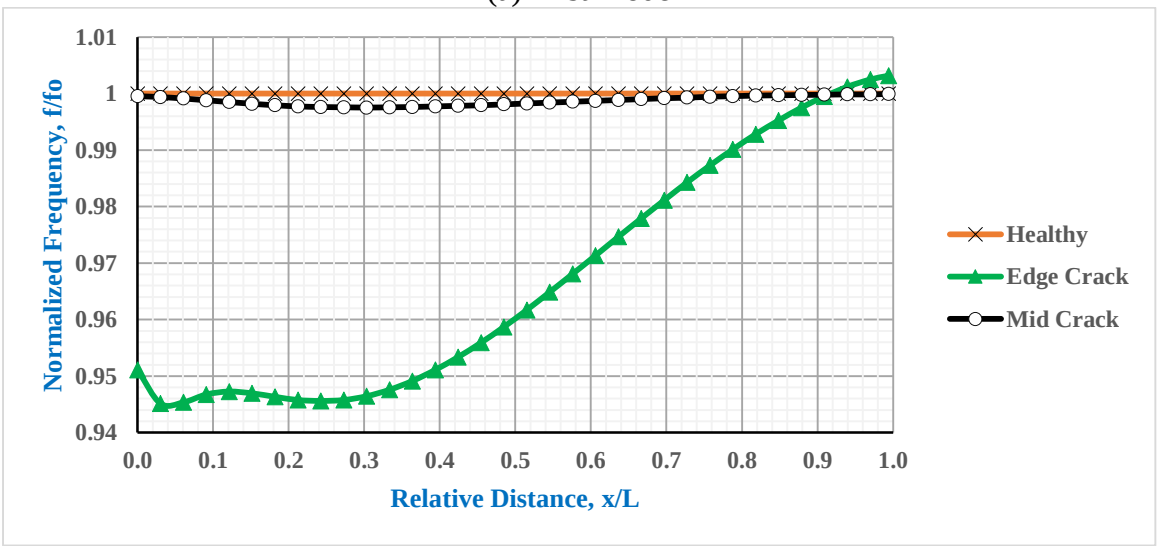

(b) Second Mode

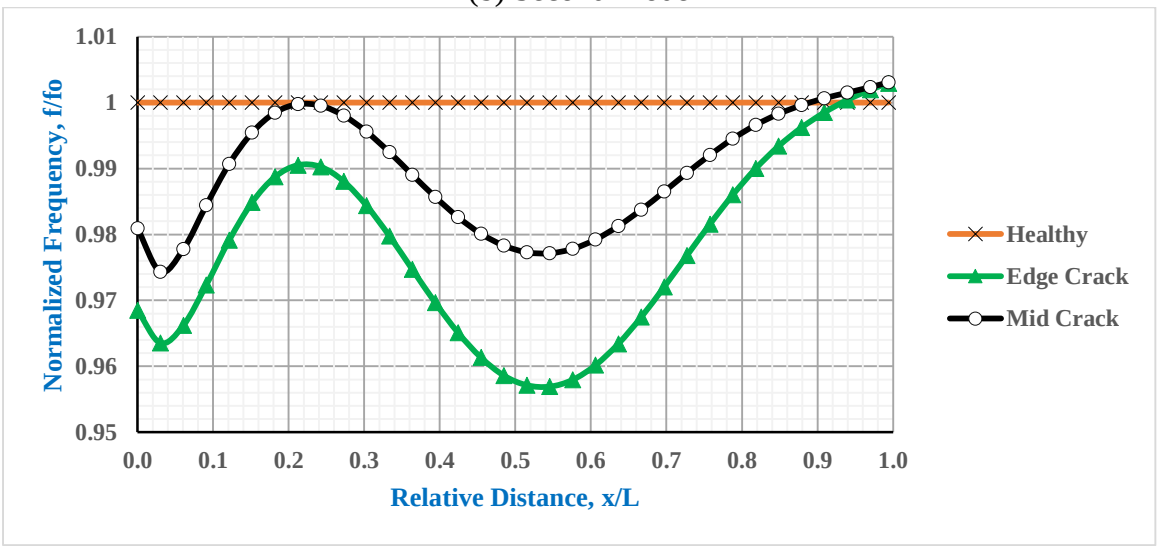

(c) Third Mode

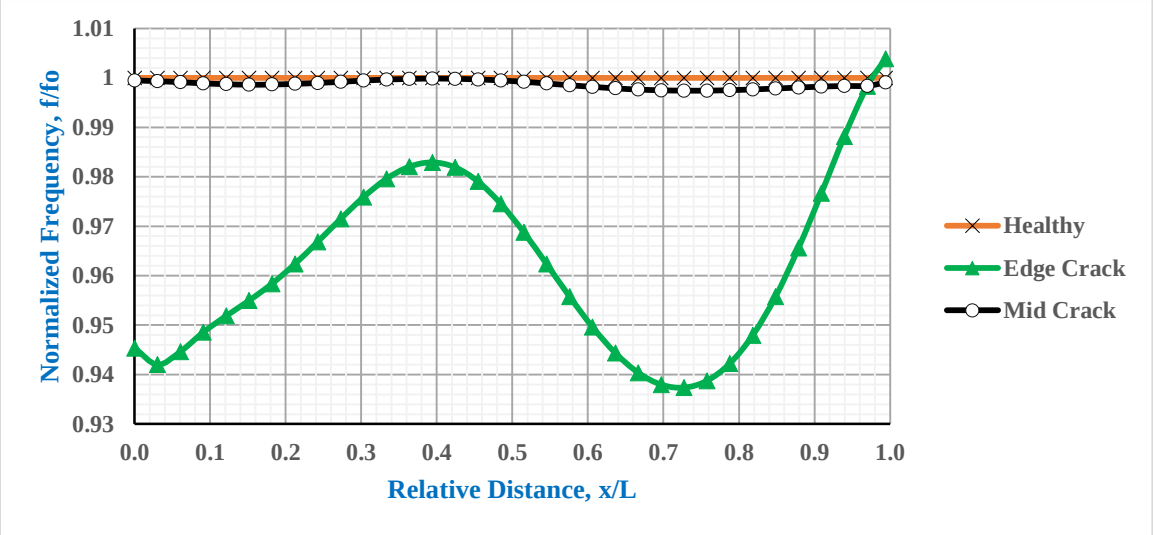

(d) Fourth Mode

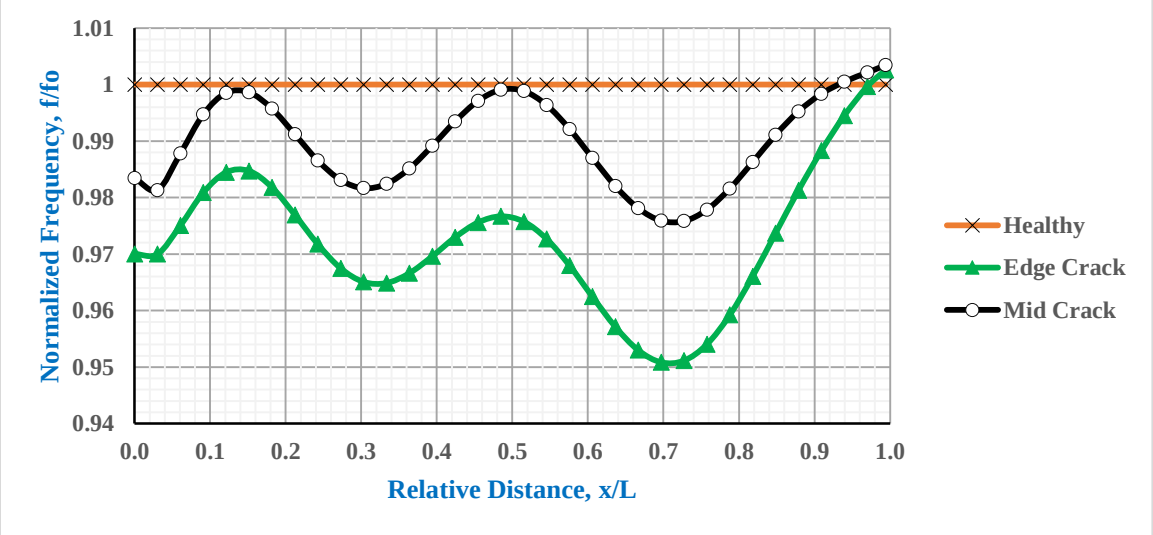

(e) Fifth Mode

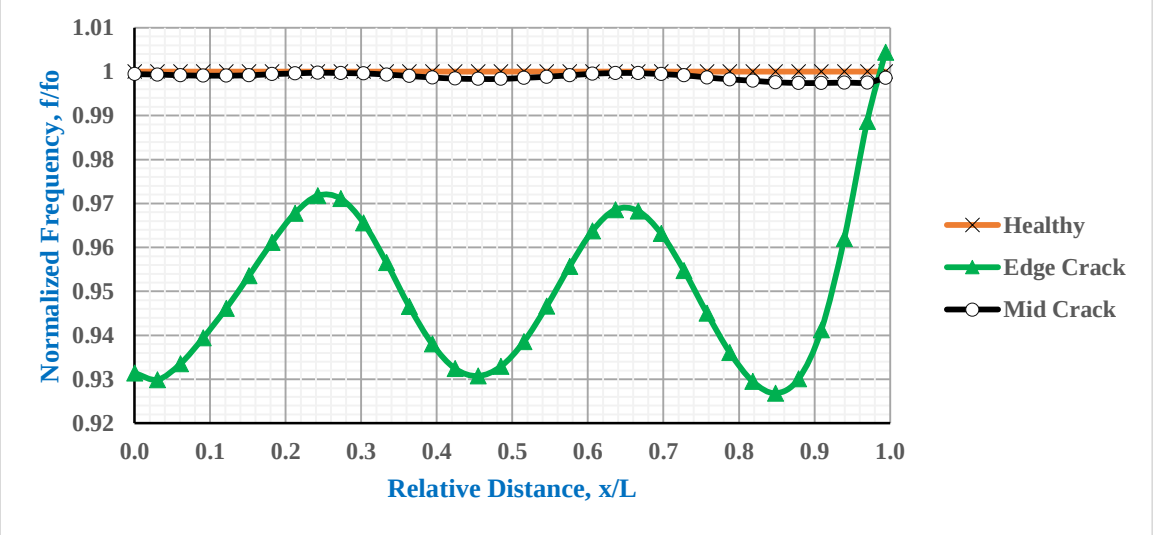

(f) Sixth Mode

Figure 4.17: Difference in Normalized Frequency Between Transverse Edge Crack (Case-5) and Transverse Mid-Crack (Case-6) along Z-axis

4.9 Case-7 and Case-8: Change of Longitudinal Crack at Edge and Mid-Positions along Z-axis

Case-7 describes the change of longitudinal edge crack positions along longitudinal direction (Z-axis). The longitudinal edge crack is generally stated as surface defect. On the other hand, case-8 describes the change of embedded longitudinal crack positions along mid Z-axis. Figure 4.18 illustrates schematic diagram these two cases. In these cases, the crack positions are changed at 10mm intervals including fixed and free end of the plate. The details of plate and crack properties are in the Table 3.1.

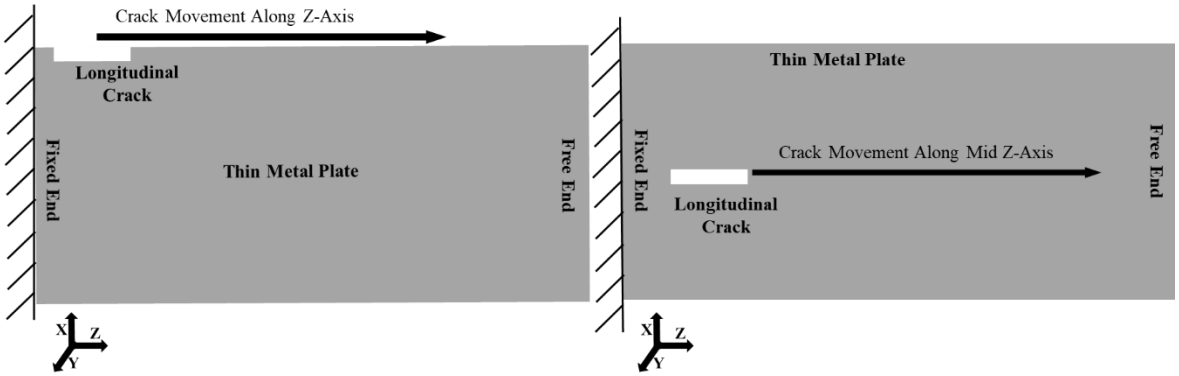

(a) Longitudinal Edge Crack (Case-7) (b) Embedded Longitudinal Crack (Case-8)

Figure 4.18: Schematic Diagram for the Change in Positions along the Z-axis of the Plate for Longitudinal Edge Crack (Case-7) and Embedded Mid-Crack (Case-8)

Figure 4.19 shows the comparison between a longitudinal edge crack (Case-7) and an embedded longitudinal crack (Case-8) of the first six modes. In the same figure, the embedded crack is mentioned as “Mid Crack”.

For longitudinal edge crack, the frequency drop is observed at fixed end, while frequency gain is observed at free end. However, it is found that for both bending and torsional modes there are very little frequency drop all over the plate. The most significant frequency drop for bending mode is 0.29% at relative distance 6.1% on 1st mode. While for torsional mode, it is 0.25% at relative distance 0% on 2nd mode. This frequency drop is negligible and this type of surface defect remain undetectable in this research.

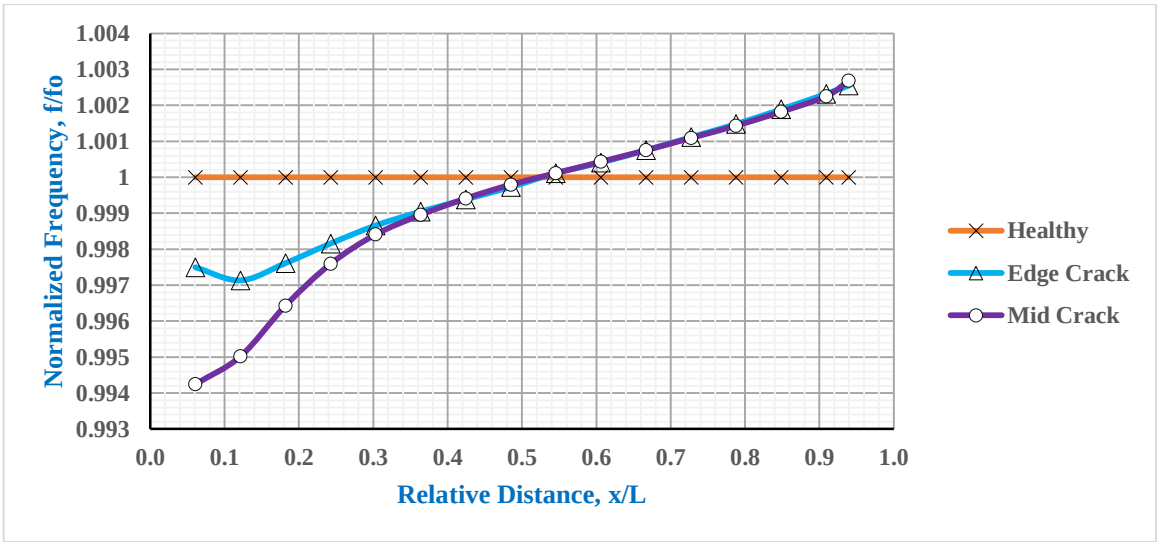

(a) First Mode

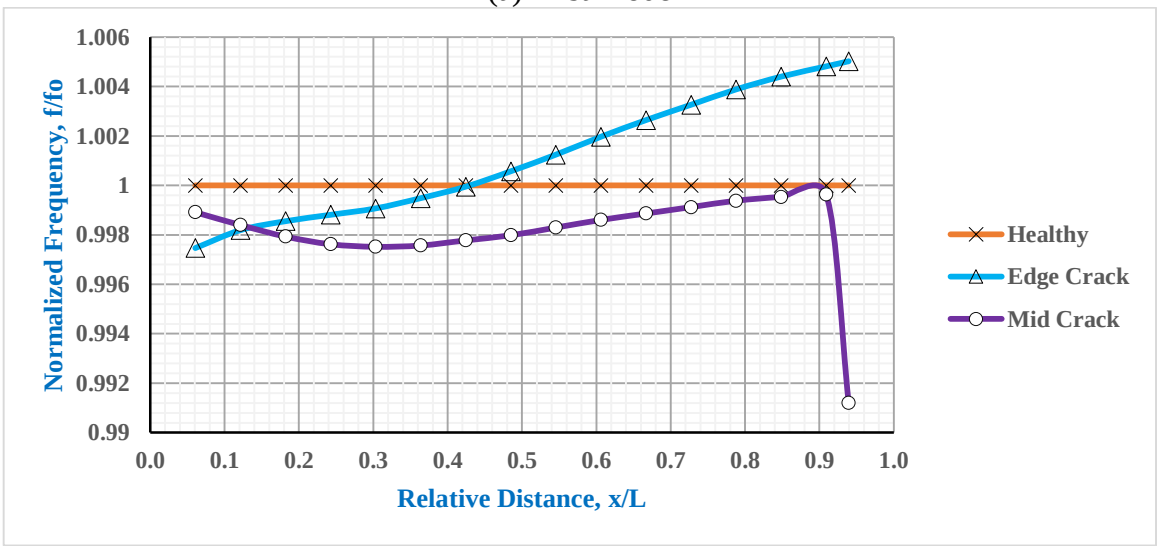

(b) Second Mode

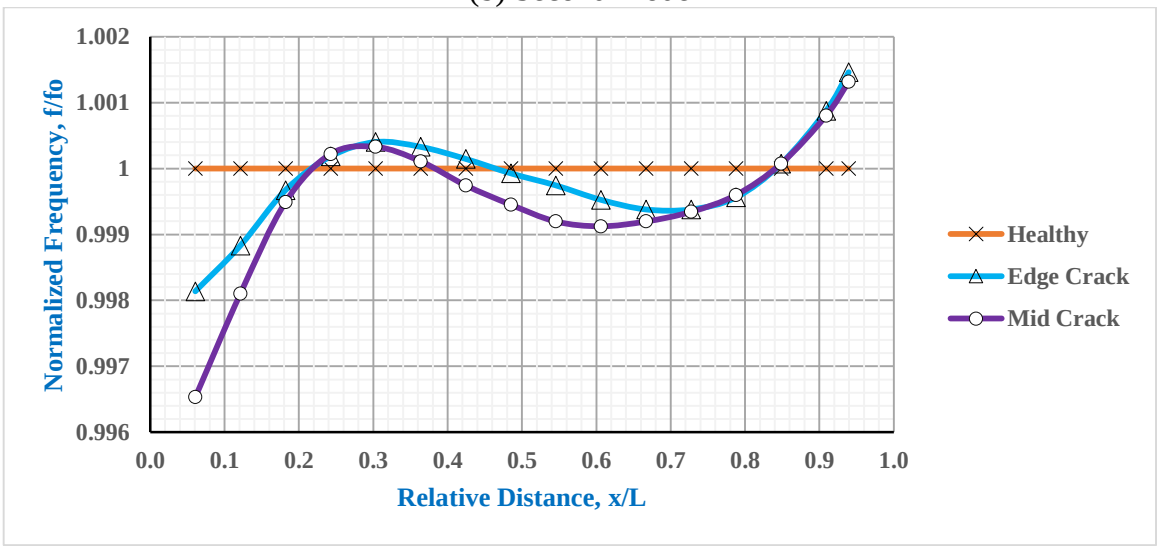

(c) Third Mode

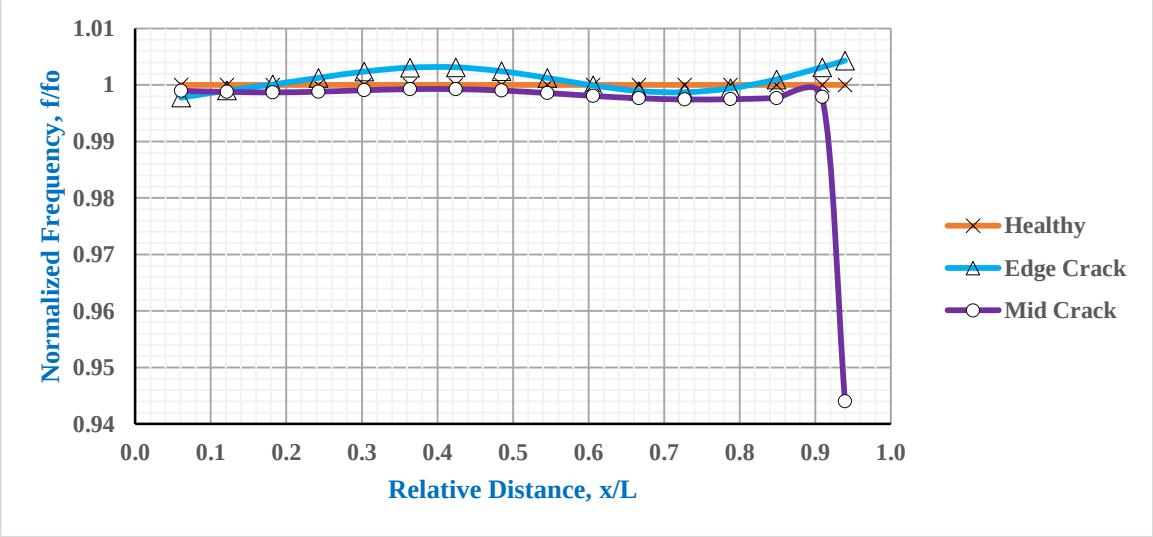

(d) Fourth Mode

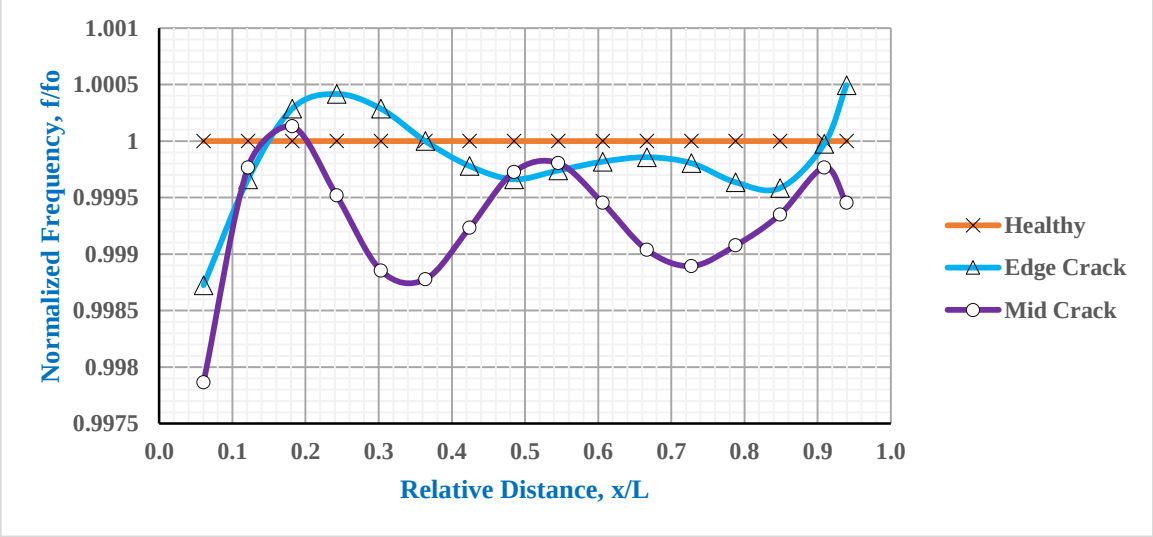

(e) Fifth Mode

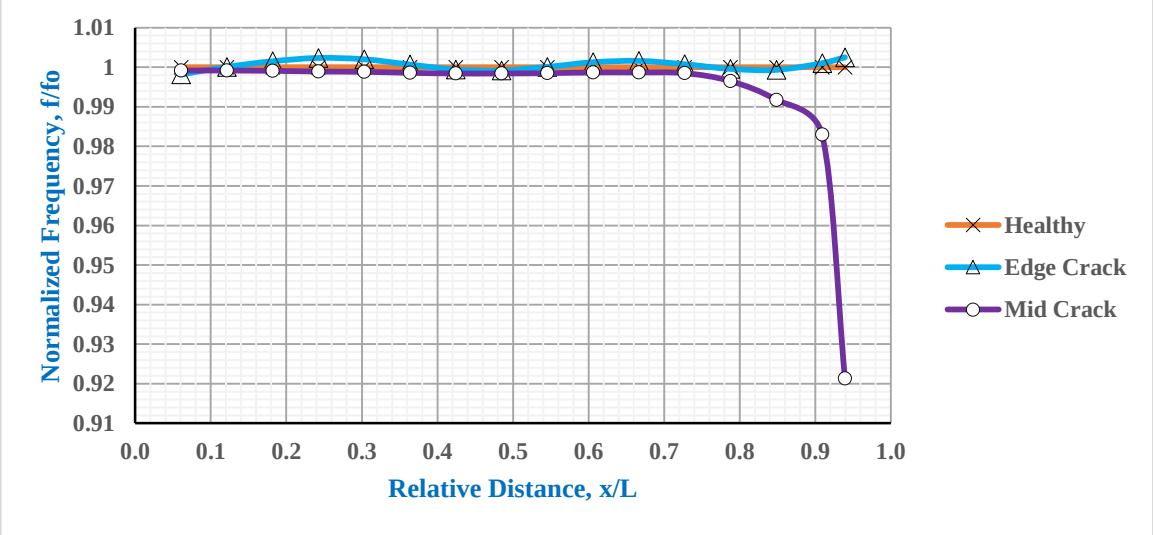

(f) Sixth Mode

Figure 4.19: Difference in Normalized Frequency Between Longitudinal Edge Crack (Case-7) and Longitudinal Mid-Crack (Case-8) along Z-axis

In bending modes, the maximum frequency drop for the embedded longitudinal crack is only 0.58% at relative distance 0% on the 1st mode. In torsional modes, the most significant frequency drop is 7.9% at the relative distance 87.9% (free end) on the 6th mode. These drops are very abrupt and sharp. This is the only crack position where the presence of embedded longitudinal mid-crack could be confirmed. It is also noticed that the magnitude of this frequency drop at free end increases with mode. Other than the free end, the maximum frequency drop is 1.7% at the relative distance of 84.8% on the 6th mode.

4.10 Case-9 and Case-10: Change of Longitudinal and Transverse Edge Crack Positions along X-axis on Free End

Case-9 describes the change of longitudinal edge crack positions along transverse direction (X-axis) on the free end of the plate. On the other hand, case-10 describes the change of transverse edge crack positions along transverse direction (X-axis) on the free end of the plate. The transverse edge crack on this axis act as a surface defect. Figure 4.20 illustrates schematic diagram these two cases. The longitudinal crack positions (case-9) and the transverse crack positions (case-10) are changed at 5 mm and 10mm intervals respectively. The details of plate and crack properties are in the Table 3.1.

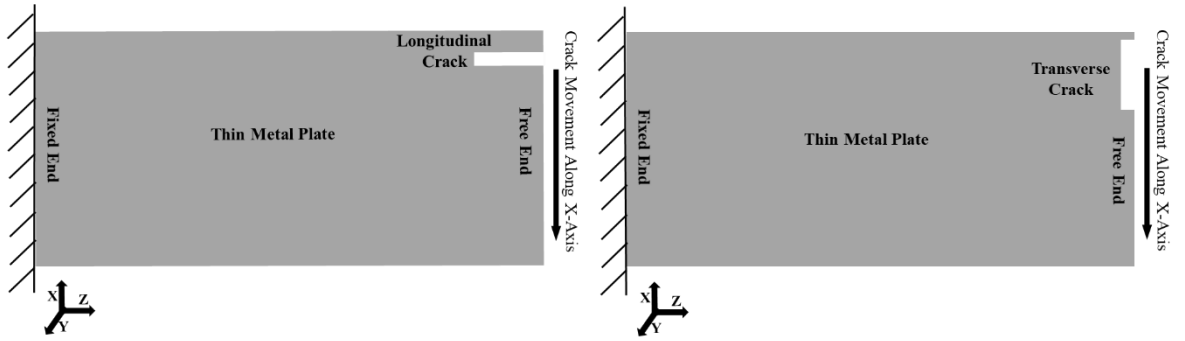

(a) Longitudinal Edge Crack (Case-9) (b) Transverse Edge Crack (Case-10)

Figure 4.20: Schematic Diagram for the Change in Longitudinal (Case-9) and Transverse (Case-10) Crack Positions along the X-axis on Free End

Figure 4.21 shows the comparisons between the change in crack positions of longitudinal edge crack (case-9) and a transverse edge crack (case-10) along X-axis for the first six modes. Here

the relative distance along X-axis is considered as the ratio of the width of the plate and the width of the plate (y/B).

For the longitudinal edge crack, it is found that, the bending modes have very little frequency change. The maximum frequency drop for this mode is 0.3% throughout the 1st mode. While for the torsional modes there are significant frequency drop from the initial edge position to the mid-position. After this point, there is significant frequency gain until the crack position reaches the final edge. The maximum frequency drop for torsional modes is 8.9% at relative distance 37.5% and 62.5% on the 6th mode.

Except the first and sixth mode, all the normalized frequency curves are parabolic when roughly 10% of both edges are not considered. The presence of a longitudinal crack at the free end can be estimated considering the fact that the bending modes having natural frequencies higher (or almost align themselves) than the healthy plate.

For the transverse edge crack (surface defect), the frequency drop for both bending and torsional modes is very low. For bending modes, the maximum frequency drop is 0.3% throughout the 1st mode. For torsional modes, the maximum frequency drop is 0.14% at relative distance 50% on the 6th mode.

For the bending modes, normalized frequency curves are higher than the frequencies of the healthy plate. In the torsional modes for transverse edge crack, the normalized curves are parabolic with symmetry along the middle of the width of plate. The troughs of these parabolas lies slightly below the frequencies of the healthy plate on the same points.

The existence of a transverse edge crack on the free end can be estimated by the presence of three parabolic curves for torsional modes and the three normalized curves higher than that of frequencies of healthy plate for bending modes.

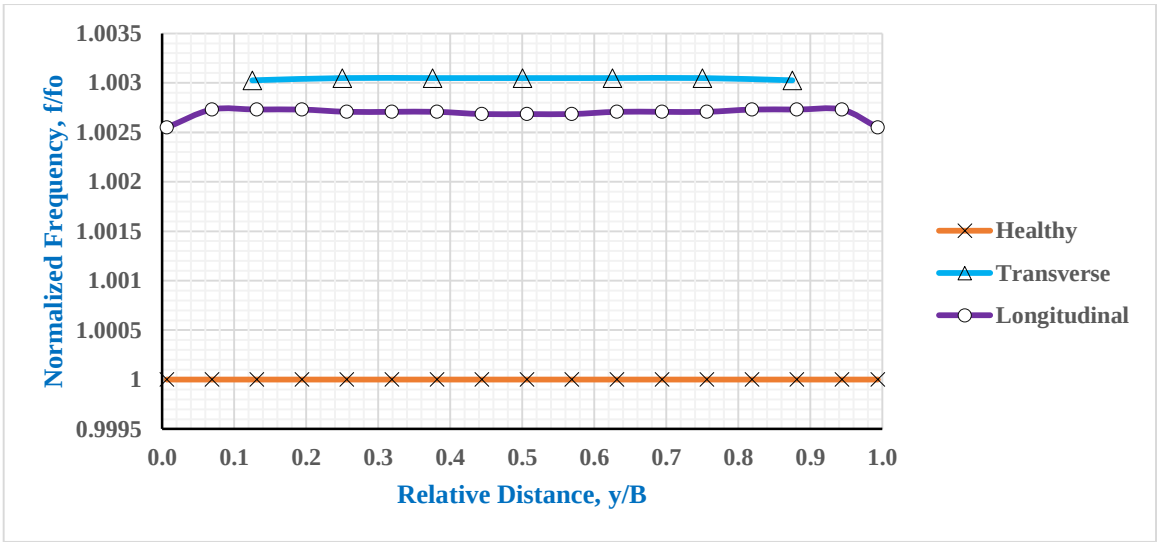

(a) First Mode

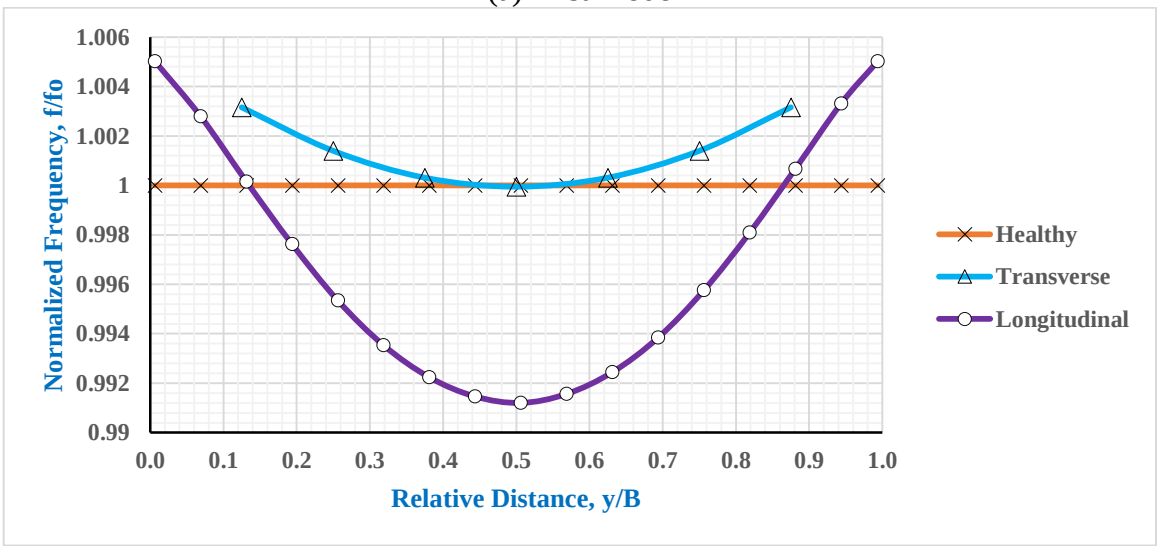

(b) Second Mode

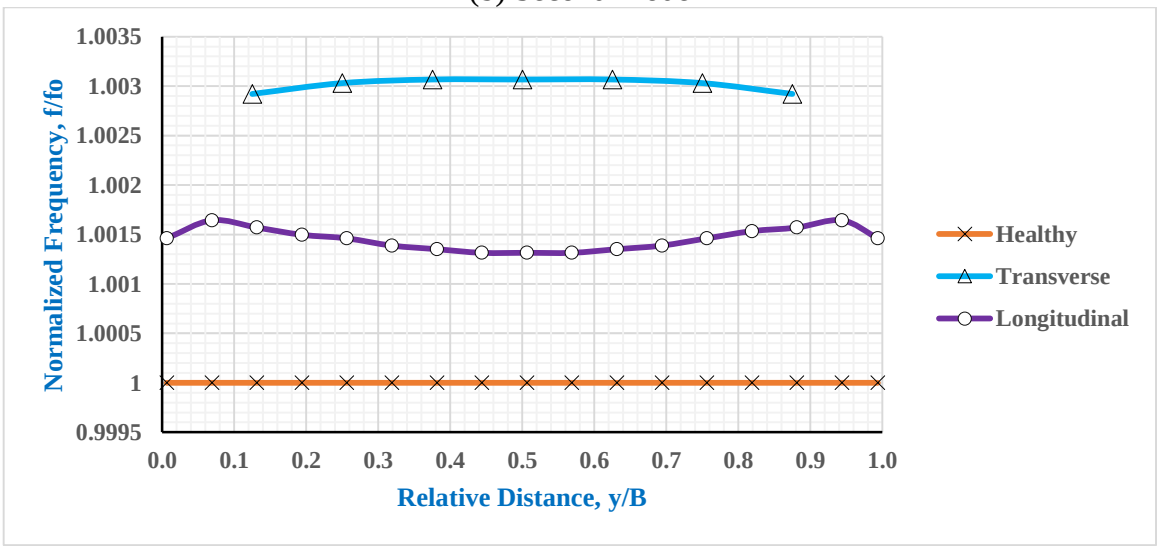

(c) Third Mode

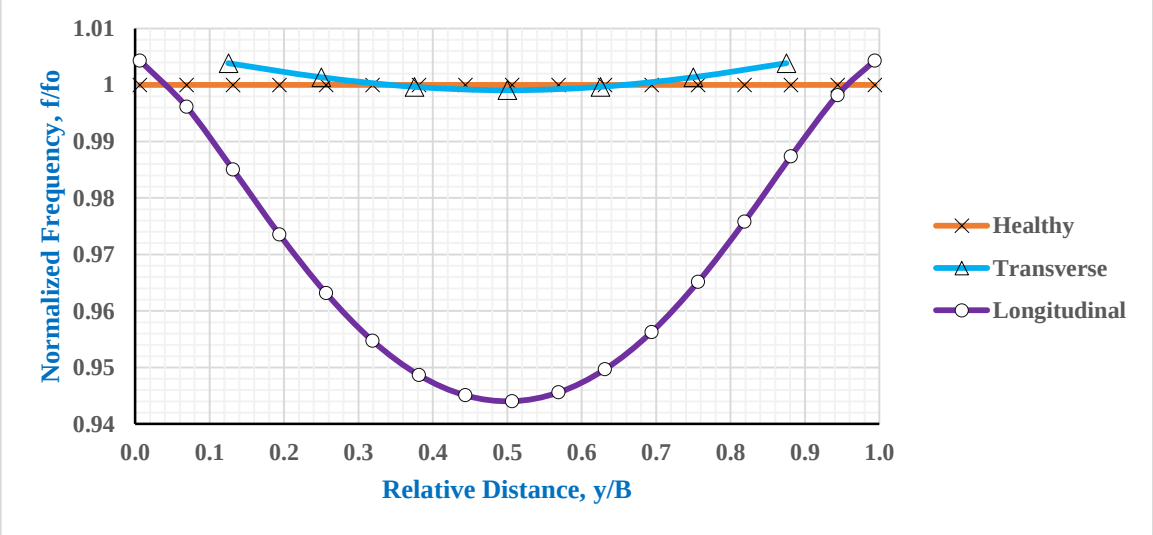

(d) Fourth Mode

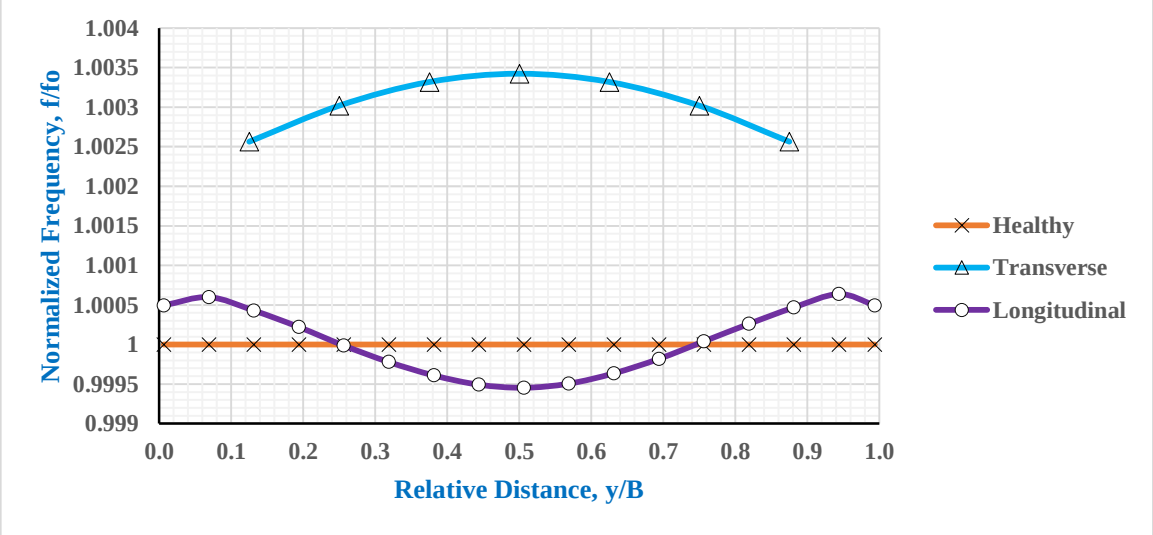

(e) Fifth Mode

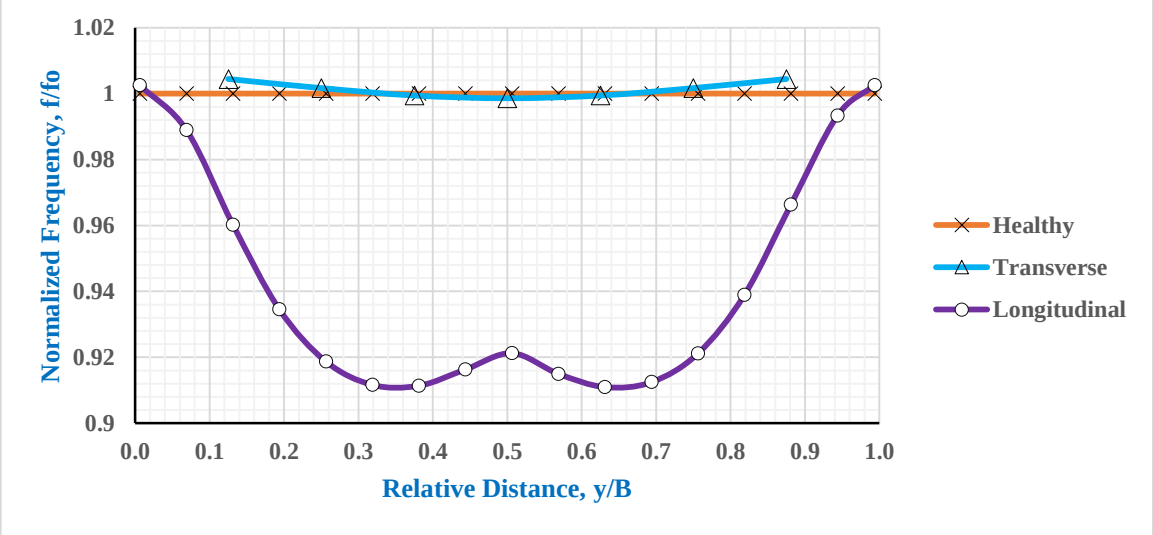

(f) Sixth Mode

Figure 4.21: Difference in Normalized Frequency Between Longitudinal (Case-9) and Transverse (Case-10) Crack Positions along the X-axis on Free End

4.11 Case-11 and Case-12: Inclined Crack Positions at Relative Distance of 21% and 79% along Z-axis

Case-11 describes the inclined crack positions near the fixed end, at relative distance of 21% of the plate along Z-axis. While case-12 describes the inclined crack positions near free end, at relative distance of 79% of the plate along Z-axis. Figure 4.22 illustrates schematic diagram of these two cases. In both these cases, the angular interval is 15^o for the span of 180^o. The details of plate and crack properties are in the Table 3.1

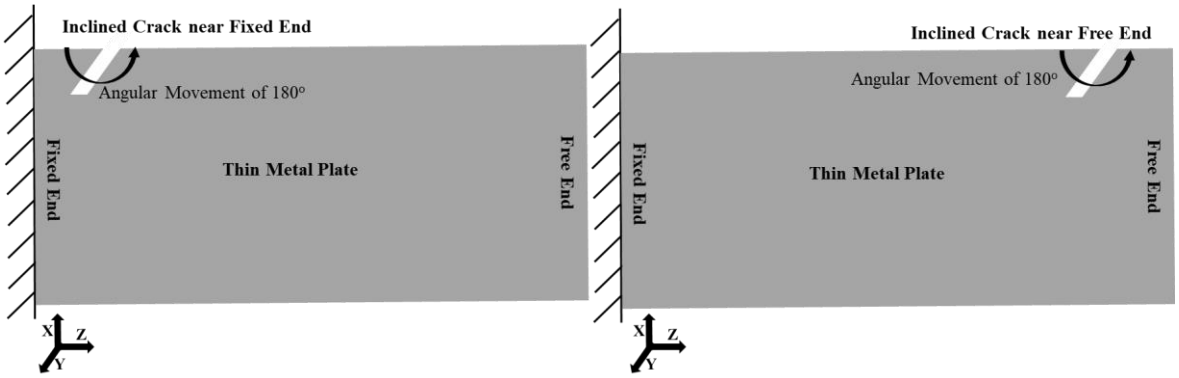

(a) Inclined Crack at x/L=21% (Case-11) (b) Inclined Crack at x/L=79% (Case-12)

Figure 4.22: Schematic Diagram for the Change in Inclined Crack at x/L=21% (Case-11) and x/L=79% (Case-12) along the Z-axis

The study of inclined crack location is taken at relative distance 21% (at 34.5mm mark) from fixed end because this region is found to have maximum frequency drop in first mode of transverse edge crack (found in case-1 to case-4). On the other hand, the study of inclined crack location is taken at relative distance 79% (at 130mm mark) from fixed end because in this region the intersection point in first mode exceeds the natural frequency of a healthy plate (found in case-1 to case-4).

From Figure 4.23, for the inclined crack at relative distance 21%, it is found that, the shape of the normalized curves are parabolic or slightly distorted parabolic with the trough in the region 60^o to 120^o. The maximum frequency drop for bending modes is 4.6% at an angle of 75^o on the

1st mode. While for torsional modes, the maximum frequency drop is 5.4% at an angle of 90^o on the 2nd mode.

From Figure 4.23, for the inclined crack at relative distance 79%, it is found that, the shape of the normalized curves are parabolic or slightly distorted parabolic (except the first mode) with the trough in the region 60^o to 90^o. The maximum frequency drop for bending modes is 4.5% at an angle of 75^o on the 5th mode. While for torsional modes, the maximum frequency drop is 6.4% at an angle of 90^o on the 6th mode.

In both these cases, for all the modes, the lowest frequency drop is at the starting and ending point of the curve where the crack angles are 0^o and 180^o. These are the location where the crack align longitudinally at the edge. The frequency drop at first and second mode are dominant at relative distance 21%, while it is dominant at fifth and sixth modes at relative distance 79%.

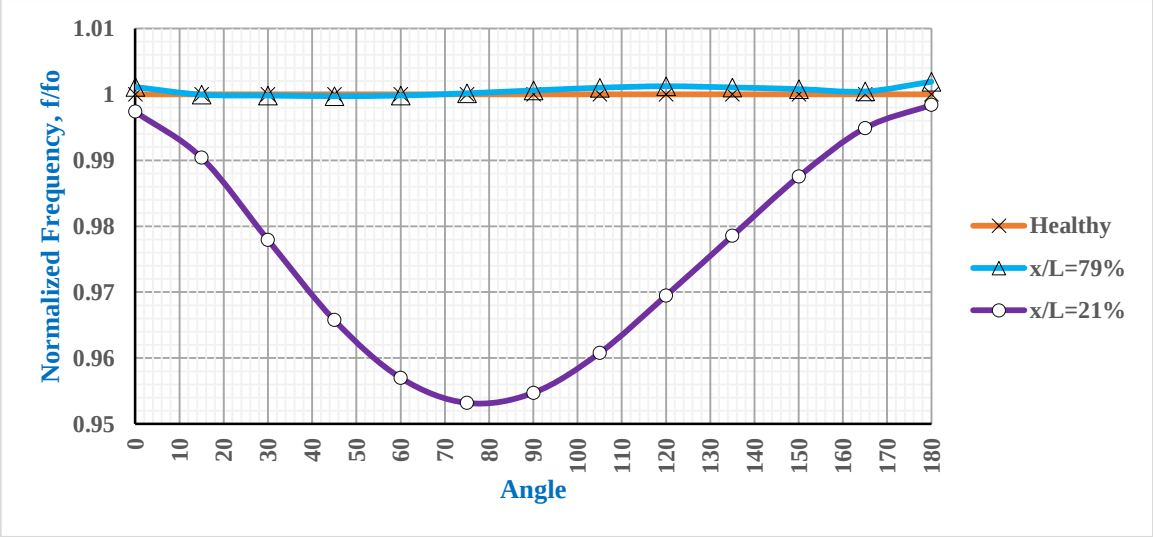

(a) First Mode

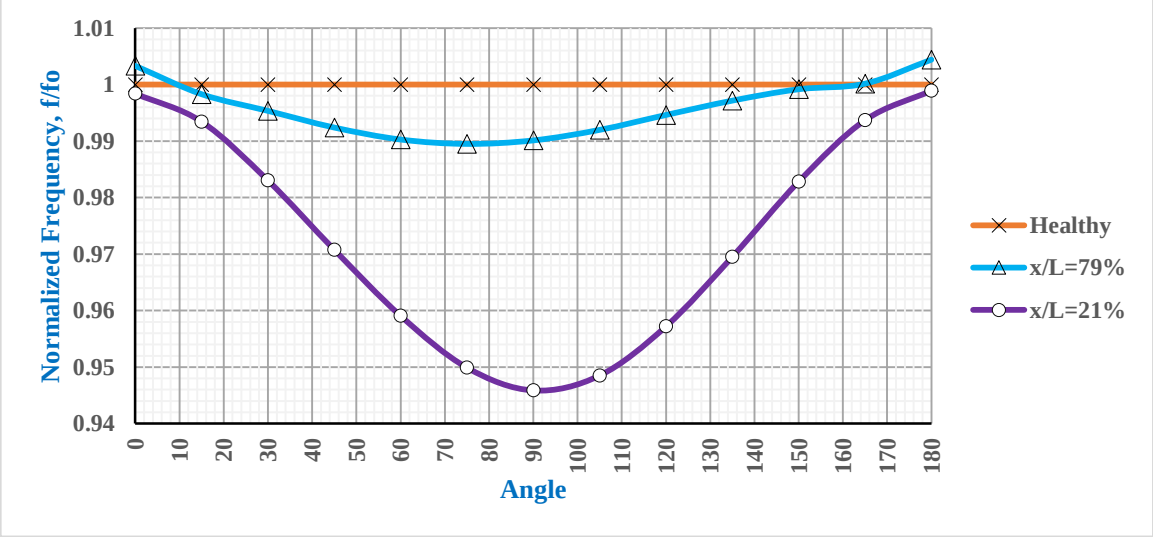

(b) Second Mode

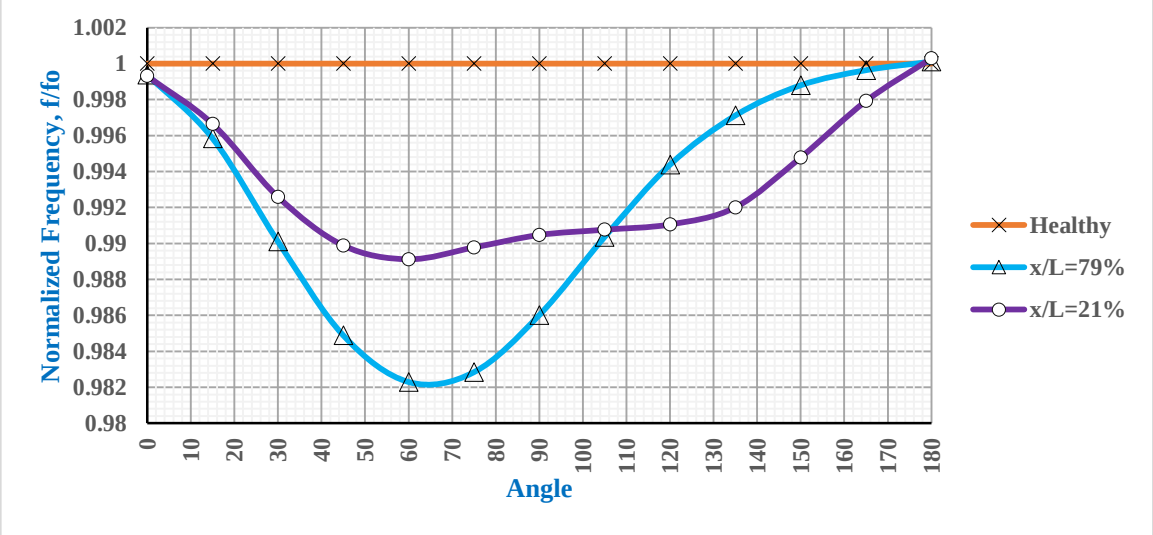

(c) Third Mode

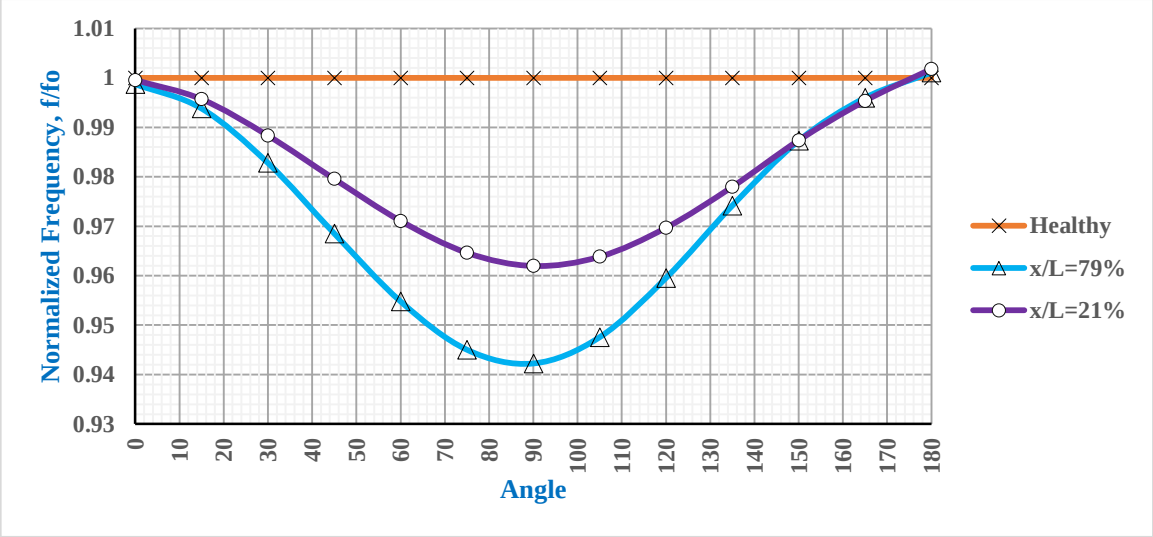

(d) Fourth Mode

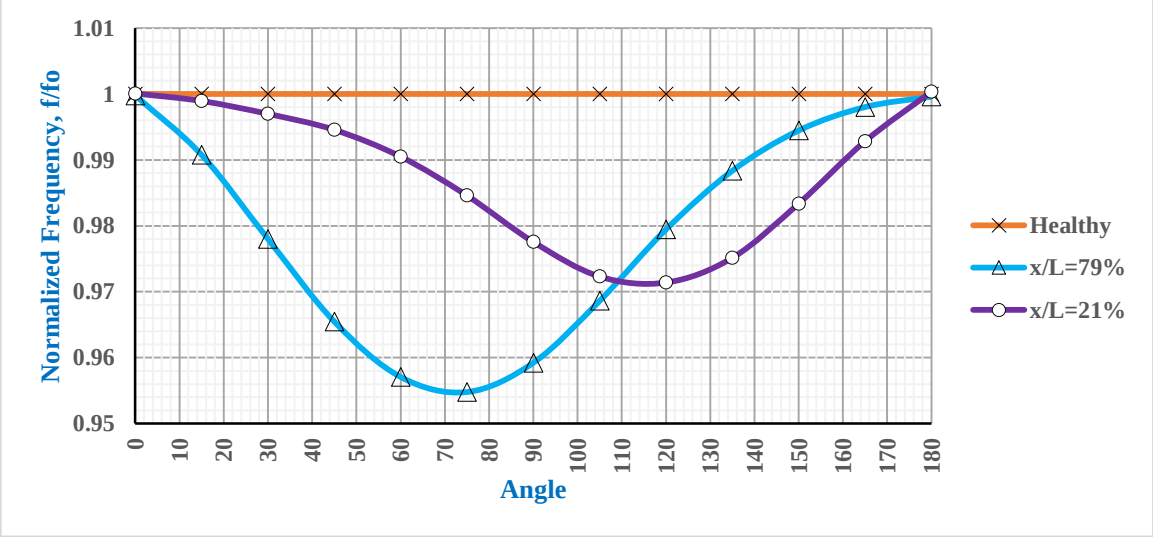

(e) Fifth Mode

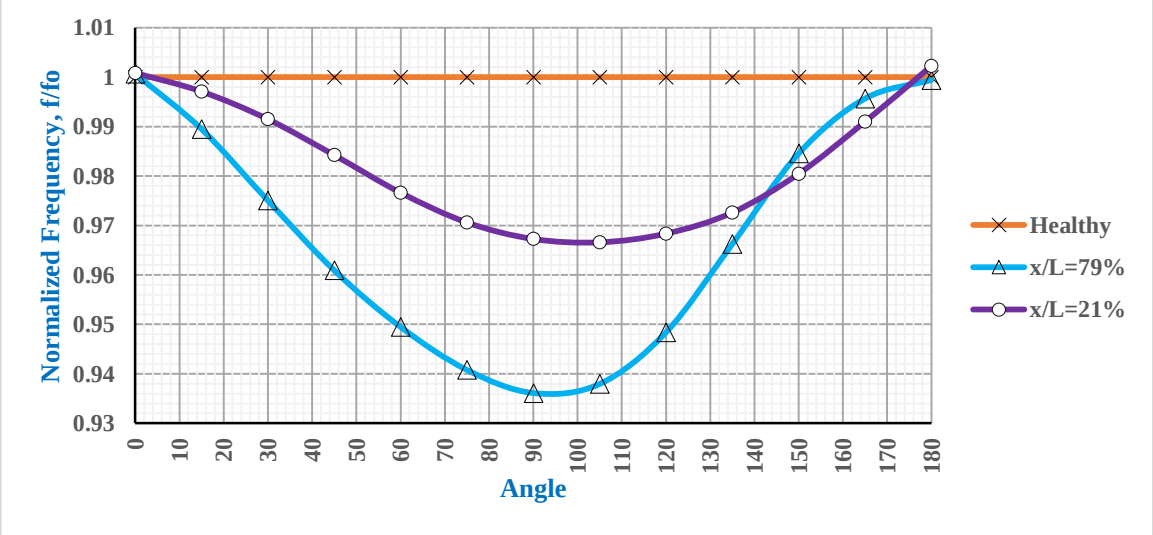

(f) Sixth Mode

Figure 4.23: Difference in Normalized Frequency Between Change in Inclined Crack at x/L=21% (Case-11) and x/L=79% (Case-12) along the Z-axis

4.12 Equivalent von-Mises Stress and Total Deformation

This is a further study of case-1 based on Static Structural Analysis using ANSYS 16.0 Workbench. In this case, the applied load is 1N at downward direction (negative Y-axis) at the mid-point of the free end of the cantilever plate, as shown in Figure 3.2. From this study, maximum and minimum of equivalent von-Mises stress and maximum total deformation is performed for the crack length of 20mm.

In Figure 4.24, the maximum stress rises to peak at relative distance of 9.1% and gradually drops linearly to a lowest point at 78.8% of relative distance. The curve then becomes parallel and align itself over the maximum stress line of the healthy plate. The maximum total deformation curve for static structural analysis follows the same pattern as maximum von-Mises stress. The curve becomes parallel to the maximum deformation of a healthy plate for a of relative distance of 90.9% to 97%. After that, the curve takes a sharp rise in deformation at the free end. Here the total deformation and maximum von-Mises stress have similar pattern.

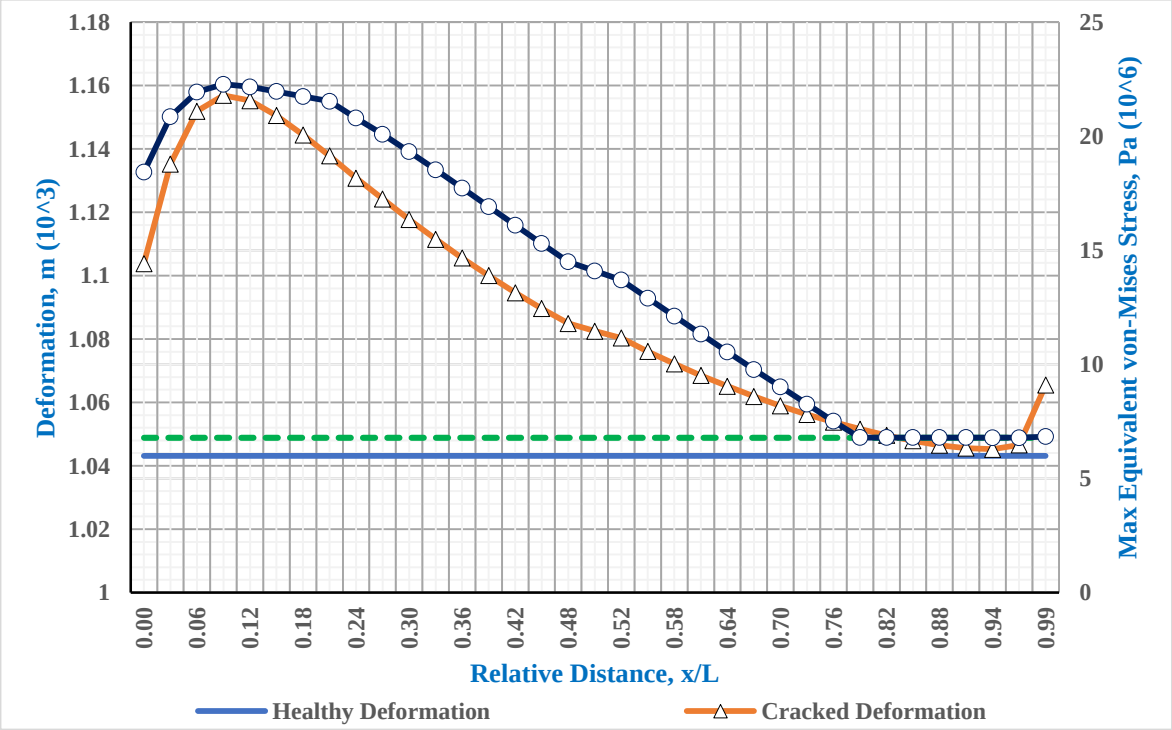

Figure 4.24: Maximum Equivalent von-Mises Stress and Deformation

Both total deformation and the modal deformation is observed along the Y-axis at the free end. The modal deformation of six modes found in Figure 4.25, also represents the rise in deflection and deformation at free end. The torsional modes typically illustrates the deflection behavior at the free end region of the cantilever plate. The deformation for bending modes less than torsional modes.

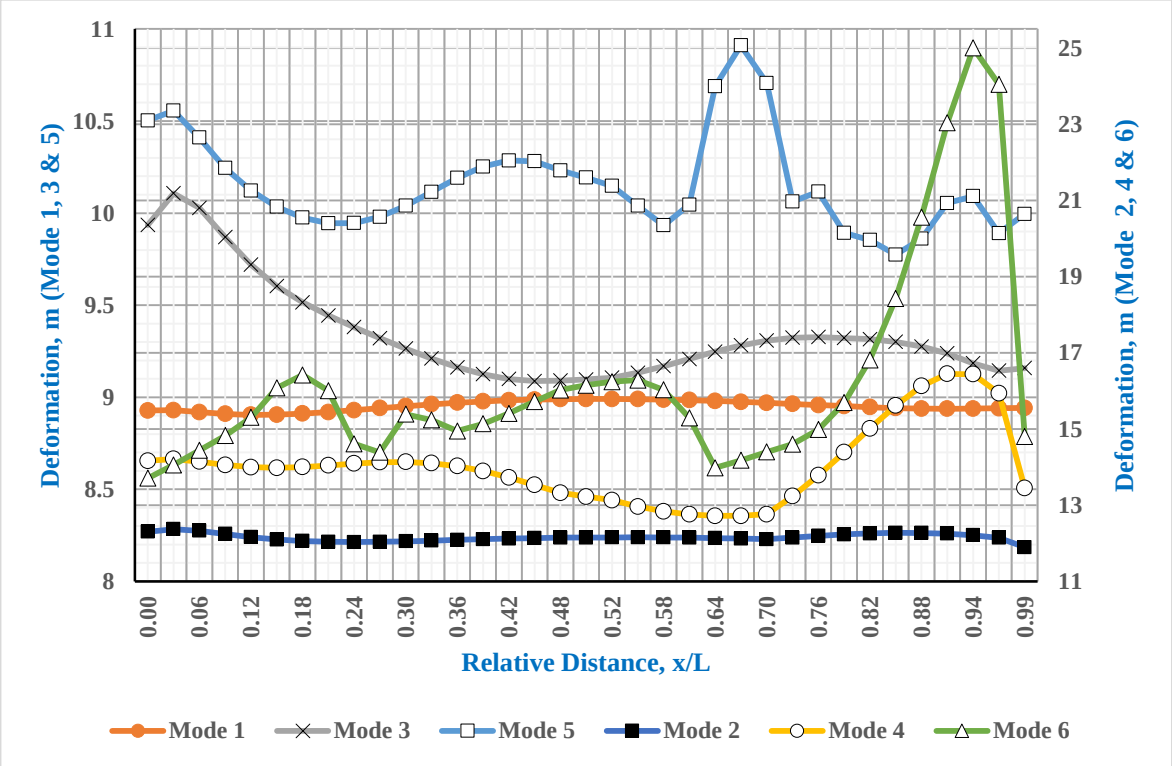

Figure 4.25: Maximum Deformation for Modal Analysis

Another interesting relationship is found between natural frequency of mode 1 and maximum von-Mises stress illustrated in Figure 4.26. Both the curves reaches their respective lowest and highest point at the same relative distance of 9.1%. These curves either cross or become parallel to their respective line of healthy plate at relative distance of 78.8%. This means that the stress curve and normalized frequency curve of mode 1 is reflection of one another.

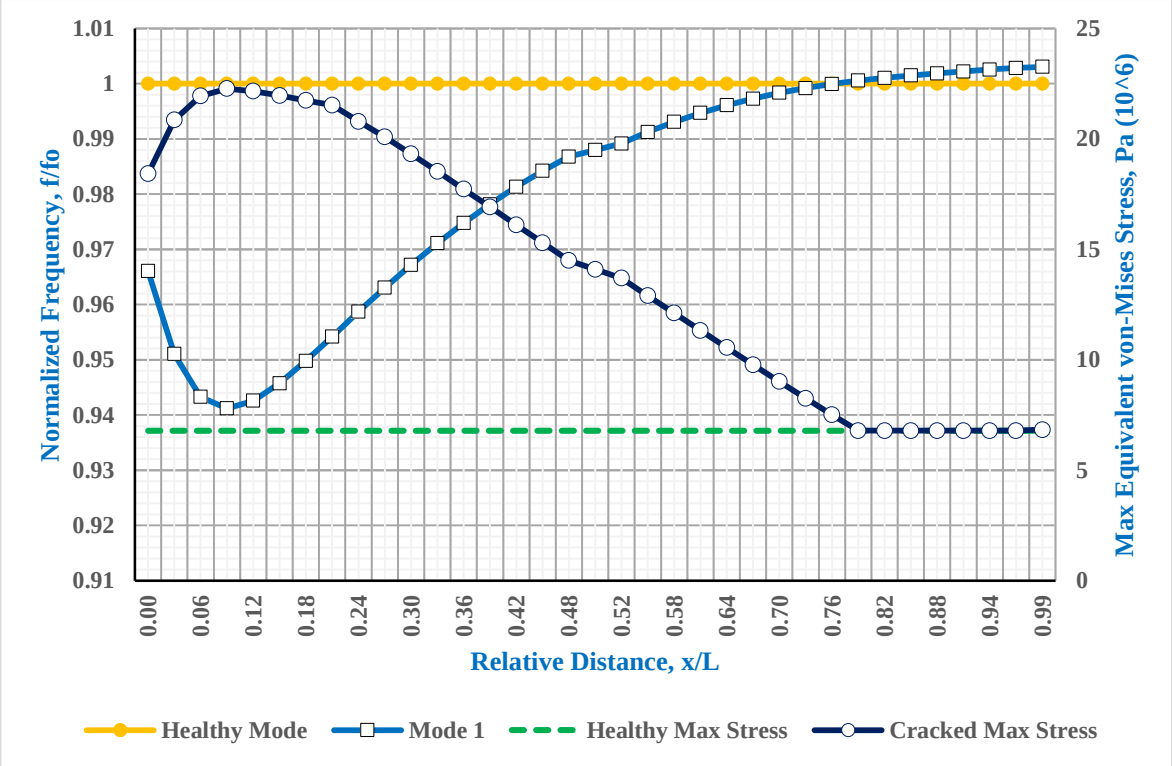

Figure 4.26: Normalized Frequency of Mode 1 and Maximum Equivalent von-Mises Stress

4.13 Mode Shapes, Stress Concentration and Total Deformation at Three Regions

The static stress analysis has been performed to observe the stress concentration due to the change of the position of the crack. As it is not harmonically excited, only the first mode condition can be observed.

In this section, brief discussion of the deformation, stress concentration and first six mode shapes are carried out on cracked and healthy plate. For cracked plate, three distinct points are selected. From the fixed end region, crack on 15mm mark on the plate is considered. This has a relative distance of 9.1%, which shows the maximum frequency drop in mode 1. The mid-point on the plate i.e., 82.5mm mark is taken which has the relative distance of 50%. From the free end region on the plate, 140mm mark is considered. This has a relative distance of 84.8%, where intersection point from mode 1 exceeds or intersect the line of the healthy plate.

4.13.1 Stress Concentration and Total Deformation on Healthy Plate

Figure 4.27 shows the total deformation and von-Mises Stress of a healthy plate when Static Structural Analysis is performed. It is understood that the deformation is maximum at free end when the stress concentration is maximum at fixed end of the healthy plate. The magnitude of stress on the healthy plate is 6.79 MPa. The minimum stress is found at the free end of the plate covering almost 15% of the area.

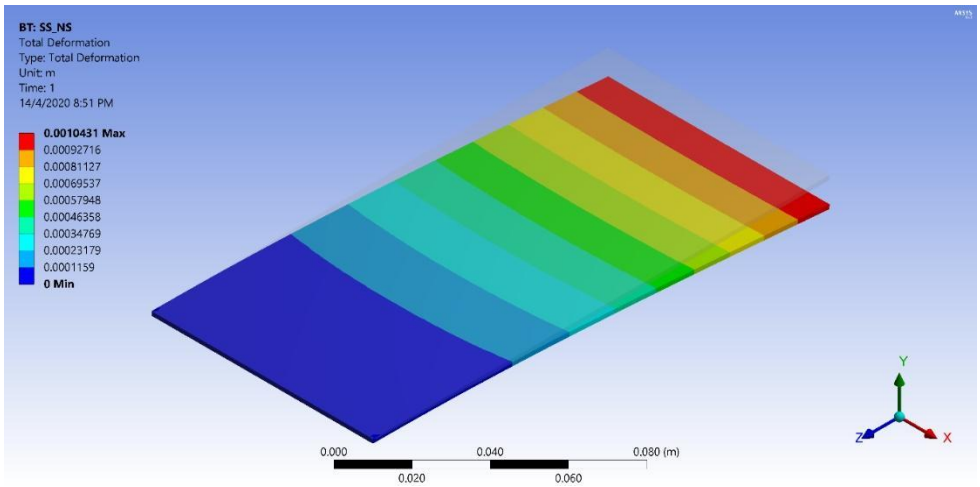

(a) Deformation when 1N force applied downwards at Free end

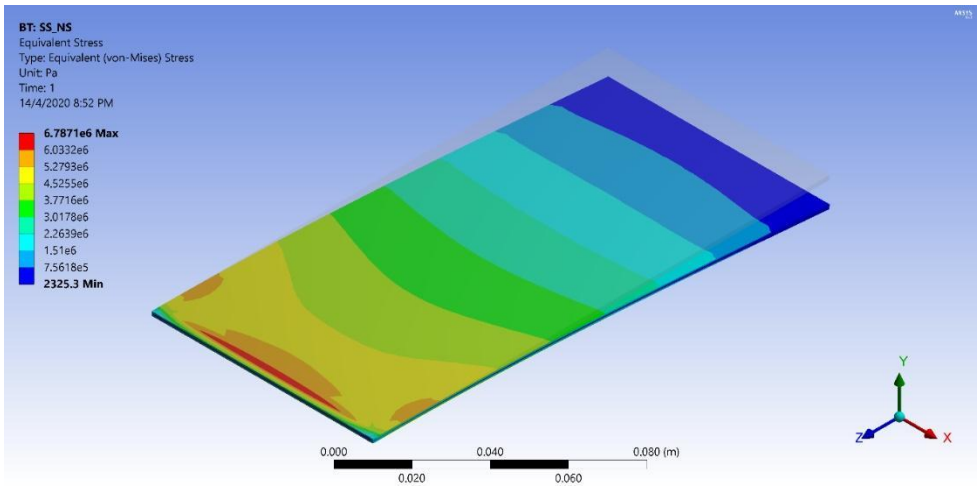

(b) von-Mises Stress

Figure 4.27: Deformation and von-Mises Stress of a Healthy Plate from Static Structural Analysis

4.13.2 Mode Shape of First Natural Frequency

Figure 4.28 illustrates the mode shapes of first natural frequency of for crack at relative distance 9.1% (near fixed end), 50% (mid-region) and 84.8% (near free end)

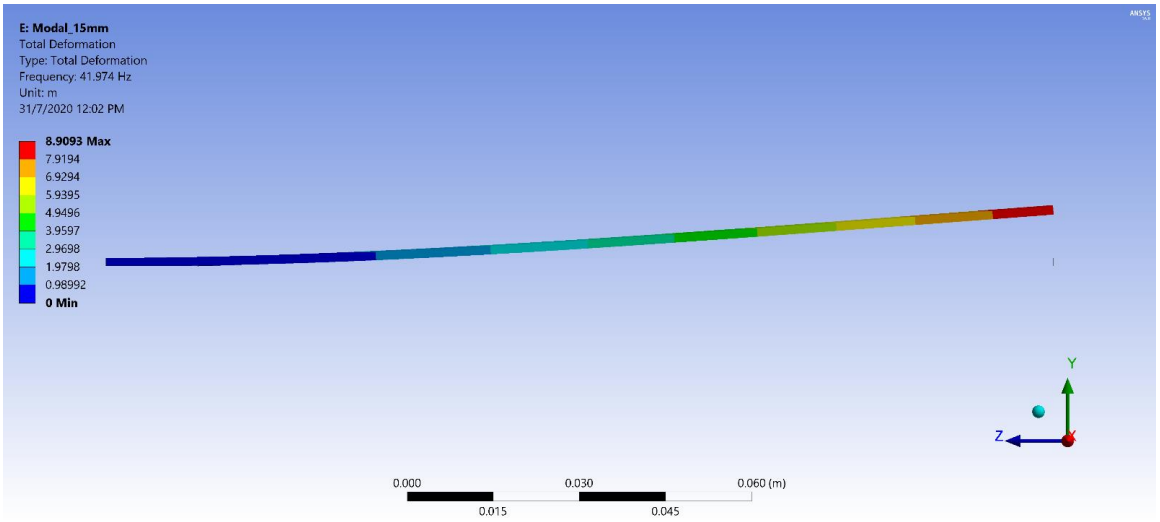

(a) Mode 1 at relative distance of 9.1% near fixed end

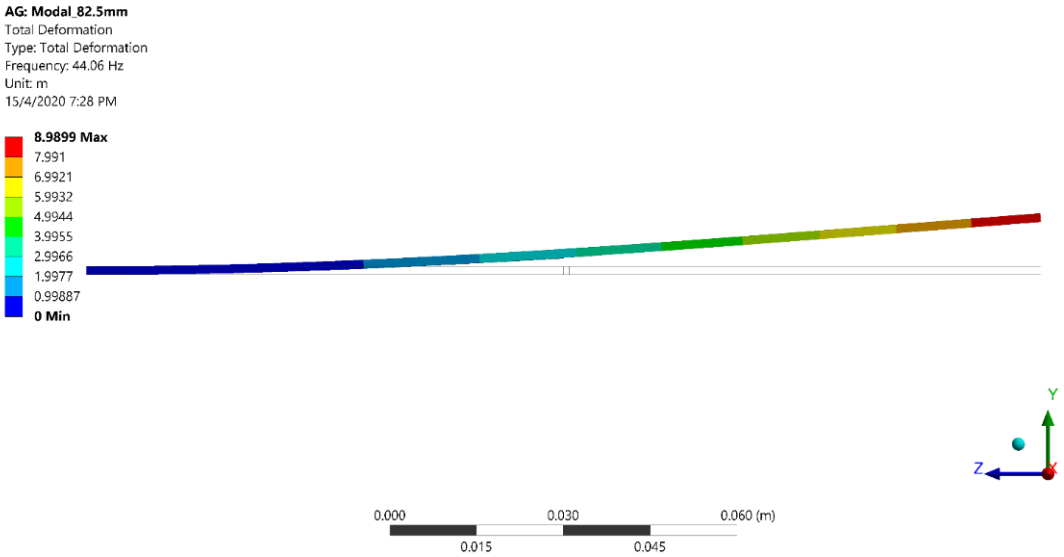

(b) Mode 1 at relative distance of 50% at Mid-region

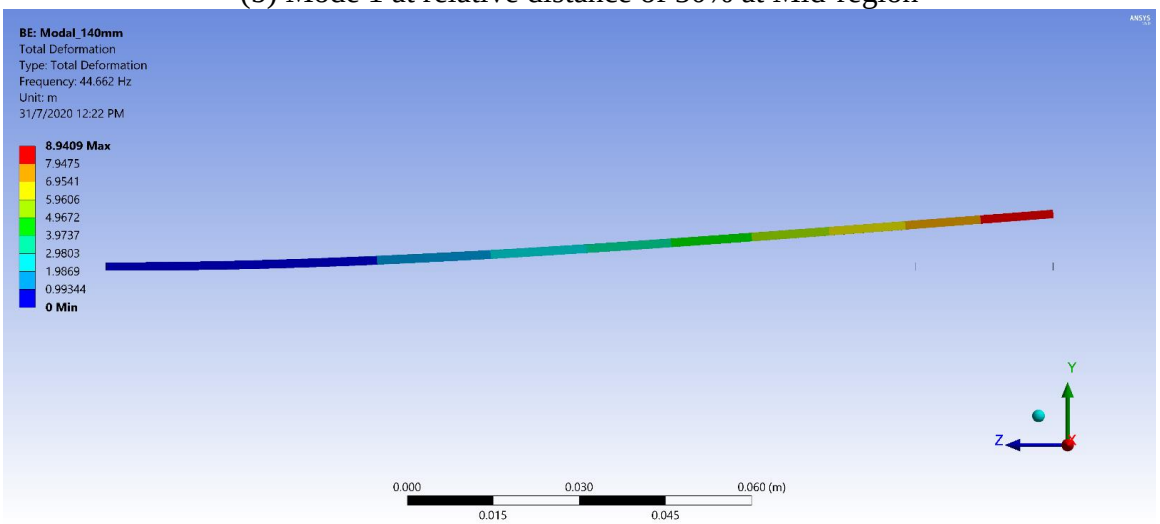

(c) Mode 1 at relative distance of 84.8% near fixed end

Figure 4.28: Mode Shape of First Natural Frequency at Three Regions

Although, the sketch of the mode shape of first natural frequency of the three regions look the same, the drop in frequency is different. The maximum drop in frequency is near fixed end, where the bend is maximum. Any crack at this area would cause the stiffness to decrease resulting in the massive drop in frequency. Moreover, due to the presence of crack in this region breathing phenomena is observed, i.e., opening and closing of the crack.

Along the mid-region, from Figure 4.26, it is understood that there would be rise in frequency. This happens because the effect on stiffness increases on the crack when any crack is found in this area. Another explanation is that due to decrease in breathing effect of the crack, the closeness of the crack decreases, as a result the stiffness of the plate increases in this region causing the natural frequency to rise.

It is discussed earlier that there exist an intersection point at free end where the normalized frequency curve crosses the frequency line of the healthy plate. At the free end, the natural frequency remain constant at maximum value and above the frequency line of the healthy plate. This happens because the effect is mass is more than that of the stiffness. This happens due to the increased deflection when the plate is loaded statically with its own mass at this area. As a result, the stored energy increase and hence increase in natural frequency. Moreover, the effect of breathing phenomena is decreased in this region than in the fixed end and mid-region.

4.13.3 Stress Concentration and Total Deformation Near Fixed End Region

From Figure 4.29, it is found that when crack is located near the fixed end region, the maximum von-Mises stress is located at the inner tip of the crack. At relative distance 9.1%, the plate reaches its maximum stress concentration of 22.27 MPa that is the highest stress value recorded for any crack position along the plate. The corresponding frequency drop is highest as found in Figure 4.26. In theory, the mass located near the fixed end carries the highest amount of strain energy. In this region the bending moment and the mode shape of curvature also reaches

the maximum value. When any piece of mass removed near the fixed end, balance of these properties is hampered and there is a massive drop in frequency in this region.

From Figure 4.24 the total deformation is the highest value for any crack positions along the plate. The minimum stress is found at the free end of the plate covering almost 50% of the area of it.

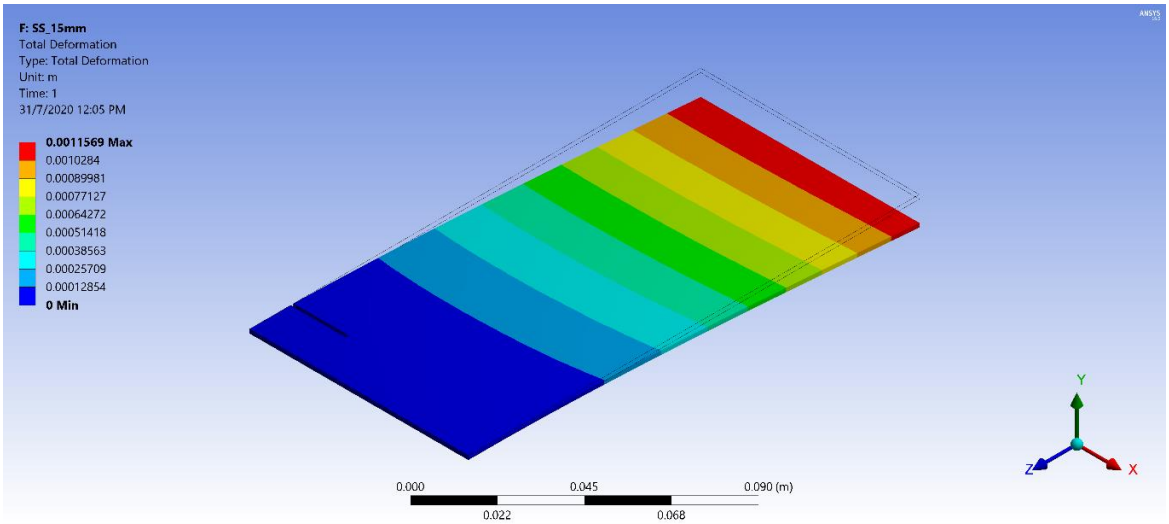

(a) Deformation when 1N force applied downwards at Free end

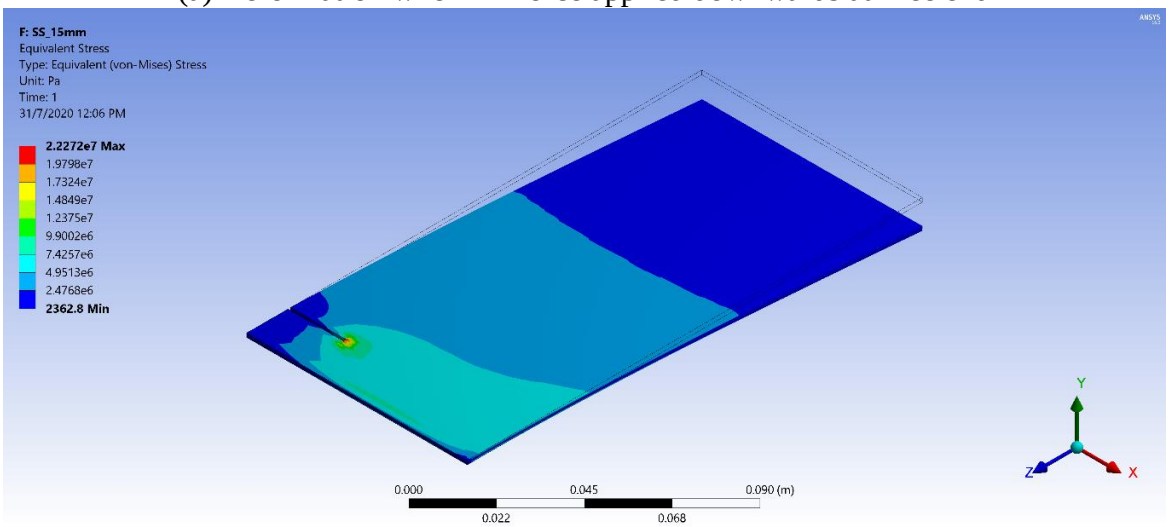

(b) von-Mises Stress

Figure 4.29: Deformation and von-Mises Stress of a Crack at Relative Distance of 9.1% Near Fixed End from Static Structural Analysis

4.13.4 Stress Concentration and Total Deformation at Mid-Region

From Figure 4.30, it is found that when crack is located near the mid- region, the maximum von-Mises stress is located at the inner tip of the crack. This magnitude of this stress is lower (14.09Mpa) than that is found near fixed end. Along with decrease in stress the deformation decreases and natural frequency increases. A possible explanation is that due to decrease in breathing effect of the crack, the closeness of the crack decreases, and the stiffness of the plate increases in this region causing the natural frequency to rise. The minimum stress is found at the free end of the plate covering almost 33% of the area of it.

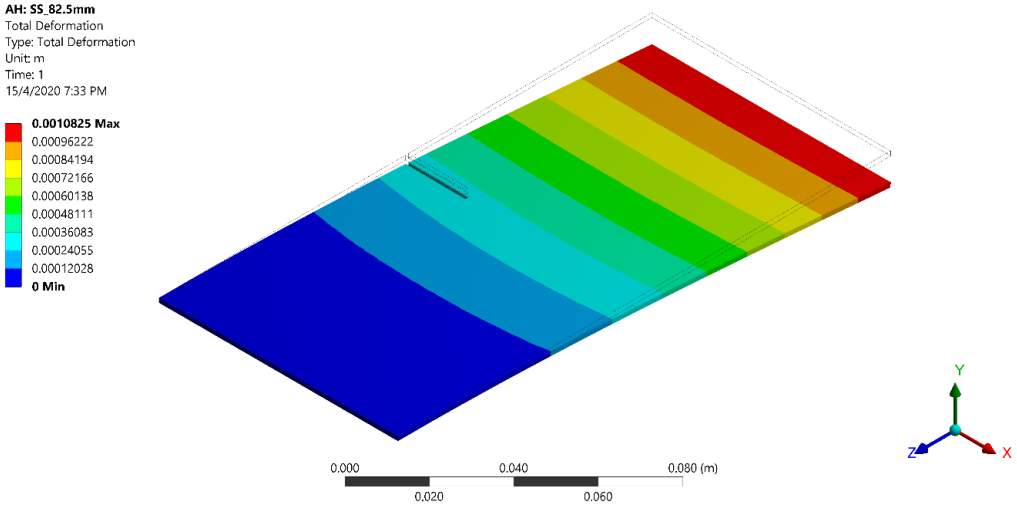

(a) Deformation when 1N force applied downwards at Free end

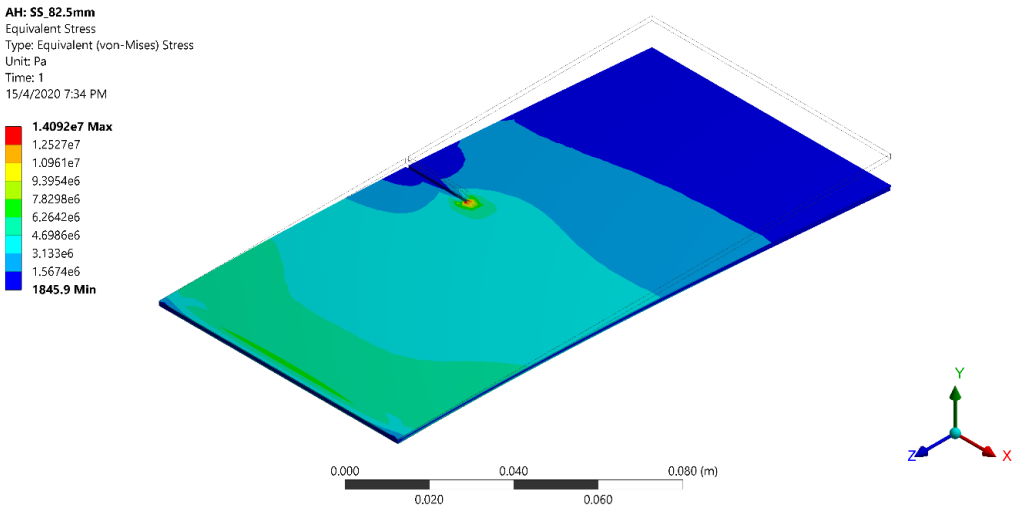

(b) von-Mises Stress

Figure 4.30: Deformation and von-Mises Stress of a Crack at Relative Distance of 50% at Mid-Region from Static Structural Analysis

4.13.5 Stress Concentration and Total Deformation Near Free End

From Figure 4.31, it is found that when crack is located near the free end region, the maximum von-Mises stress is located near the fixed end of the cracked plate. This magnitude of this stress is lowest (6.79MPa) than that is found near fixed end and in mid-region. The magnitude of the stress for this cracked plate and the healthy plate is the same and shows similar deformation.

For rest of the crack locations until the end of free end the magnitude remains constant as shown in Figure 4.26. As the stress becomes constant in this region, the total deformation and the natural frequency of mode 1 also remain constant in this region. This is the region the intersection point is located where the natural frequency of the cracked plate intersects the equation of natural frequency line of the healthy plate.

In this region, the breathing effect reaches to minimum and deflection of the plate becomes maximum. A possible explanation for increased natural frequency is that due to increased deflection of the free end due the presence of crack, the plate is loaded statically with its own mass. As a result, the stored energy increase and hence increase in natural frequency. The minimum stress is found at the free end of the plate covering almost 10 to 15% of the area.

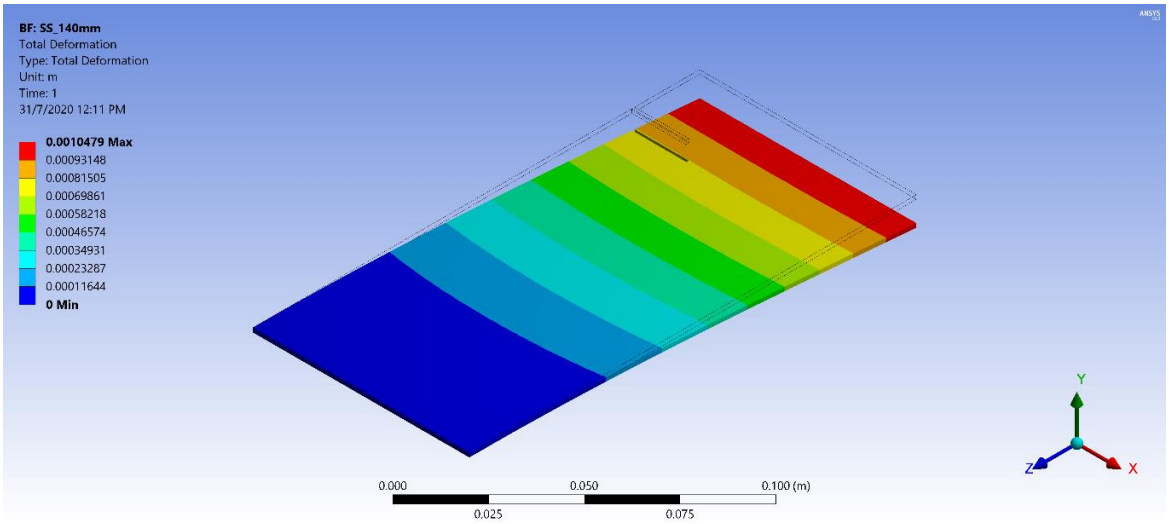

(a) Deformation when 1N force applied downwards at Free end

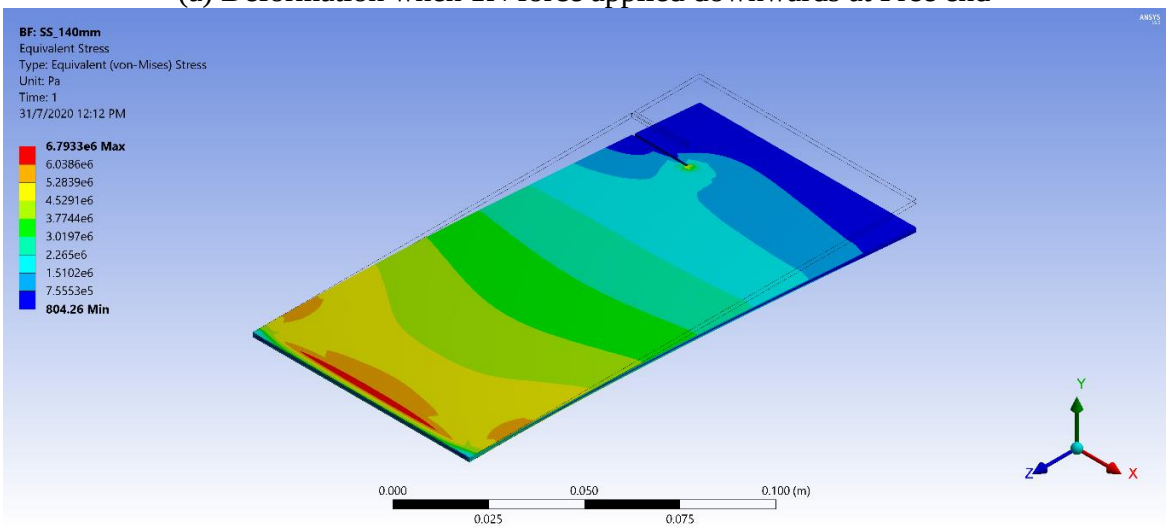

(b) von-Mises Stress

Figure 4.31: Deformation and von-Mises Stress of a Crack at Relative Distance of 84.8% at Free End from Static Structural Analysis

4.13.6 Other Mode Shapes at Three Regions

The explanation of mode shapes are already discussed on section 4.2 and 4.3. Moreover, section 4.13.2 explains the first mode shape of the three regions of the plate. Rest of the mode shapes (from mode 2 to mode 6) is explained in this section.

Figure 4.32 shows the rest of the mode shapes (from mode 2 to mode 6) of crack located at relative distance of 9.1% near fixed end. Similar to healthy plate, for first bending mode and torsional mode there is one nodal point each. For second bending and torsional mode, there are two nodal points and so on. The nodal point increases for subsequent increase in number mode each mode.

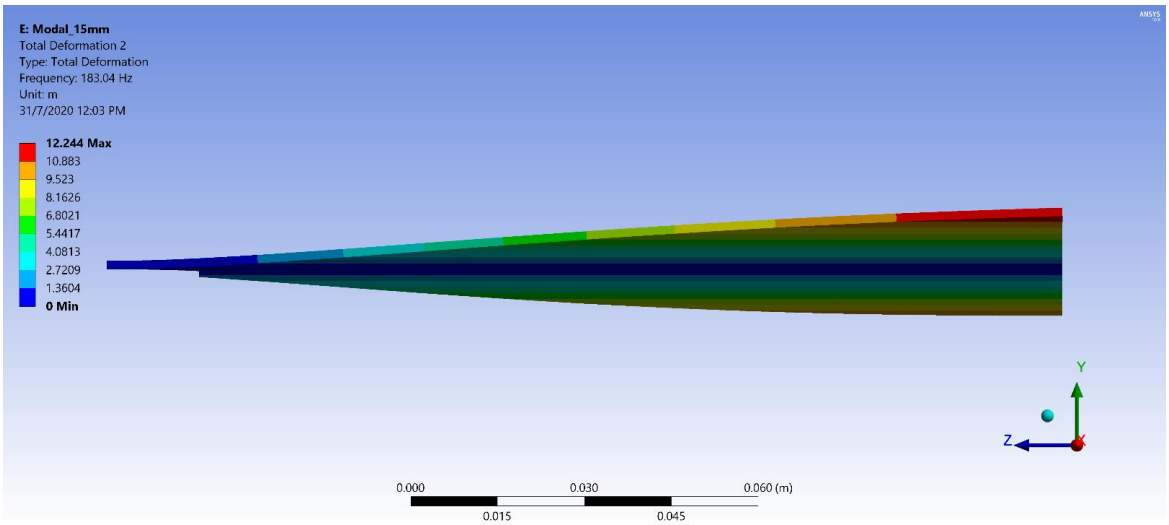

(b) Modal Deformation at Mode 2

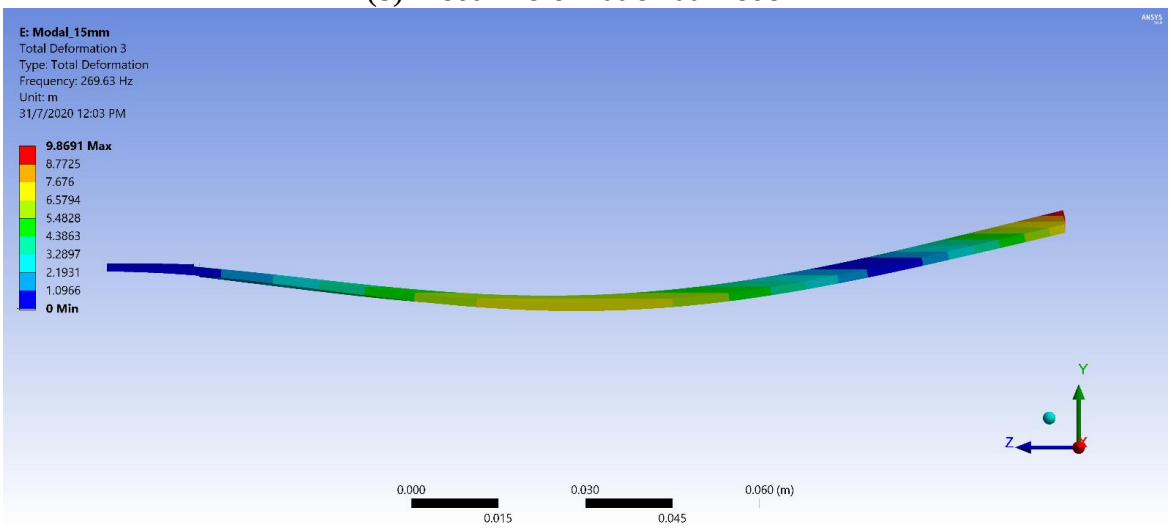

(c) Modal Deformation at Mode 3

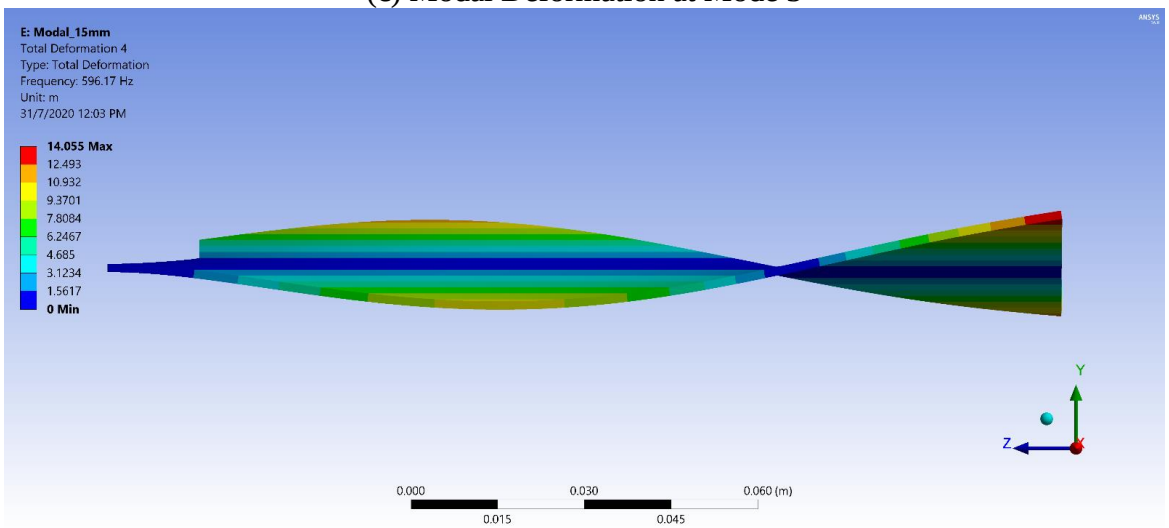

(d) Modal Deformation at Mode 4

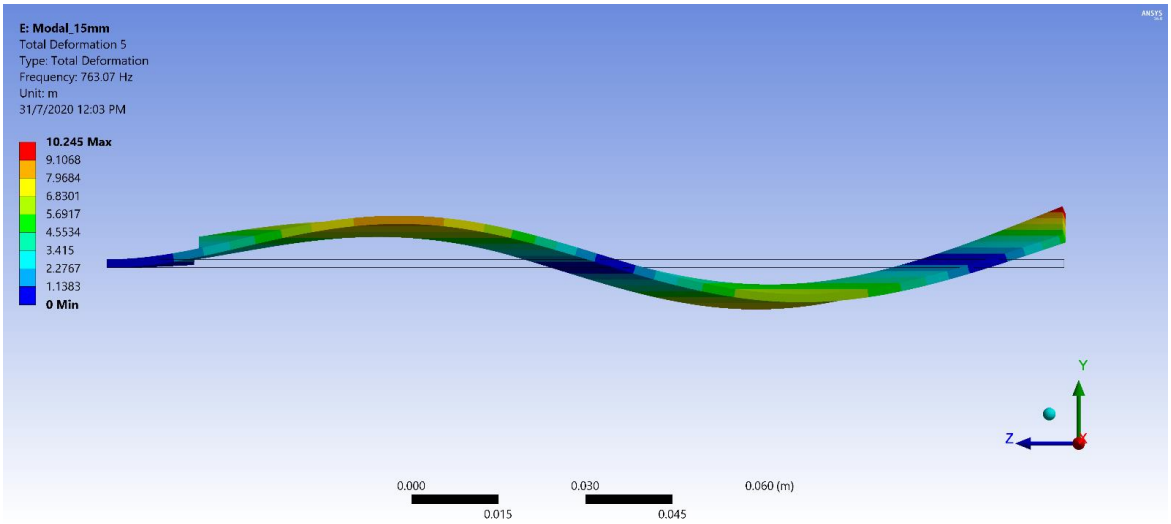

(e) Modal Deformation at Mode 5

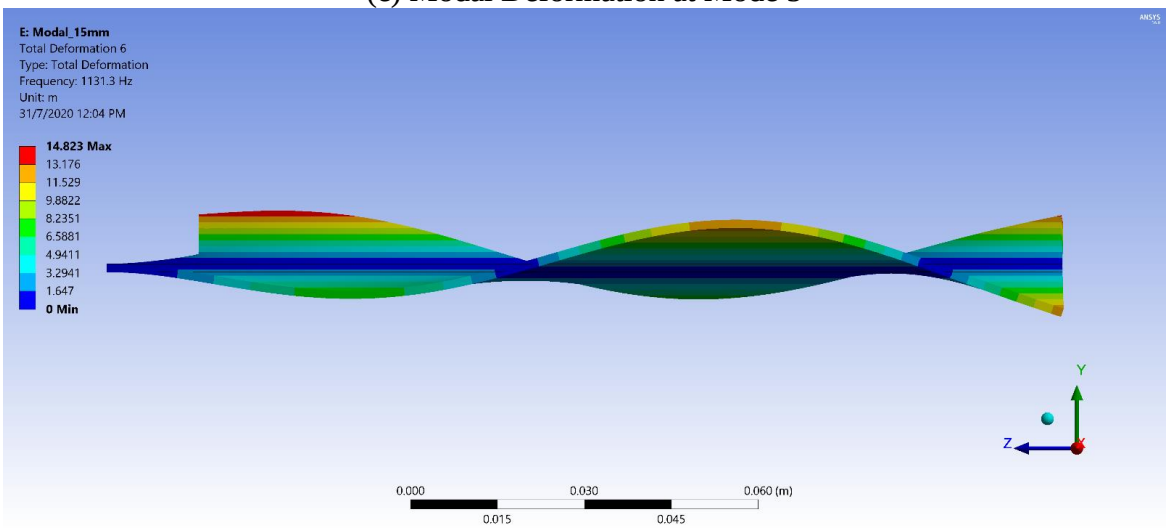

(f) Modal Deformation at Mode 6

Figure 4.32: Other Mode Shapes (Mode 2 to Mode 6) of Crack at Relative Distance of 9.1% Near Fixed End

Figure 4.33 shows the rest of the mode shapes (from mode 2 to mode 6) for crack located at relative distance of 50% at mid-region. The linear motion in bending modes and the angular motion in torsional modes behave the same way as explained in section 4.2 and 4.3. The number of nodal points also remains the same as before. However, the effect of breathing phenomena decreases in this region than in the fixed end.

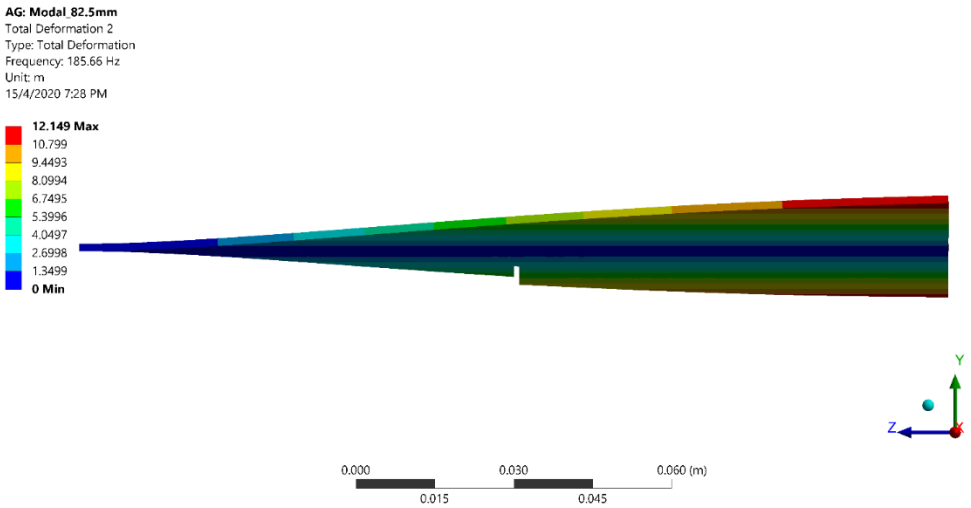

(b) Modal Deformation at Mode 2

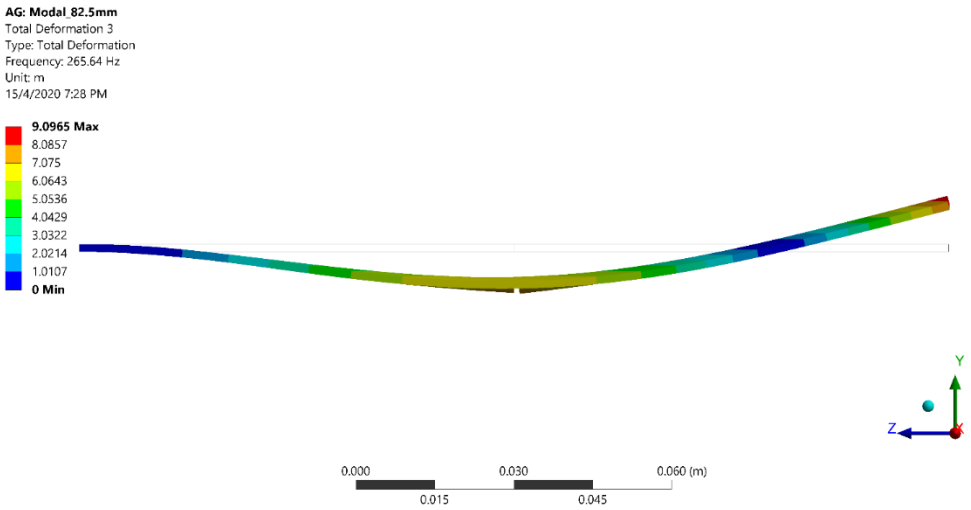

(c) Modal Deformation at Mode 3

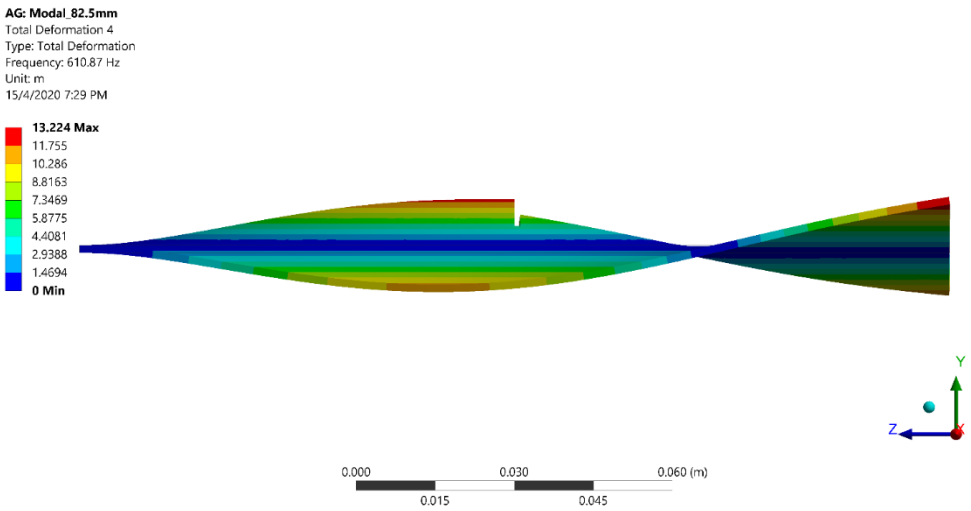

(d) Modal Deformation at Mode 4

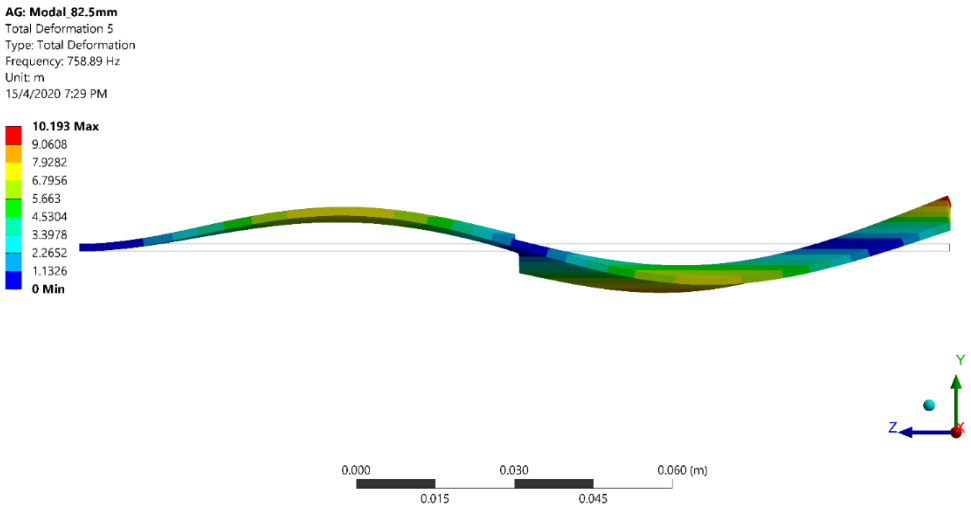

(e) Modal Deformation at Mode 5

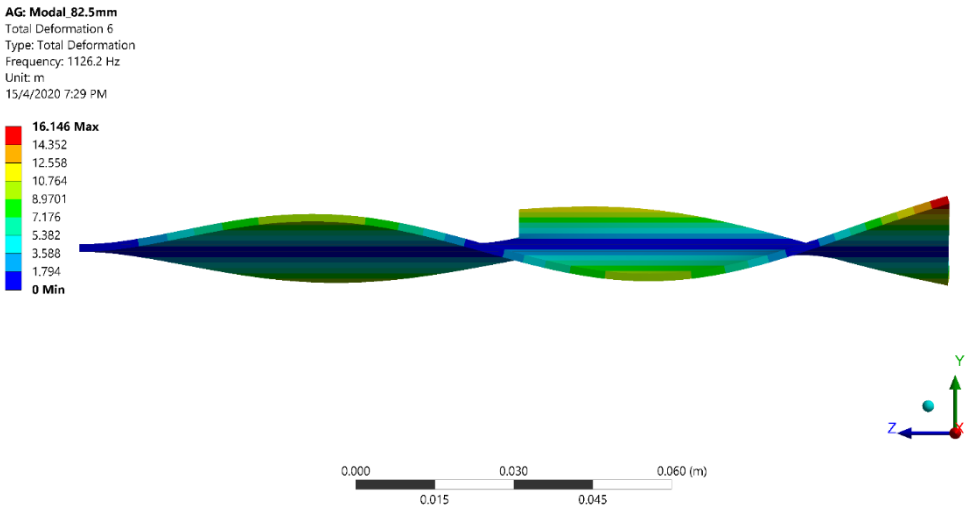

(f) Modal Deformation at Mode 6

Figure 4.33: Other Mode Shapes (Mode 2 to Mode 6) of Crack at Relative Distance of 50% at Mid-Region

Free: Figure 4.34 shows the rest of the mode shapes (from mode 2 to mode 6) for crack located at relative distance of 84.8% at free end region. The linear motion in bending modes and the angular motion in torsional modes behave the same way as explain before. The number of nodal points also remains the same as before. However, the effect of breathing phenomena is decreased further in this region than in the fixed end and mid-region.

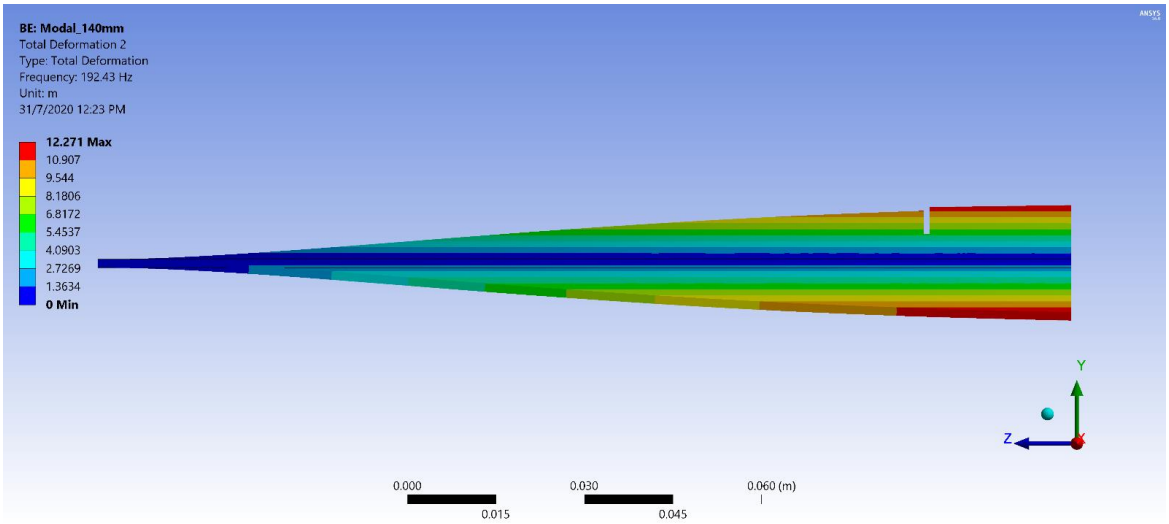

(b) Modal Deformation at Mode 2

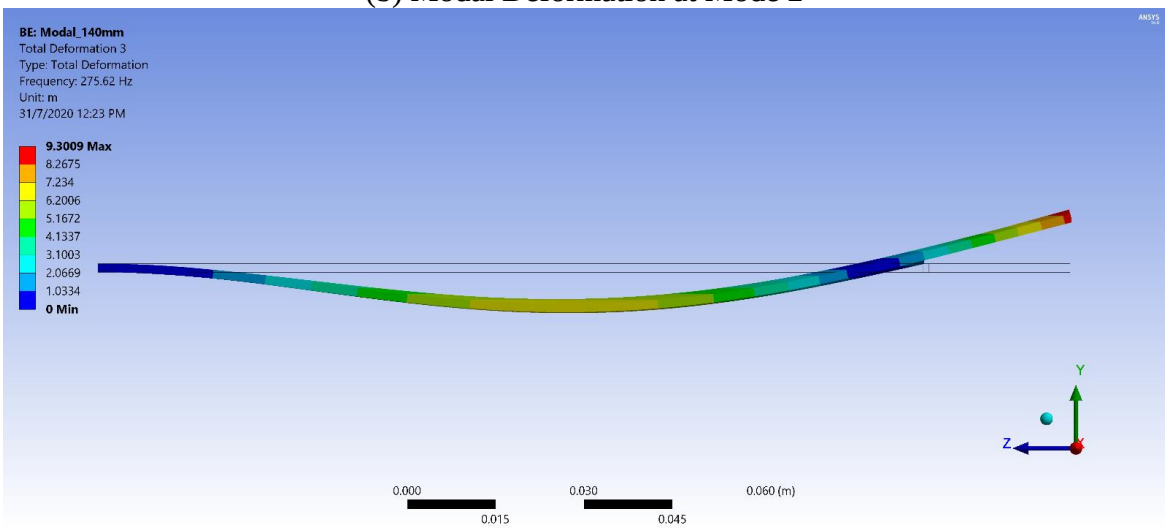

(c) Modal Deformation at Mode 3

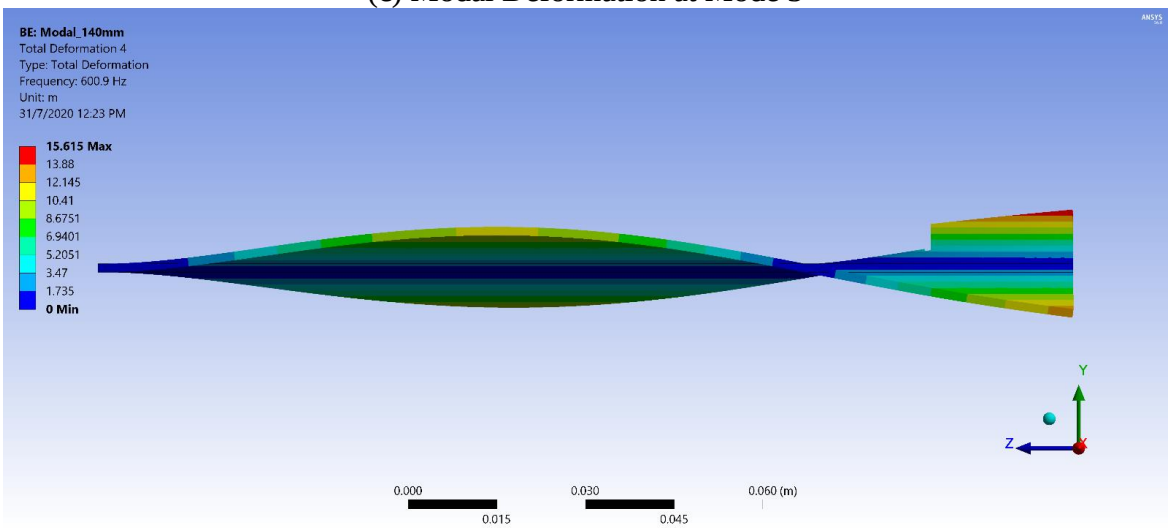

(d) Modal Deformation at Mode 4

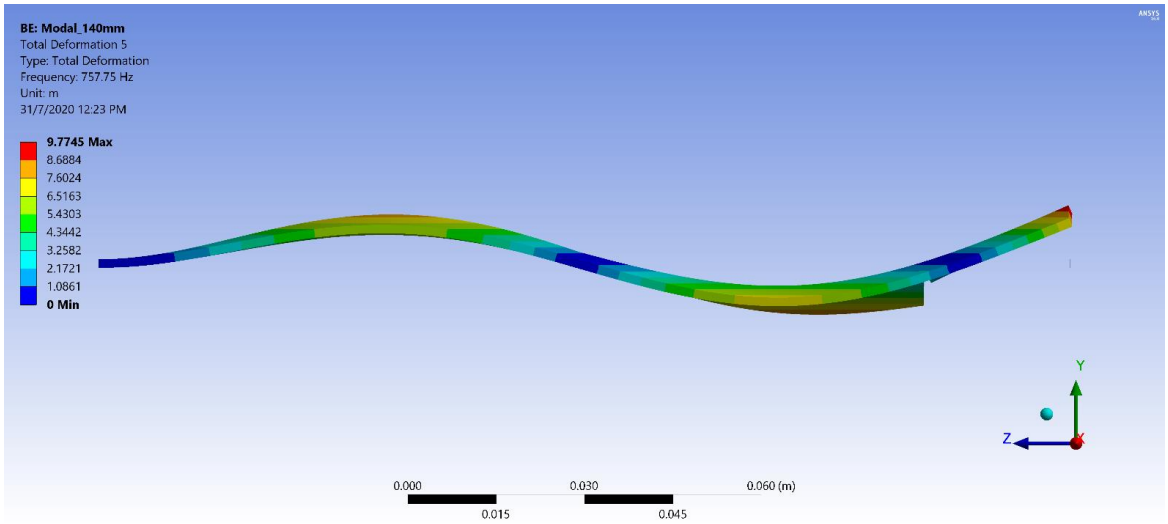

(e) Modal Deformation at Mode 5

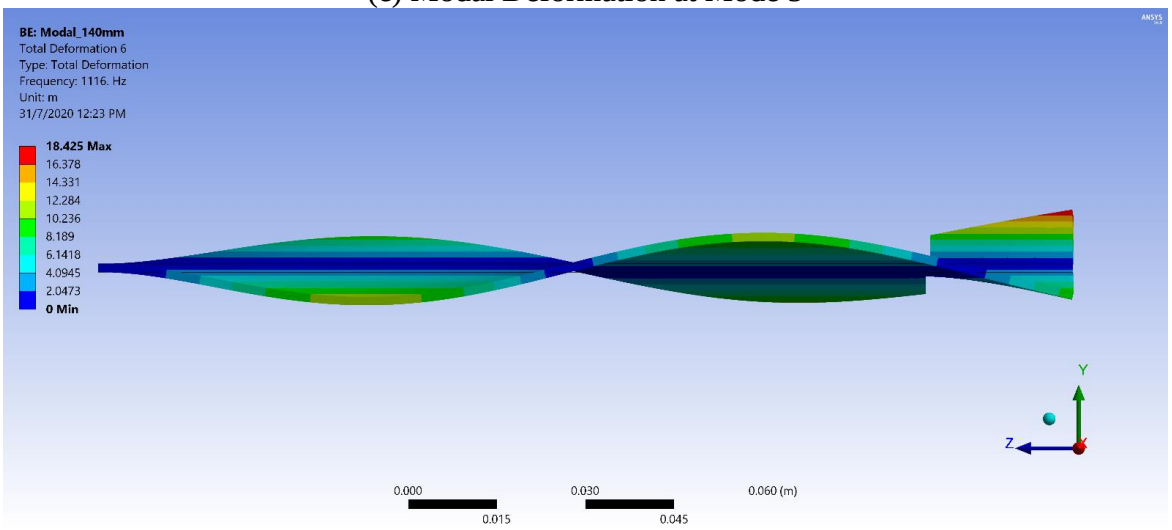

(f) Modal Deformation at Mode 6

Figure 4.34: Other Mode Shapes (Mode 2 to Mode 6) of Crack at Relative Distance of 84.8% at Free End

Chapter 5

Detection of Cracks

5.1 Detection of Cracks of all Cases

Based on the problem specifications mentioned on section 3.4 and Figure 3.6, the Table 5.1 is prepared for the detection of crack on the metal plate. This table is self-explanatory and summarized the percentage of maximum frequency drop for the presence of crack on the plate. The cracks are detectable based on simulation and mode shapes.

Table 5.1: Summary of Crack Detection in the Research

		Frequency Drop		
Case	**Case Description**	**Bending Mode**	**Torsional Mode**	**Remarks**
1	Transverse Edge Crack along Z-axis (AA)	Have Distinct Pattern	Have Distinct Pattern	Detectable
	Max Frequency Drop	*5.9% at x/L=9.1% on 1st Mode*	*7.4% at x/L=84.8% on 6th Mode*	
2	Change of Transverse Edge Crack Lengths along Z-axis	Similar Pattern as Case-1 Larger the Crack Length: -Higher the Frequency Drop -Intersection Point Moves towards Free End	Similar Pattern as Case-1 Larger the Crack Length: -Higher the Frequency Drop -Intersection Point Moves towards Free End	Detectable when Crack Length is more
	Max Frequency Drop *(a=10,20,30mm)*	*1.8%, 5.9% & 11.4% respectively at x/L=9.1% on 1st Mode*	*1.4%, 7.4% & 20% respectively at x/L=81.8%, 84.8%, 90.9% on 6th Mode*	
3	Change of Transverse Edge Crack Widths along Z-axis	Similar Pattern as Case-1 Larger the Crack Width: -No Effect on Frequency Drop -Intersection Point Moves towards Fixed End	Similar Pattern as Case-1 Larger the Crack Width: -No Effect on Frequency Drop -Intersection Point Moves towards Fixed End	Detectable when Crack Length is more irrespective of crack width
	Max Frequency Drop *(b=0.5,1.0,1.5mm)*	*5.7%, 5.9% & 6.0% respectively at x/L=9.1% on 1st Mode*	*7.1%, 7.4% & 7.6% respectively at x/L=84.8% on 6th Mode*	
4	Change of Crack Depths along Y-axis	Very Little change until crack is thorough	Very Little change until crack is thorough	Detectable when thorough
	Max Frequency Drop	*0.87% at Fixed End (c/H<1)* *5.9% at Fixed End (c/H=1)* *on 1st Mode*	*0.92% at Free End (c/H<1)* *7.4% at Free End (c/H=1)* *on 6th Mode*	
5	Transverse Edge Crack along Z-axis (SS)	Have Distinct Pattern Similar to Case-1	Have Distinct Pattern Similar to Case-1	Detectable
	Max Frequency Drop	*5.8% at x/L=9.1% on 1st Mode*	*7.3% at x/L=84.8% on 6th Mode*	

		Frequency Drop		
Case	**Case Description**	**Bending Mode**	**Torsional Mode**	**Remarks**
6	Embedded Transverse Crack along Mid Z-axis	Similar Pattern as Case-1	Very Low	Detectable
	Max Frequency Drop	*4.2% at x/L=6.1% on 1st Mode*	*0.26% at x/L=90.9% on 6th Mode*	
7	Longitudinal Edge Crack along Z-axis	Very Low	Very Low	Undetectable (Surface Defect)
	Max Frequency Drop	*0.29% at x/L=6.1% on 1st Mode*	*0.25% at x/L=0% on 2nd Mode*	
8	Embedded Longitudinal Crack along Mid Z-axis	Very Low	Very Low but Sharp Drop at Only Free End	Detectable only at Free End
	Max Frequency Drop	*0.58% at x/L=0% on 1st Mode*	*1.7% at x/L=84.8% on 6th Mode* *7.9% at x/L=87.9% on 6th Mode (Free End)*	
9	Longitudinal Edge Crack along X-axis	Very Low	Visible at Mid-Region	Detectable at Mid Region
	Max Frequency Drop	*0.3% throughout the 1st Mode*	*8.9% at y/B=38.1% & 63.1% on 6th Mode*	
10	Transverse Edge Crack along X-axis	Very Low	Very Low	Undetectable (Surface Defect)
	Max Frequency Drop	*0.3% throughout the 1st Mode*	*0.14% at y/B=50% on 6th Mode*	
11	Inclined Crack Positions near Fixed End on Z-axis	Moderate (First two Modes)	Moderate (First two Modes)	Detectable when Inclined Crack at 60^o to 120^o
	Max Frequency Drop	*4.6% at Angle=75^o on 1st Mode*	*5.4% at Angle=90^o on 2nd Mode*	
12	Inclined Crack Positions near Free End on Z-axis	Moderate (Last two Modes)	Moderate (Last two Modes)	Detectable when Inclined Crack at 60^o to 90^o
	Max Frequency Drop	*4.5% at Angle=75^o on 5th Mode*	*6.4% at Angle=90^o on 6th Mode*	

It is seen that surface defects (case-7 and case-10) for both longitudinal and transverse direction could not be traced from the research. While the inclined cracks (case-11 and case-12) within the angle between 60^o to 120^o could only be traced if the crack positions are within the nodal region. Torsional modes (case-6) have no effect on embedded transverse crack at mid-axis along longitudinal direction because of the twisting moment is zero. The embedded crack would only be detectable through bending modes, with the limitation that the crack position must be near nodal region. On the other hand, embedded longitudinal crack at mid-axis along longitudinal direction (case-8) would remain undetectable throughout the axis. The only crack location where crack detection is possible is at the free end of the plate. It is only found on the torsional modes where the frequency drop is abrupt and sharp on the normalized frequency curve. Crack, which is not completely thorough, (case-4) would remain undetectable in the research. Crack width have negligible effect on frequency drop (case-3). Therefore, the change in crack length plays vital role in detection of crack. The larger the crack length the higher the frequency drop (case-2).

Considering all the above and the Figure 4.6 into account, it is observed that number of bends (i.e. number of nodes) in case of bending increases with increased modes. Similar things happen in case of torsional modes for increased number of twists. Any crack that is located in this region experiences massive frequency drop than any other regions. This is because the influence of stiffness of the plate is greater in this region.

5.2 Experimentation

From the modal analysis, it is expected that the significance difference of 6% to 10% and more could be detectable through experimentation. Moreover, carrying out harmonic analysis could result change of amplitudes in different positions and using frequency response function (FRF), amplitude and natural frequency could be obtained. Besides, the variation of amplitude for cracked plate and the healthy plate could be attained and distinguished. The obtained results could be validated through experimentation and could be used for detection of crack, although the change of natural frequency is not very high. Unfortunately, the research only considered the results from numerical simulation of different cases. Due to outbreak of COVID-19, no experimentations were conducted. If experimentation would have been done, the results attained could be verified for further analysis. In that case, harmonic analysis could have been incorporated to authenticate the results analytically in some specific cases with more significant differences for detection of cracks.

Chapter 6

Conclusion and Recommendation

6.1 Conclusion

Most of the scientific research is conducted with cantilevered cracked beam with different approaches into account for detecting cracks. These include bilinear effect, modal analysis and harmonic analysis along with mathematical derivation. The research is inspired because very few scientific works are investigated on thin metal cantilever plates for detection of crack. Detailed parametric study is conducted on an edge crack, which is thorough in nature. The research consists of several cases. Studies of different crack orientations (transverse, longitudinal and inclined) and crack sizes (crack length, crack width and crack depth) are done over relative distance along the longitudinal (Z-axis), transverse (X-axis) and depth (Y-axis) directions. Different materials (aluminum alloy and structural steel) is also taken into account. The study of each of these cases are simulated on ANSYS 16.0 workbench and designed over SolidWorks. The results of numerical analysis (modal analysis) is correlated with stress concentration, deformation, deflection and breathing effect of the crack on the plate. Taking the natural frequency of the healthy plate as the base of the comparison, any deviation due to presence in crack is noted and to identify the most significant locations on the plate where the change is maximum. The work has been validated with a scientific paper [3] of Tao et al.

For a transverse crack along longitudinal (Z-axis) direction (case-1), the change of frequency is more in torsional modes than bending modes. In both bending and torsional modes, the maximum frequency drop shift towards the free end with the increased number of modes.

In other observation, it is found that as the crack length increases (case-2), the frequency drop increases and the intersection point moves towards the free end. This is found in both simulation results and solutions with regression equations. For all six modes in three distinct regions (fixed end, mid-region and free end), there is increase in frequency drop with increase in crack length (further study). Moreover, for larger crack length, there is always more frequency drop at fixed end (48.1% and 56%) than in mid-region (22.7% and 44.5%) and

lowest at free end (1.7% and 26.1%) when considering mode 1 and 2 only. On the other hand, the frequency drop is higher at free end (29.3% and 32.3%) when considering mode 5 and 6.

It is noticed (in case-3) that as the crack width increases, the frequency drop remains constant and the intersection point moves towards the fixed end. This is confirmed in both simulation results and solutions with regression equations. When the crack width increases, in further study of case-3, the frequency drop increases at fixed region and frequency gain increases at free region for mode 1 and 2. The maximum significant difference is 9.7% and 9.0% at fixed end for mode 1 and 2 respectively.

When the crack depth is increased (in case-4), the frequency drop remains constant until crack depth to plate thickness (c/H) ratio becomes 75% and more. After this point, there is a rapid drop of frequency drop until the crack is thorough.

It is deduced that metal (case-5) and metal alloy (case-1) have the same normalized frequency curve as they follow same pattern and trend plotted over relative distance. The torsional modes found in normalized frequency curves have the same line of progression with little difference. While the bending modes found in normalized frequency curves take place at certain gap though they follow the same pattern of progression. In this case, natural frequency of aluminum alloy is greater than structural steel indicating greater stiffness in aluminum alloy. Both bending and torsional modes, the maximum drop in frequency shifts towards the free end with increase in mode.

It is observed that at all the locations the frequency drop in transverse edge crack (case-5) is massive than embedded mid-crack (case-6). For transverse mid-crack, torsional modes have little significance with maximum frequency drop of 0.26% at relative distance 90.9%. While in bending modes, the frequency curves of embedded mid-crack have the same pattern as edge

crack but the frequency drop lower (maximum frequency drop 4.2% on 1st mode) than transverse edge crack (maximum frequency drop 5.8% on 1st mode).

The maximum frequency drop in bending modes is 0.29% for longitudinal edge crack (case-7) and 0.58% for embedded longitudinal mid-crack (case-8). These are located near fixed end on 1st mode. While in torsional modes, maximum frequency gain is observed at free end in case-7. However, in case-8, sharp frequency drop is noticed. Both these cracks are undetectable. Only the embedded longitudinal mid-crack can be detected at free end with the presence of sharp frequency drop in torsional modes.

The bending modes of both longitudinal edge crack (case-9) and transverse edge crack (case-10) is negligible along the transverse direction. The frequency drop for longitudinal edge crack at mid-region is detectable when torsional mode is considered. The maximum frequency drop is 8.9% on 6th mode. The transverse edge crack (surface defect) remains undetectable.

Most of the frequency curves for inclined crack at relative distance 21% (case-11) and 79% (case-12) are parabolic or slightly distorted parabolic. Considering the torsional modes, the lowest frequency drop is found at the starting and ending point of the normalized frequency curve where the crack angles are 0^o and 180^o. These are the locations where the crack align longitudinally at the edge (surface defect). On the other hand, the maximum frequency drop is found when the crack angle is 90^o, the crack location where the crack orientation is transverse at the edge. For inclined crack near fixed end, mode 1 and 2 are dominant and maximum significant difference found within this region. While near free end, mode 5 and 6 are dominant and maximum significant difference found within this region.

6.2 Recommendation

As crack length plays an important role, further analysis should be done with increased crack length. Moreover, static structural analysis should be done of these increased crack lengths, to understand the behavior of crack more. Experimentation of some specific cases where cracks are more prone to detection should be performed first to verify the obtained simulation results. Harmonic analysis should be performed to get wide range of amplitude. A comparison could be made to note the major differences in detection of cracks in a cantilever beam and thin cantilever plate.

References

1. Shen, M.-H. H. and Chu, Y. C., “Vibrations of Beams with a Fatigue Crack”, Computers & Structures, Vol. 45, Issue 1, 17 September 1992, pp. 79-93.

2. Chondros, T.G., Dimarogonas, A.D. and Yao, J., “Vibration of Beam with a Breathing Crack”, Journal of Sound and Vibration, 239 (1), 2001, pp. 57-67.

3. Tao, N., Ma, Y., Jiang, H., Dai, M. and Yang, F., “Investigation on Non-Linear Vibration Response of Cantilevered Thin Plates with Crack Using Electronic Speckle Pattern Interferometry”, The International Conference on Experimental Mechanics 2018 (ICEM18), Brussels, Belgium, 2 (8), 1–5 July 2018, pp. 539.

4. Orhan, S., “Analysis of Free and Forced Vibration of a Cracked Cantilever Beam”, NDT & E International, Volume 40, Issue 6, September 2007, pp. 443–450.

5. Tufisi, C., Gillich, G.-R. and Aman, A.T., “The Effect of a Crack Near the Fixed End on the Natural Frequencies of a Cantilever Beam”, Vibroengineering PROCEDIA, Vol. 23, 2019, pp. 37-42.

6. Shinde, Y.D. and Katerkar, S.D., “Vibration Analysis of Cantilever Beam with Single Crack using Experimental Method”, International Journal of Engineering Research & Technology (IJERT), Vol. 3, Issue 5, May – 2014, pp. 1644-1648.

7. Praisach, Z.I., Minda, P.F., Gillich, G.-R. and Minda, A.A., “Relative Frequency Shift Curves Fitting Using FEM Modal Analyses”, Proceedings of the 4th WSEAS International Conference on Finite Differences - Finite Elements - Finite Volumes - Boundary Elements, April 2011, pp. 82-87.

8. Gillich, G.-R., Wahab, M.A., Praisach, Z.I. and Ntakpe, J.L., “The Influence of Transversal Crack Geometry on the Frequency Changes of Beams”, International Conference on Noise and Vibration Engineering, September 2014, pp. 485-498.

9. Rao, Singiresu S.. Mechanical Vibration, Fourth Edition, Pearson, 2004.

10. Anderson, T.L., Fracture Mechanics - Fundamentals and Applications. Third Edition, Taylor and Francis.

11. Andreaus, U. and Baragatti, P., “Fatigue Crack Growth, Free Vibrations, and Breathing Crack Detection of Aluminium Alloy and Steel Beams”, The Journal of Strain Analysis for Engineering Design, 44 (7), 2009, pp. 595-608.

12. Al-Waily, M. and Deli, A., “A Suggested Analytical Solution of Buckling Investigation for Beam with Different Crack Depth and Location Effect”, International Journal of Energy and Environment, Vol.7, Issue 3, 2016, pp. 201-216.

13. Charalambides, P.G. and Fang, X.M., “The Mechanics of a Cantilever Beam with an Embedded Horizontal Crack Subjected to an End Transverse Force, Part A: Modelling. Mechanics”, Materials Science & Engineering, Vol 5, 2016.

14. Liu, J., Zhu, W.D., Charalambides, P.G., Shao, Y.M., Xu, Y.F. and Fang, X.M., “A Dynamic Model of a Cantilever Beam with a Closed, Embedded Horizontal Crack Including Local Flexibilities at Crack Tips”, Journal of Sound and Vibration, Vol. 382 (10), November 2016, pp. 274-290.

15. Soliman, E.S.M.M, “Influence of Crack Inclination Angle on Isotropic Cracked Cantilever Beam”, J Fail. Anal. and Preven., Vol. 20, 2020, pp. 1065–1080.

16. Jena S.P. and Parhi D. R., “Response Analysis of Cracked Structure Subjected to Transit mass – a Parametric Study”, Journal of Vibroengineering, Vol. 19, Issue 5, 2017, pp. 3243-3254.

17. Gillich, G.-R., Maia, N.M.M., Mituletu, I.-C., Praisach, Z.-I, Tufoi, M. and Negru, I., “Early Structural Damage Assessment by Using an Improved Frequency Evaluation Algorithm”, Latin American Journal of Solids and Structures, 12(12), 2015, pp. 2311-2329.

18. Barad, K. & Sharma, D. and Vyas, V., “Crack Detection in Cantilever Beam by Frequency based Method”, Procedia Engineering, 51, 2013, pp. 770-775.

19. Elshamy, M., Crosby, W.A. and Elhadary, M., “Crack Detection of Cantilever Beam by Natural Frequency Tracking using Experimental and Finite Element Analysis”, Alexandria Engineering Journal, Vol. 57, Issue 4, December 2018, pp. 3755-3766.

20. Gillich, G.-R., Tufoi, M., Korka, Z., Stanciu, E. and Petrica, A., “The Relations between Deflection, Stored Energy and Natural Frequencies, with Application in Damage Detection”, Romanian Journal of Acoustics and Vibration, 13, 2016.